5-1-2010

Genetic contributions to brain fiber architecture and neuroanatomical alterations in alcohol dependent individuals : a correlation study

Vibhati Kulkarny

Vibhati V. Kulkarny
Candidate

Biomedical Sciences
Department

This dissertation is approved, and it is acceptable in quality and form for publication:

Approved by the Dissertation Committee:

Nora Perrone-Bizzozero, Chairperson

GENETIC CONTRIBUTIONS TO BRAIN FIBER ARCHITECTURE AND NEUROANATOMICAL ALTERATIONS IN ALCOHOL DEPENDENT INDIVIDUALS: A CORRELATION STUDY

VIBHATI V. KULKARNY

B.S., Psychobiology, University of California, Los Angeles, 2003

DISSERTATION

Submitted in Partial Fulfillment of the
Requirements for the Degree of

Doctor of Philosophy
Biomedical Science

The University of New Mexico
Albuquerque, New Mexico

May, 2010

DEDICATION

I dedicate this work to my parents Vijay and Karuna Kulkarny for being my support and ever flowing encouragement throughout my life. They have taught me many things throughout the years, the most important being the value of a good education and to always do my best. I also want to dedicate this to my younger sister, Amruta Kulkarny, who is my other half, without her emotional support, hours of encouragement and funny anecdotes, this part of my life would have taken much longer. Thank you, my family, for all the love, support and encouragement; I couldn't have done this without you.

ACKNOWLEDGEMENTS

I would like to acknowledge my mentors Dr. Nora Perrone-Bizzozero and Dr. Kent Hutchison for supporting me through the trials and tribulations of my graduate career. Dr. Perrone-Bizzozero's enthusiasm for science, and inquisitive nature made my graduate career an educational and exciting experience. She taught me that "data is data," and no matter what it is, positive or negative, it can be interpreted. I respect and admire her as a person, a mother, a scientist and as a mentor. My co-mentor Dr. Hutchison, provided a new, cutting-edge opportunity for my graduate career where I was given free range to prove myself. This path, a rare sight in graduate school, demonstrated Dr. Hutchison's trust, compassion and faith in me and my capabilities, for which I am deeply grateful. Drs. Andrea Allan and Michael Wilson provided additional insight in the fields of statistics and genetics, respectively. Dr. Allan's expertise in alcohol research and statistical analyses, as well as her guidance, care and compassion, has fostered me into the scientist I am today. Dr. Wilson's discussions and knowledge in the field of genetics were immensely helpful, as was his NeuroGenetics class, which inspired the second part of this dissertation. I would also like to thank my committee for their scientific guidance, undeterred encouragement, and immense amount of support and complete faith in my victory.

I would like to acknowledge Marilee Morgan who took me under her wing when I started in the Neurogenetics Lab and essentially taught me the basics of microarrays and how to clean up large amounts of genotype data. I would like to thank my friends and labmates Flora Soto-Endicott, Dr. Eric Claus and Robert Chavez, for providing me with

information about AD, offering scientific advice and for teaching me how to run FSL, DTIStudio, IDL and TBSS, respectively.

I would also like to thank Dr. Fernando Valenzuela, Dr. Dan Savage, and Dr. Rebecca Hartley, my previous committee on studies for supporting me through my previous thesis and for encouraging me not to quit, but to push through to success. I would like to acknowledge Dr. Martina Rosenberg and Sayuri Nixon for their help and company in the wet lab on the previous project, as well.

Lastly, I would like to acknowledge my parents for letting me be a student for another five years, my sister for her encouragement, and my friends for their love and support during my long pursuit of the PhD.

GENETIC CONTRIBUTIONS TO BRAIN FIBER ARCHITECTURE AND NEUROANATOMICAL ALTERATIONS IN ALCOHOL DEPENDENT INDIVIDUALS: A CORRELATION STUDY

BY

VIBHATI V. KULKARNY

ABSTRACT OF DISSERTATION

Submitted in Partial Fulfillment of the
Requirements for the Degree of

Doctor of Philosophy
Biomedical Science

The University of New Mexico
Albuquerque, New Mexico

May, 2010

GENETIC CONTRIBUTIONS TO BRAIN FIBER ARCHITECTURE AND NEUROANATOMICAL ALTERATIONS IN ALCOHOL DEPENDENT INDIVIDUALS: A CORRELATION STUDY

by

Vibhati V. Kulkarny

B.S., Psychobiology, University of California, Los Angeles, 2003
Ph.D., Biomedical Sciences, The University of New Mexico 2009

ABSTRACT

Alcohol dependence (AD) is a complex addictive disorder, affecting 5.4% of the general population during a lifetime (Kessler, 2005) and has a complex heterogenous phenotype, with behavioral, morphological, and genetic components. Alcohol use can cause gray matter and white matter tissue damage. The extent of alcoholism's effect on brain matter structure in young adults is less known. Assessement of low and high alcohol dependent individuals was derived from DSM-IV. FSL based Magnetic Resonance Imaging (MRI) and quantitative fiber tracking derived from diffusion tensor imaging (DTI) assessed morphological alterations of 6 gray matter structures involved in addiction and 10 white matter structures that show connectivity of these structures in 26 low AD and 19 high AD individuals. Candidate SNPs were chosen relating to synaptic plasticity and myelination (BDNF, NTRK2, NFKB1, MAG, OLIG2) and each individual was genotyped. Alcohol dependence affected the volumes of the caudate-putamen, the accumbens, the amygdala and the hippocampus. The uncinate fasciculus was also affected by level og AD, showing smaller mean diffusivity (MD), quantified separately for axial diffusivity (AxD), a marker of axonal intergrity, and radial diffusivity (RD), a

marker of myelin integrity. Exploratory associations of AD, morphological alterations and SNPs, showed significant correlations and trends, but was not well defined due to a small subject population. The present research shows evidence that behavioral diseases are associated with identifiable neuroanatomic alterations, and do form relationships with specific SNPs. Additional information is needed when studying a specific, yet multifactorial disease, such as AD, but nonetheless, we advocate the use of neuroimaging measures in genetic studies.

TABLE OF CONTENTS

LIST OF FIGURES

LIST OF TABLES AND GRAPHS

CHAPTER 1: INTRODUCTION

1.1 Imaging Genetics (IG)

With the advent of advances in molecular biology, neuroimaging, genetics and psychopathology, opportunities have arisen to study the interplay of genes, brain and behavior within a translational framework. This strategy, in use at present, in which genetic effects on brain function can be explored using neuroimaging, is titled "imaging genetics" (Viding E et al, 2006). Identifying specific genes that contribute to risk for illnesses can provide critical information on the causes of these diseases that may lead to the development of novel diagnostic and therapeutic strategies.

The publication of the reference human genome sequence (Venter et al 2001; Lander et al 2001) has led to the process of identifying common variations in the sequences and the impact on the gene and its function and how that variation alters human biology. Imaging, with its capacity to quantify detailed anatomical structure and function within human subjects, is a tool for characterizing the functional genetics in human circuitry. This presents a new specified field for science integrating genes, endophenotypes and neuroimaging.

Examining this relationship between genes and neural systems was initially called "Imaging Genetics (IG)" (Hariri, Drabant and Weinberger, 2006). The essence of "imaging genetics" rests on two general concepts; the effectiveness in delineating biological pathways and mechanisms by which individual differences in function emerge and show a biased risk for a clinical disease; and, application of imaging and genetics to study the susceptibility and development of the specific pathology in question.

In the context of a clinical disease state, genes represent the blueprint that either directly, or indirectly, in concert with the environment, results in the disease. Additionally, those same genes offer the ability to identify at-risk individuals and molecular pathways and mechanisms for treatment. Variations in this blueprint, that impact gene function, will contribute largely to the resultant complex pathological disease. In the case of biological diseases, protein coding genes appear to be the only consistent risk factors that have been identified across populations, accounted for by inheritance (Moldin and Gottesman, 1997).

Genetic epidemiological studies have examined the relationship between specific genetic polymorphisms and diseases and have shown unclear results (Malhotra and Goldman, 1999). There are two reasons for this. First, due to individual variability in observed behavior and subjectivity of this assessment, it is necessary to have large sample populations, often exceeding a hundred subjects, to identify even small gene effects (Glatt and Freimer, 2002). Furthermore, subgroups may exist which obscure the effects in the broader group (e.g. age, gender, etc). Second, the effects of genes are not expressed directly at the level of the disease, but are mediated by their molecular and cellular effects on information processing at the cellular level and more globally, in the human body.

Genes are directly involved in the function of brain regions related to cognitive processes, and because of this, functional polymorphisms in genes may be related to the function of neural systems mediating behavioral outcomes (**Figure 1**). This approach utilizes an exploration of specific genes, not the genome, molecular mechanisms and systems, and pathology of an illness. "Imaging Genetics" is a unique tool by which to

explore the functional impact of brain relevant polymorphisms with the idea of then understanding their impact on the human body or behavior.

Functional imaging methods provide information on the integration and interaction of specific anatomical regions in large scale spatially distinct networks during cognitive or behavioral responses. This type of data is essential for understanding the physiology of information processing at the systemic level, and may be sensitive to pathological changes seen in individuals with disorders (Gothelf et al, 2005; Hirvonen et al, 2006; Seidman et al, 2006). Neuroimaging methods are successfully applied to analyze neurological and psychiatric disorders and there is growing evidence that addictions are associated with alterations in brain structure and function (Thompson et al, 2004). Neuroimaging techniques require no more than a few minutes, to a couple of hours, of subject participation to acquire data sets which reflect hundreds of repeated measures of brain structure (Magnetic Resonance Imaging, MRI) and function (functional Magnetic Resonance Imaging, fMRI). Most importantly, these techniques, MRI, fMRI, EEG/ MEG (Electroencephalography/ Magnetoencephalography), PET (Positron Emission Tomography) are non-invasive and the efficiency allows for the ability to investigate the specificity of a gene's influence on multiple brain regions and systems in a single subject in a single session. The capacity of these techniques is to produce rapid results of differences in brain structure *in vivo* for the study of genetic variation. Taken together, these types of data suggest that markers of brain function may be more sensitive to subtle genetic variations than overt behavior (Hariri and Weinberger, 2003).

The search for genetic loci involved in disorders is hampered by the genetic complexity of an illness; heterogeneity characterizes AD expression, comorbidity with other disorders that distort clinical presentation. Genes predispose an individual to a neurological or psychiatric illness and can be transmitted without expression as a clinical phenotype. The interest arises in developing endophenotypes, indicators of processes mediating between genotype and phenotype as an important strategy to deal with the complications. Endophenotypes are behavioral or physical characteristics that represent the biological features in the gene to behavior pathway. Specifically, they are markers that are genetically correlated with disease liability, and can be measured in affected or unaffected individuals. They provide greater power to localize and identify disease related quantitative trait loci (QTLs) (Balngero et al, 2003). It maybe possible that genes act more directly on an endophenotype, more than a clinical classification, and thus, a study may be more efficient in leading to a candidate gene. Endophenotypes may provide information about neurochemical pathways leading from the genes to the clinically diagnosed behavior. Biological endophenotypes are measureable intermediate phenotypes that are generally closer to the action of the gene (Gottesman and Gould, 2003). Although neurological and psychiatric illnesses are typically identified through behavioral observation, these illnesses are closely associated with brain structures. Advances in neuroimaging indicate that particular diseases preferentially disturb specific neuroanatomic structures. Furthermore, the distribution of structural differences reflects the underlying pathology. For example, hippocampal/ limbic system atrophy points to addiction and cerebellar atrophy in Karsokoff's syndrome points to chronic alcoholism. These alterations seen in affected individuals often predate overt symptom expression in

a less severe form (Fleisher et al, 2005). Previous literature has focused on electrophysiologic measures that are representative of AD subjects. AD individuals show evidence of several abnormalities in electrophysiologic functioning including differences in all three bands of a resting EEG versus controls (Porjesz B et al. 2005). Numerous additional studies suggest that electrophysiologic endophenotypes can be used as biological markers and may be utilized in genetic analyses. Biological endophenotypes are measurable intermediate phenotypes that are generally closer to the action of the gene (Gottesman and Gould, 2003). In conclusion, findings of neuroanatomical alterations in affected individuals and with increased genetic risk for the disease suggest that at least a portion of the indices could be endophenotypic markers (McDonald et al, 2004).

The complete process involves identifying a genetic polymorphism (e.g. single nucleotide polymorphism, SNP) within a candidate gene, one which has an impact at the molecular level and has a distribution that involves information pathway in the brain. At a fundamental level, all three concepts--genetics, neuroimaging and human behavior--are linearly linked within "imaging genetics." IG provides a starting point for further characterization of molecular and functional effects of candidate genes in brain systems that are involved in a specific behavior. As such, the contributions of variances in these systems to complex psychopathologies can be understood from their genetic origins.

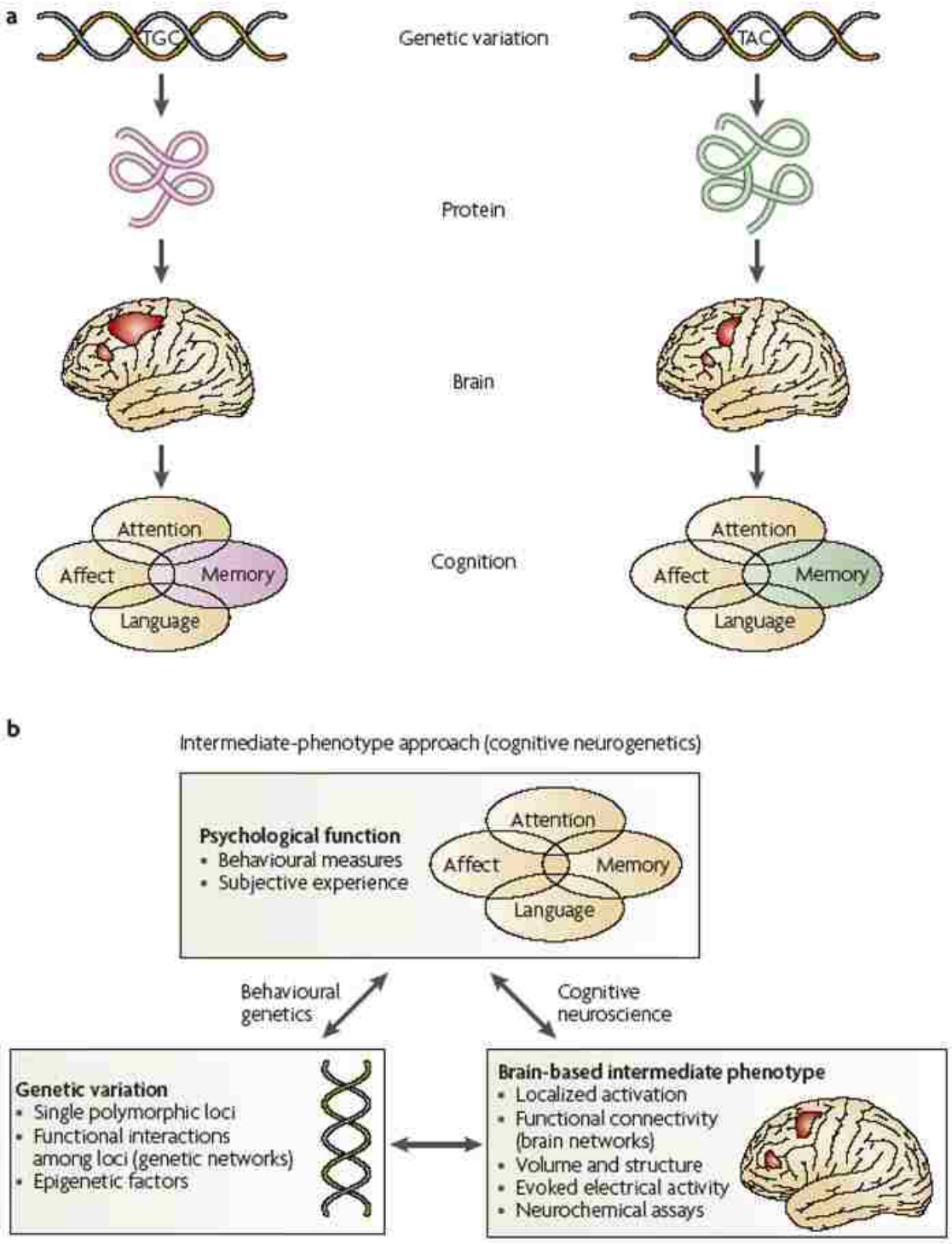

Figure 1. Integrating behavioral neuroscience and genetics through the intermediate phenotype approach. (a) Variations in genes can lead to variations in function, yet many steps exist between. (b) Numerous sub-disciplines study the different links in the causal chain from gene to behavior. (Green et al, 2008).

1.2 Epidemiology of Alcohol Dependence Syndrome (ADS)

1.2.1 Alcohol Dependence Syndrome (ADS)

Alcohol dependence, a common disorder with heterogeneous etiology, as described in the DSM-IV is a psychiatric diagnosis describing a measure in which an individual uses alcohol despite significant areas of dysfunction, evidence of physical dependence, and/or related hardship. Alcohol dependence is acknowledged by the American Medical Association as a disease with a characteristic set of signs and symptoms with a progressive course. For a person to meet criteria for Alcohol Dependence (OMIM #103780) within the criteria listed in the DSM-IV, they must meet 3 of a total 7 possible criteria within a 12-month period.

The first 2 criteria are related to physiological dependence: tolerance and withdrawal. The 3rd and 4th criteria establish a pattern of losing control of drinking by breaking drinking rules or failing at attempts to quit or cut back. The 5th and 6th criteria are indicative of a progression of addiction as more and more time is spent on drinking and changes in lifestyle result. The seventh criterion for Alcohol Dependence is met when a person continues to drink despite being aware that their drinking is causing or exacerbating some psychological or physiological problem(s).

Alcohol Dependence is differentiated from alcohol abuse by the presence of symptoms such as tolerance and withdrawal. Both alcohol dependence and alcohol abuse are sometimes referred to by the less specific term “Alcoholism.” Alcohol dependence syndrome (ADS) is a classification of alcoholism proposed by Edwards and Gross in 1976 and formally defined by the World Health Organization. This system standardizes terminology and differentiates between two disorders: alcohol abuse, disabilities that

result from excessive drinking, and alcohol dependence, tolerance and withdrawal (**Figure 2**). Alcohol dependence refers to alcohol as an addictive agent and remission, as defined within DSM-IV, and the measure can be attained despite continued use of alcohol. That is, a patient can be in sustained remission yet still be drinking alcohol so long as the patient does not meet the 3 out of 7 criteria.

The alcohol dependence syndrome is seen as a cluster of seven elements and not all elements may be present in each individual case, but the diagnosis is sufficiently consistent and coherent to be recognized clinically. Also, the syndrome exists in degrees of severity rather than a categorical absolute. Thus, the question is not 'whether a person is dependent on alcohol', but 'how far along the scale of dependence has a person progressed.'

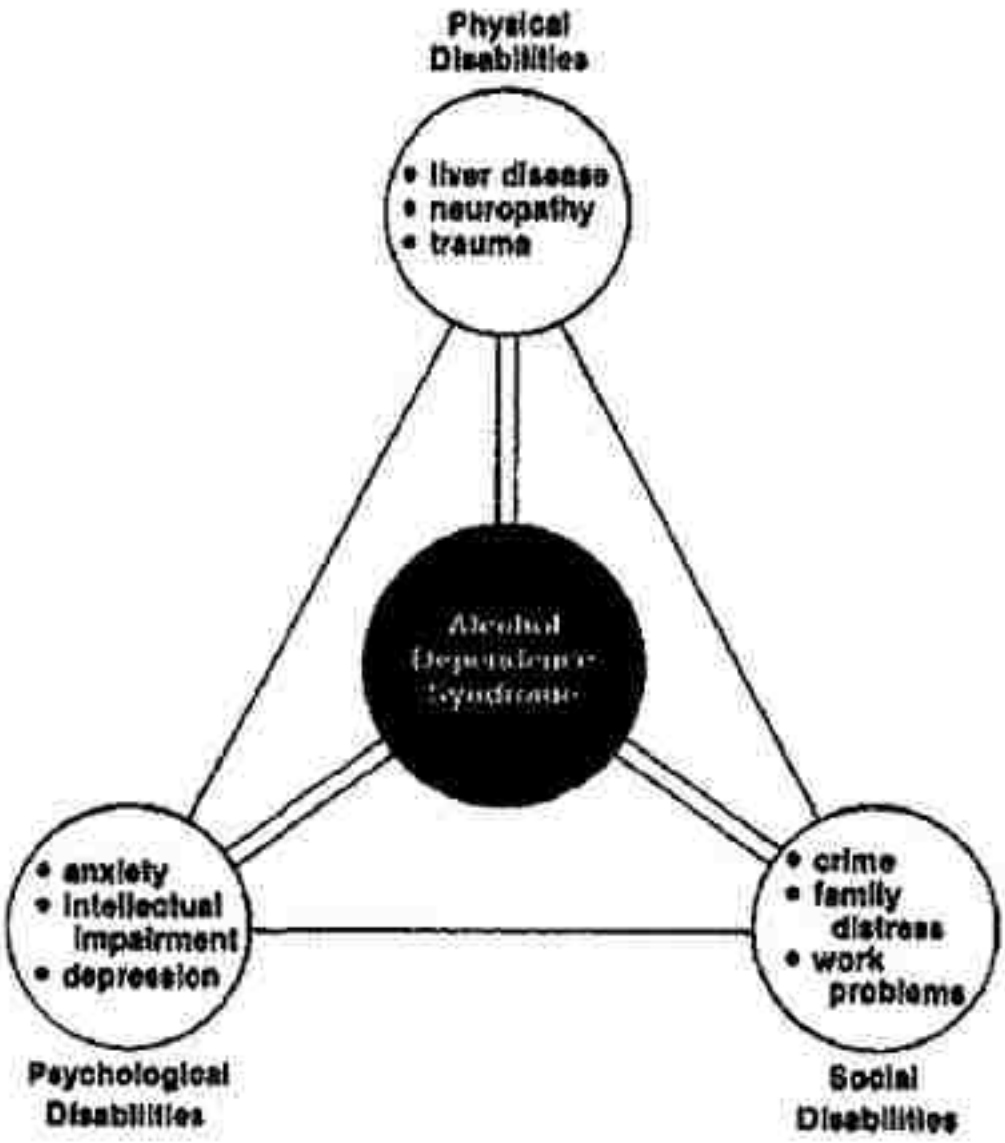

Figure 2. Differentiation of alcohol dependence syndrome from alcohol related disabilities (Skinner and Allen, 1982).

1.2.2 Alcohol Dependence Syndrome: Diagnosis

The ADS scale provides a quantitative measure of the severity of alcohol dependence consistent with the concept of the alcohol dependence syndrome. The printed instructions for the ADS refer to the past 12-month period. However, instructions can be altered for use as an outcome measure at selected intervals (e.g., 6, 12, or 24 months)

following treatment. ADS scores have proven to be highly diagnostic with respect to a DSM diagnosis of alcohol dependence, and have been found to have excellent predictive value with respect to a DSM-IV diagnosis. The ADS is used in wide variety of settings for screening and assessment of alcohol dependence. Several studies have used the ADS with adolescents. The ADS can be used for screening and case finding in a variety of settings including health care, corrections, general population surveys, workplace, and education. A score of 9 or more is highly predictive of DSM diagnosis of alcohol dependence.

In 1981, Skinner identified an Alcohol Dependence Factor that correlated with chronic social debilitation and psychopathology, deriving a 29-item Alcohol Dependence Scale. Skinner and Allen's study in 1982 found that the dependence syndrome is assessed reliably (internal consistency=0.92) with a brief self-report scale and that the syndrome correlates in predictable ways with clinic attendance, physical symptoms and psychosocial problems in the subject's life. The 29 items that form the ADS questionnaire encompass four key aspects of the syndrome: (1) loss of behavioral control (i.e. blackouts, gulping drinks) (2) psychoperceptual withdrawal symptoms (i.e. hallucinations) (3) psychophysical withdrawal symptoms (i.e. hangovers, deliriums tremens), and (4) obsessive-compulsive drinking style (i.e. sneak drinks, hidden drinks, drink availability). The advantage of using the AD Scale is that it may be used to order individuals along a continuum of alcohol dependence rather than make a discrete diagnosis of alcoholic and non-alcoholic (Skinner and Allen, 1982). The following elements are the template for which the degree of dependence is judged:

1. Narrowing of the drinking repertoire.
2. Increased salience for alcohol over other competing responsibilities.
3. An acquired tolerance to alcohol.
4. Withdrawal symptoms.
5. Relief or avoidance of withdrawal symptoms by further drinking.
6. Subjective awareness of compulsion to drink.
7. Reinstatement after abstinence.

Specifically, the high correlation between alcohol dependence and adverse consequences from drinking demonstrated that the Alcohol Dependence Scale provides the proper information for defining levels of dependence. The ADS can be used for basic research studies where a quantitative index is required regarding the severity of alcohol dependence. For clinical research, the ADS scale is a useful screening and case-finding tool.

1.2.3 ADS: Incidence in the human population

Alcohol dependence is a widespread disorder, affecting about 10% of the population (Sher et al, 2005). Approximately 5-7% of the adult U.S. population is diagnosed with alcohol dependence, a complex addiction having a heritability of at least 50% in both men and women (Reich et al, 1998). About 12% of American adults have had an alcohol dependence problem at some time in their life (Hasin et al, 2007). From the estimated 27 million Americans exhibiting AUD--alcohol abuse or alcohol dependence—the average age of onset is 22 years and 72% of this population has one 2-5 year-long episode (Hasin et al, 2007).

1.2.4 ADS: Genetic Associations

Vulnerability to alcohol dependence is most likely caused by multiple interacting genes, each contributing to the phenotype and symptoms of addictions or brain damage. AD is essentially a behavioral disorder in nature and the etiology is likely to involve dysfunction in brain systems; therefore, genes encoding neural substrates mediating these dysfunctions represent the most obvious susceptibility genes. In particular, the brain systems involved in the motivational aspects of addiction are considered to be disrupted sufficiently to produce the characteristic loss of control of consumption and drug seeking.

Crabb et al. in 1990 reviewed biologic markers for increased risk of alcoholism and concluded that liability to alcoholism is controlled by a major effect with or without additional multifactorial effects. Twin, adoption and family studies have shown that genetic factors play a considerable role for risk and symptoms of alcohol dependence (Goodwin, 1975). Alcohol use leads to addiction, dependence, or tolerance and these phenomena create adaptive responses at the cellular level so that if the drug is removed, the neuroadaptations are revealed, leading to manifestation of withdrawal symptoms (**Figure 3**). Again, AD is differentiated from alcohol abuse by the presence of symptoms such as tolerance and withdrawal. In the case of AD, withdrawal is the presentation of symptoms (e.g. agitation, delirium tremens, depression, seizures and death) that occur upon the abrupt discontinuation/separation or a decrease in dosage of alcohol. Substantial evidence suggests that this cellular adaptive process is mediated, at least in part, by changes in gene expression (Nestler et al., 1994). Morphometric studies of gray matter suggest that neurons in the frontal lobe are selectively damaged (Kril and Harper, 1989) and thus, the frontal cortices, important in judgment, decision-making, and other

executive functions (Rahman et al, 1999) have been chosen as a focus for addiction and alcoholism. Lewohol et al in 2000 selected this region from post-mortem tissue of alcoholic individuals for DNA microarray analysis. This analysis revealed expression levels of 400 genes of which 163 were found to differ by 40% or more between alcoholic and non-alcoholic individuals. Specifically, a significant decrease in myelin-related genes, PLP, MAG, Mal, and MBP, in the frontal cortex indicated that alcohol abuse directly or indirectly affects the transcription of these proteins. Hill et al (2004) studied families containing 330 alcoholic individuals identified, through multipoint linkage analyses, loci on chromosomes 1, 2, 6, 7, 10, 12, 14, 16, and 17. Several linkage studies give evidence for many chromosomal loci, where--among others--glutamatergic and dopaminergic genes are located (Edenberg and Foroud, 2006). Genetic association studies that have shown a relationship between alcohol dependence and numerous neurochemical/neurotransmitter systems and neuroimaging studies provide further support for the role of alterations in these systems in the pathogenesis of alcohol dependence (Wong et al., 2003).

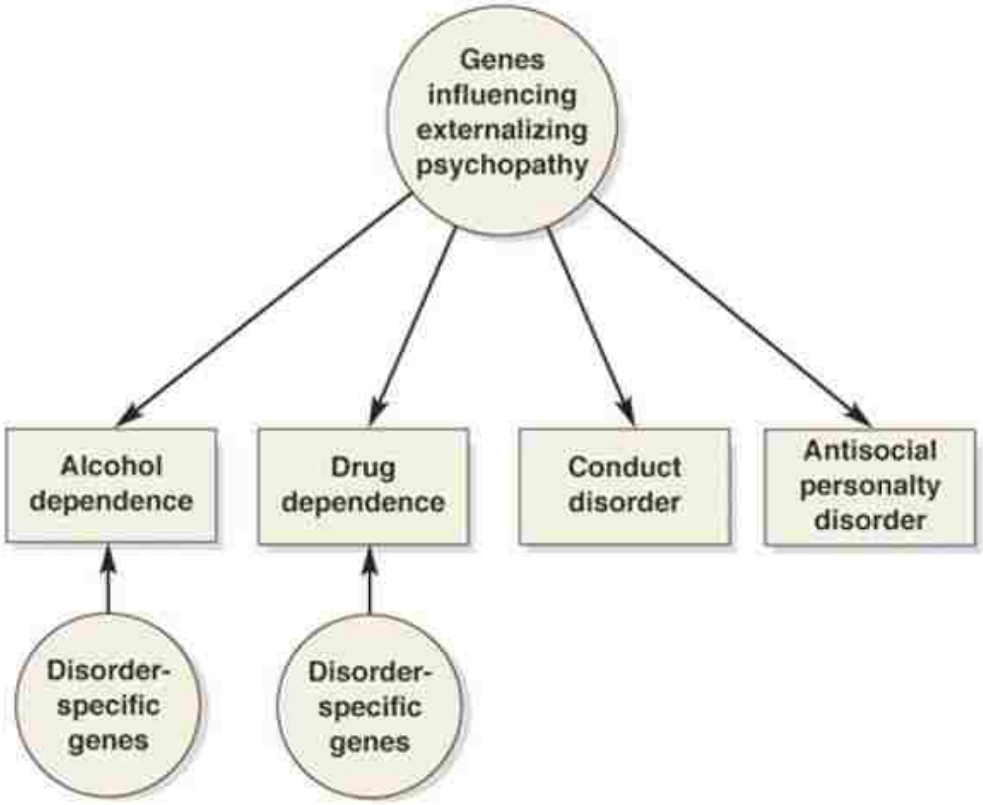

Figure 3. Model illustrating influences on genetic factors on the development of AD. Some of the proposed genetics factors have a disorder specific influence (Dick and Agarwal, 2008).

1.2.5 Alcoholism and Depression

The Collaborative Study on Genetics of Alcoholism (COGA) identifies genes contributing to alcoholism and related traits, including depression. Psychopathological studies have observed that alcoholism and affective disorders interact and can coexist; the vulnerability to both alcoholism and depression can run in families (Merikangas and Gelernter, 1990; Merikangas et al., 1994). In 2002, Nurnberger et al, defined three phenotypes- "alcoholism", "alcoholism and depression," and "alcoholism or depression"- and analyzed whether these phenotypes were linked to specific chromosomal regions.

The analysis found a genetic linkage to an area on chromosome 1 suggesting that a gene or genes in this area may predispose individuals to alcoholism and depression that may be alcohol induced. Alcoholism and depression tend to occur together in families where both disorders are transmitted. The limitation of this study is that by design it focused on familial linkage analysis and did not represent the spectrum of people who are AD, depression or both.

1.3 Neuro-Imaging Techniques for Neuroanatomical Studies

1.3.1 History of Neuroimaging: AD

Chronic alcoholism has been associated with global changes in brain morphology, such as cortical and sub-cortical atrophy. The first documented case of damage due to chronic alcoholism, using pneumoencephalography (Brewer and Perrett, 1971) showed brain shrinkage and was easily confirmed using CT scans of heavy drinkers and alcoholics (Cala et al., 1985). Postmortem study of alcoholic subjects has identified damage in white matter and identified demyelination (Lewohl et al., 2000), microtubule disruption (Paula-Barbosa and Tavares, 1985) and axonal deletion, as well as morphological degeneration involving cell processes (Harper et al., 1987). Also, volume reduction arising from shrinkage, reduction in cell counts, size, or neuronal processes has been reported (De la Monte, 1988; Harper and Kril, 1990, 1991). Although, these studies have been essential in identifying gross neuroanatomical damage in alcoholism, the post-mortem fixation process and collapse of certain regions, does not reflect the alcohol-related effects on the living brain (Pfefferbaum et al., 2004). In vivo conventional magnetic resonance imaging (MRI) studies have provided convergent validity for the damage observed in alcoholic subjects post-mortem and are generally consistent with the

neuropathological literature regarding white matter volume reduction in the cerebrum (Pfefferbaum et al, 1992).

1.3.2 Magnetic Resonance Imaging (MRI): Physics

The brain is mainly composed of water molecules and when an individual is placed within a powerful magnetic field of the scanner (a diffusion–weighted pulse sequence) these protons align with the direction of the field. A second radiofrequency electromagnetic field is then briefly turned on causing the protons to absorb some of its energy. When this field is turned off the protons release the obtained energy at a radiofrequency that is detected by the scanner. The position of protons in the body can be determined by applying additional magnetic fields during the scan that allow an image of the brain to be constructed, slice by slice. Diseased or damaged tissues, such as tumors or plaques, are detected due to the different rates of reaching equilibrium states for all the protons in the region of interest (ROI). By changing the parameters on the scanner, using additional magnetic fields, a contrast between different tissues is created (Lauterbur et al., 1989, **Figure 4**). MRI uses no ionizing radiation and is generally a very safe procedure.

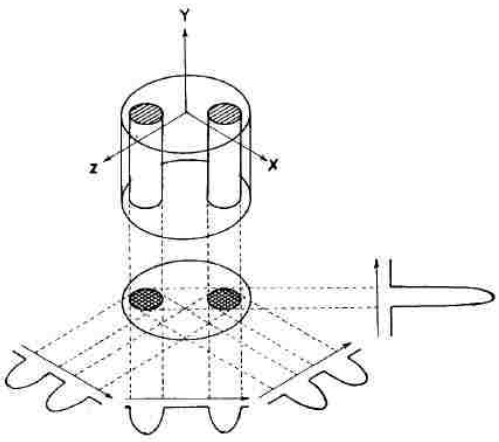

Figure 4. Relationship between a 3D object and its 2D projection along the y-axis and four 1D projections at 45deg intervals in the xz-plane. The arrows indicate the gradient directions (Lauterbur PC, 1989).

1.3.3 Diffusion Tensor Imaging (DTI): Physics

Structural MRI enables quantification of bulk volume and a few aspects of tissue quality but does not assess the microstructure of brain tissue and its components, such as axons, microtubules, and myelin. By contrast, diffusion tensor imaging (DTI) permits in vivo quantification of the directionality, coherence and microstructural integrity of white matter tracts (Moseley et al., 1990; for reviews on method and application in human studies see Basser and Jones, 2002; Kubicki et al., 2002; Sullivan and Pfefferbaum, 2005).

The intrinsic property of water diffusion in human brain tissue provides information about the structural characteristics of the tissue. When the diffusion of water molecules is unconstrained (e.g. CSF), it is characterized by Brownian motion. The resulting molecular displacement produces a Gaussian distribution where the movement has no directional preference and is, therefore, "isotropic." When motion is restricted by boundaries with a predominant direction, such as the walls of a white matter tract, the diffusion is greater in parallel to the tract and thus is "anisotropic" (**Figure 5A**). White matter is highly organized in fiber bundles that restrict water and so, the orientation of the diffusion depends on the orientation of the specific fiber tracts observed. The axon's cytoskeleton consists of axoplasm and organelles, and this includes neurofilaments, mitochondria, and microtubules. The axon bundles are organized as fasciculi, commissures, and fibers linking brain regions. With disease or trauma, the cytoskeleton that has high anisotropy in healthy white matter, is disturbed and results in lower anisotropy (Arfanakis et al., 2002). In addition to this extracellular spaces between fibers will sequester fluid and provide space for water movement, also contributing to

anisotropy. Anisotropy is calculated in a within voxel basis and is expressed as a fraction—fractional anisotropy (FA) for a ROI (Pierpaoli and Basser, 1996). The way to conceptualize the information on FA is to view it geometrically (see **Figure 5C**). The tensor effectively fits the angular variation of the diffusion direction values to the shape of a 3D ellipsoid. Anisotropic diffusion within white matter is modeled with an elongated ellipsoid, indicating directionality of the water molecules. The 3 directions of eigenvectors are diagonalized and averaged to obtain the FA value (Mukherjee P et al, 2008). A tract or structure with high FA is indicative of restricted diffusion typically in a normal organized tissue. The FA of CSF is near 0 and can approach a value of 1 in the corpus callosum. DTI studies in alcoholism are revealing abnormally low FA in white matter brain structures, in particular the corpus callosum, implying damage to fiber/tract structure (**Figure 6**).

In DTI, water diffusion, meaning the thermal motion of water molecules is also measured. The diffusion constant relates to the average displacement of a molecule over an area to the observations of time. The mean diffusivity (MD) is the diffusion constant measured in a clinical state, reflecting the limitation that in vivo diffusion cannot be separated from other sources of water mobility, such as active transport, flow along pressure gradients and changes in membrane permeability (Mukherjee P et al, 2008). Therefore, MD is characterized by the overall mean-squared displacement of molecules (average ellipsoid size) and the overall presence of obstacles to diffusion, where each of the three axes ADCx, ADCy, ADCz and the average diffusivity is (ADCx + ADCy + ADCz)/3=MD White matter tracts with tightly packed coherently oriented fiber bundles hinder water displacement perpendicular to the direction of the fibers, resulting in larger

apparent diffusion coefficient (ADC_x) values parallel to the tracts rather than orthogonal to them (Chenevert TL et al, 1990). In the healthy human brain the MD in white matter is 0.64-0.71 x 10^{-3} mm^2/s and a variable rate of decline in the MD value reflect speed of growth, maturation and an increase in axonal integrity (Mukherjee et al, 2001; Hermoye L et al, 2006). The conventional explanation for reduced MD is membrane permeability changes, better axonal integrity, cellular swelling and decreased volume but increased tortuosity of the extracellular space (Duong et al, 1998). Reduction of radial diffusivity may be attributed to myelination as this modulates the diffusion anisotropy originating from cell membranes by creating an additional barrier (Beaulieu, 2002). Furthermore, the lack/disruption of myelin sheath has been found to increase radial diffusivity without affecting axial diffusivity (Song et al., 2002).

The primary eigenvector is important for WM tracking because this vector indicates the orientation of the axonal fiber bundles. Therefore, it is also known as "axial diffusivity" (AxD) and is specifies the rate of diffusion along the orientation of the fibers. The second and third eigenvectors are orthogonal to the primary eigenvector, and their associated values give the magnitude of diffusion in the plane transverse to the axonal bundles. Hence, the mean of these two eigenvectors is also known as "radial diffusivity" (RD).

Structural brain imaging has provided clear evidence that long-term consumption of alcohol is associated with reductions in brain volume but fails to provide evidence of a connection to vulnerability of these tissues to damage. DTI can therefore provide visual depictions of white matter fiber systems, which can be measured with quantitative fiber

tracking. The advantage of quantitative fiber tracking is that DTI metrics are derived only from fibers identified in a region of interest.

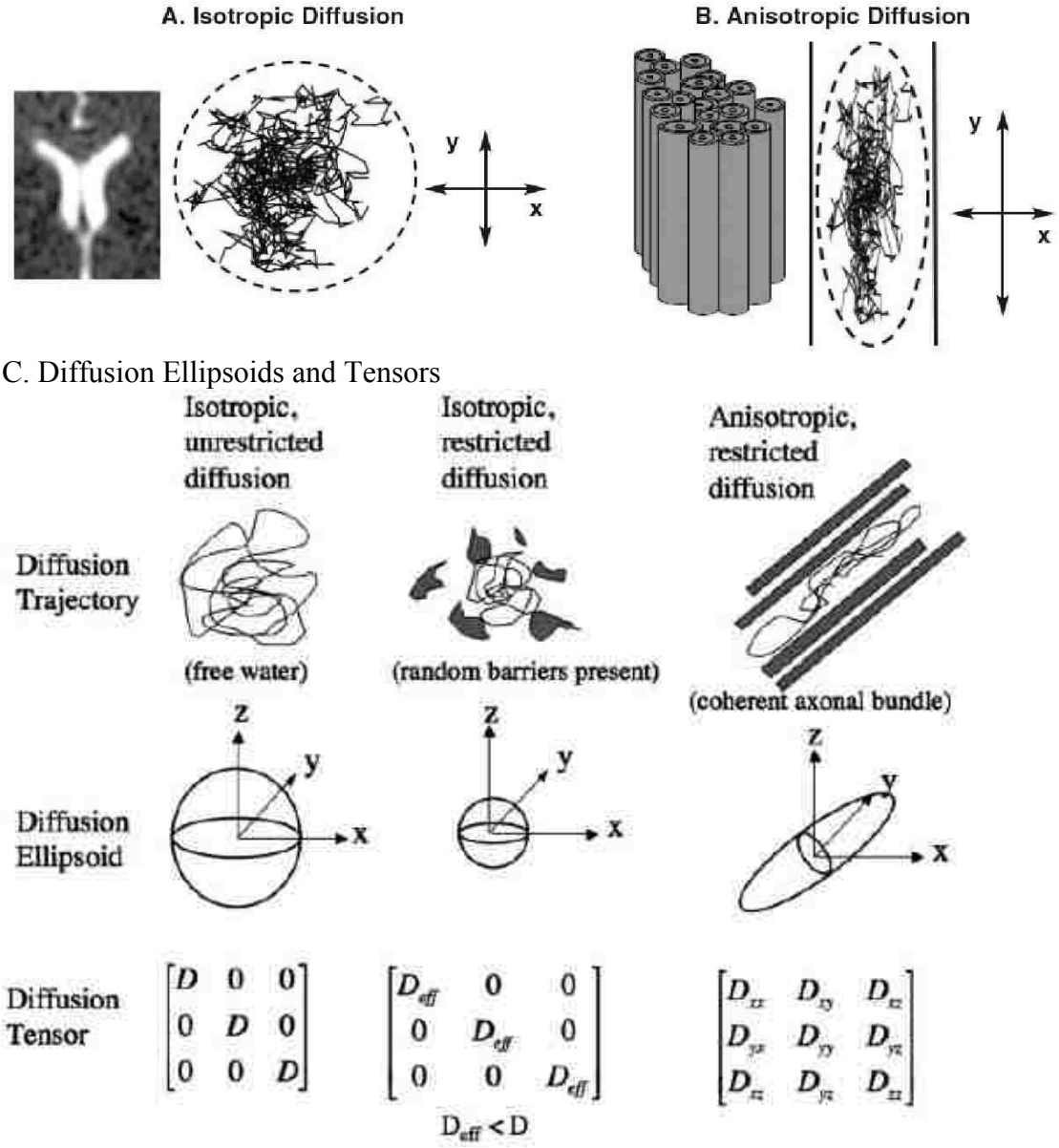

Figure 5. Isotropic and anisotropic diffusion. (A) Motion is unconstrained, i.e. the ventricles, diffusion is isotropic, meaning motion occurs equally and randomly in all directions. (B) Motion is constrained, i.e. white matter tracts, diffusion is anisotropic, meaning that motion is oriented more in one direction than another (Rosenbloom et al, 2003). (C) The diffusion ellipsoids and tensors for isotropic unrestricted diffusion, isotropic restricted diffusion, and anisotropic restricted diffusion (Mukherjee P et al, 2008).

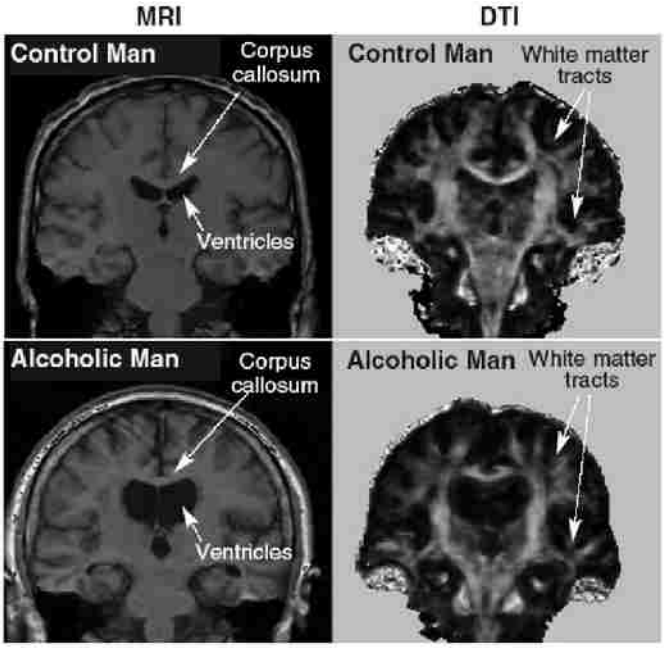

Figure 6. Coronal images display the MRI and DTI studies of a healthy man (upper) and age-matched alcoholic subject (lower). The MRI shows a thinner corpus callosum displaced upward by enlarged ventricles and on the DTI less delineation of white matter tracts in the alcoholic subject is visible (Pfefferbaum and Sullivan, 2003).

1.3.4 Neuroanatomical Damage in AD: Gray Matter

Neuroimaging has enabled longitudinal study of the examination of alcoholism's course through periods of drinking. Controlled studies have revealed evidence of alcohol-related brain structural and functional modifications—some permanent, some transient and some compensatory. In 1975, Tarter and colleagues suggested that prolonged alcohol abuse results in effects that are most pronounced in the anterior region of the brain, extending from the frontal lobe through the dorso-medial nucleus of the thalamus and associated basal regions. Both cortical gray matter (Fein et al, 2002) and white matter sustain widespread loss (Pfefferbaum et al, 1992). Alcohol-related volume deficits observed in the frontal lobes (Pfefferbaum et al, 1997), anterior hippocampus (Sullivan et al, 1995; Agartz et al, 1999), mammillary bodies and cerebellum (Shear et al,

1996), and corpus callosum (Hommer et al., 1996; Pfefferbaum et al., 1996). In this section I will provide a brief summary of the major findings for these brain regions.

The prefrontal cortex is the most complex and highly developed of the neocortical regions in the human brain. It functions as a massive association cortex with afferent and efferent connections to all other neocortical regions, as well as to the cingulate, limbic system and the basal ganglia. In 1998, Pfefferbaum and colleagues showed, in a 5-year longitudinal study, brain volume shrinkage in prefrontal cortex with additional loss in the anterior superior temporal cortex and lateral and third ventricle enlargement in alcoholics. Neuropsychological studies have reported selective alterations of frontal executive functions, such as planning or problem-solving ability, in neurologically normal alcoholic patients (Pishkin et al., 1985). Moderate neuronal loss has been reported in the frontal cortex and in the cingulate gyrus of alcoholic subjects (Kril and Harper, 1989). Quantitative morphometric studies show brain volume shrinkage that relates to a reduction in the volume of the white matter in the cerebral hemispheres rather than volume changes in the cerebral cortex. Harper et al (1985) showed a mean reduction of 4.6% in white matter volume, and de la Monte (1988) found a 6.1% to 17.5% reduction.

Major areas of the limbic system include the hypothalamus, amygdala, hippocampus, septal nuclei, and anterior cingulate gyrus. Functions of the limbic system include mediating learning and memory and contributing to emotions. These regions have essential roles in alcoholism (see **Figure 7**).

The amygdala (AMG) is a small almond-shaped structure deep inside the antero-inferior region of the temporal lobe that is partially controlled by the brain's dopamine system (Salgado-Pineda et al., 2005), and is an essential part of the brain’s reward and

emotion circuitry. It is a heterogeneous brain area consisting of 13 nuclei and cortical regions and their subdivisions. The amygdala connects with prefrontal cortex, the hippocampus, the septal nuclei, and the medial dorsal nucleus of the thalamus. This system responds to alcohol and produces feelings of pleasure when positive reinforcement occurs (Koob, 2003). Koob, 2003 describes that neuropharmacologic studies in animal models have provided evidence for neurochemical mechanisms in specific brain reward and stress circuits that become dysregulated during the development of alcohol dependence. There are multiple neurotransmitter systems that converge on the extended amygdala that become dysregulated during the development of alcohol dependence, including gamma-aminobutyric acid, opioid peptides, glutamate, serotonin, and dopamine. In addition, the brain stress systems may contribute significantly to the allostatic state. During the development of alcohol dependence, corticotropin-releasing factor may be recruited, and the neuropeptide Y brain antistress system may be compromised. These changes in the reward and stress systems are hypothesized to maintain hedonic stability in an allostatic state, as opposed to a homeostatic state, and as such convey the vulnerability for relapse in recovering alcoholics. It is well known that excessive chronic drinking is accompanied by a broad spectrum of emotional changes ranging from apathy and emotional flatness to deficits in comprehending emotional information, but their neural bases are poorly understood. In a recent study using fMRI, Marinkovic et al, 2009, observed clear evidence of differences between abstinent long-term alcoholics and non-alcoholic controls in amygdala activation to emotional materials, suggesting that the amygdala can control or affect the outcome of addiction to alcohol.

The hippocampus (HPC) is a three-layer sheet of neurons located on the floor of each lateral ventricle within the temporal lobes and adjacent to the amygdala. As part of the limbic system, it is involved in motivation and plays a central role in memory formation (Ramsey et al, 2002). The HPC consists of interfolded layers of the dentate gyrus and cornus ammonis, which is continuous with the subiculum, which in turn merges with the parahippocampal gyrus. It is a well-known fact that alcohol is a teratogen affecting the hippocampal development and function Structural neuroimaging studies have demonstrated a reduction of hippocampal volume in alcoholics (Agartz et al, 1999; Pfefferbaum and Sullivan, 2002). One study demonstrated hippocampal volume reduction in heavy, chronically drinking, alcohol dependent subjects compared with non-alcoholic controls (Makris et al, 2008, see **Figure 8**). In 1997, Harding et al showed the loss of hippocampal volume in humans and attributed it to changes in white matter and in 2002, Roberto et al, showed that chronic alcoholism in the rat, significantly impairs hippocampal long term potentiation.

The thalamus serves as a major junctional complex that modulates input to the PFC (Nauta, 1971, 1972). Volume shrinkage in the thalamus (Sullivan et al, 2003), caudate and putamen occurs in alcoholics. Sullivan et al (2003) has also observed significant volume shrinkage in the nucleus accumbens of recently drinking alcoholics relative to subjects that were sober for a month.

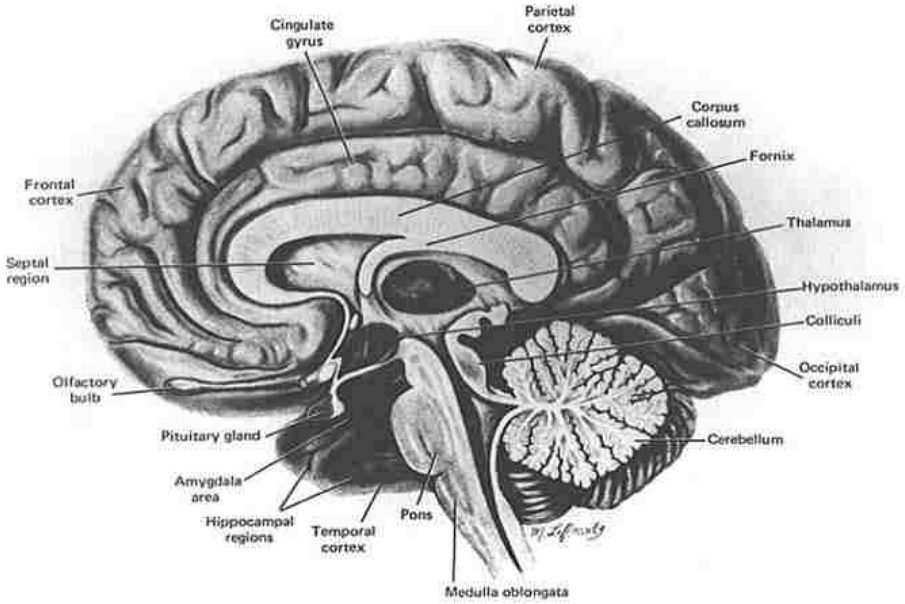

Figure 7. Cross section of the human brain. Cortical, limbic, and cerebellar regions are highly vulnerable to alcoholism damage. Among the regions discussed presently are the amygdala, hippocampus, and thalamus (Oscar-Berman and Bowirrat, 2005).

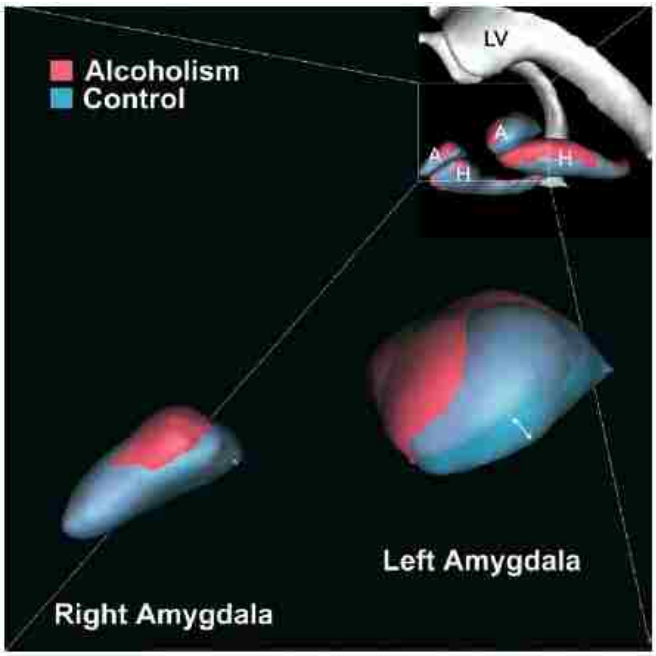

Figure 8. The hippocampus and amygdala are shown as 3D isosurfaces. The average shape of the HPC and AMG of control subjects is coregistered and superimposed on the average shape of these structures in the subjects with alcoholism. As seen in the figure there is a more pronounced volume reduction in the left amygdala (Makris N et al., 2008).

1.3.5 Neuroanatomical Damage in AD: White Matter Tracts and Bundles

Structural MRI studies have shown that white matter subadjacent to the cortex, corpus callosum (Hommer D et al., 1996; Pfefferbaum A et al., 2006; Estruch R et al., 1997), and pons (Sullivan EV et al. 2001, 2006) is affected in terms of macrostructural volume deficits in uncomplicated alcoholism. MRI studies also show thinning of the corpus callosum in older alcoholic men (Pfefferbaum et al., 1996) and a higher incidence of large white matter hyperintensities (WMHIs) than matched controls (Jernigan et al, 1991; Pfefferbaum et al., 1992). WMHI can reflect several processes—including edema, demyelination, gliosis or excess cerebro spinal fluid (CSF). MRI studies have reported that the greatest cortical and sub-adjacent white matter loss occurs in the frontal lobes (Pfefferbaum et al., 1997). Initial studies using DTI in uncomplicated alcoholism have reported abnormally low anisotropy in regionally defined white matter of alcoholic men (Pfefferbaum et al., 2000) and women (Pfefferbaum and Sullivan, 2002). In these studies both men and women showed deficits in the callosal genu and centrum semiovale, and men showed additional deficits in the callosal splenium (see Figure 9). The damage of the cerebral cortex in chronic alcoholism also results in corpus callosum atrophy with a decrease in area, thickness of genu, and splenium (Oishi et al., 1999). The corpus callosum is reduced in thickness in alcoholics when compared to age- and sex- matched controls (Harper and Kril, 1988; Pfefferbaum et al., 2000). A survey of multiple brain fiber systems revealed a differential pattern of alcoholism's effect on regional FA with functional consequences attributable in part to compromised fiber microstructure with signs of myelin degradation (Pfefferbaum, et al., 2008). In Pfefferbaum's 2008 study 11 major white matter bundles were assessed using DTI in 87 alcoholics and 88 healthy

controls. Alcoholism affected FA and MD of several fiber bundles including the frontal forceps, internal and external capsules, fornix, and superior, cingulate and longitudinal fasiculi. In conclusion, these previous studies and results indicating an interruption of intra- and inter- voxel coherence of white matter tracts provides *in vivo* evidence that alcoholism disrupts white matter microstructure.

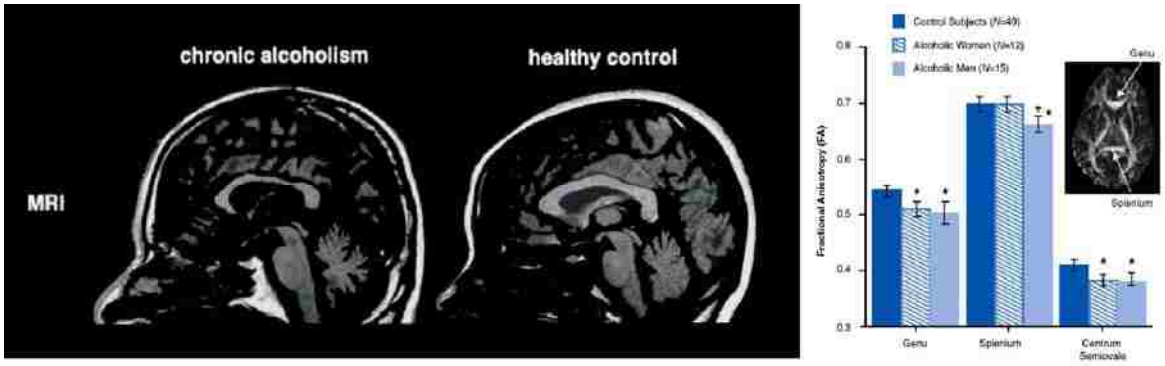

Figure 9. White matter damage. (A) T1-weighted image of MRI in a chronic alcoholic (>83ml alcohol consumption everyday for 10 years) and a healthy control (Oishi M et al. 1999). (B) Alcoholic subjects, men and women, have lower fractional anisotropy (FA) in the genu of the corpus callosum, the centrum semiovale. Male subjects also have a lower FA for the splenium. (Rosenbloom MA et al., 2003).

1.4 Genetics and Alcohol Dependence

1.4.1 Genetics: Alcoholism and Candidate Genes

Genes are the biological toolbox with which one negotiates the environment (Hariri and Weinberger, 2003). Numerous questions come to mind with such a statement: How does a gene affect brain structure and information processing with regard to certain personality traits or cognitive abilities, and how does it increase risk for a neuropsychiatric disorder? How many genes contribute to a particular complex behavior, clinical symptom, or disease? What genetic overlap exists across behaviors, symptoms and diseases? How large are the effects of candidate genes on particular brain functions?

The "candidate gene association" approach has been a popular strategy for attempting to answer all of the questions above. Genetic associations are a test of a relationship between a particular phenotype and a specific allele of a gene. This approach begins with a selecting of biological aspect of a particular condition or disease, then identifying the variants in genes thought to impact the candidate biological process, and next searching for evidence that the frequency of a particular variant is increased in populations having the disease or condition. A significant increase in allele frequency in the selected population is evidence of an association. When a particular allele is significantly associated with a particular phenotype, it is potentially a causative factor in determining that phenotype. There are, however, caveats to the design and interpretation of the association studies. Among them are linkage disequilibrium, ancestral stratification and whether a particular genetic variation observed is of major relevance to a distinct human condition. (Glabus, 1994)

1.4.2 Strategies for Gene Identification in AD

Molecular genetic techniques were defined by the introduction of polymerase chain reaction (PCR) in 1983 (Saiki, et al, 1988) which replicated and analyzed DNA sequences and their structure. Specific stretches of DNA that are closely linked to the genes that underlie the trait in question identifies Quantitative Trait Loci (QTLs) and alleles, individual variations of DNA in a distinct region, constitutes a polymorphism. Polymorphisms are used for genetic analysis: DNA sequences in non-coding DNA regions with repeats that vary in frequency are microsatellite markers. The exchange of single nucleotides in the DNA is the origin of single nucleotide polymorphisms (SNPs) that are found in coding or non-coding DNA.

There are numerous and sufficient experimental ways of combining molecular methods and the epidemiological data to detect the contribution of genes to AD- linkage studies and association studies.

Quantitative Trait Loci

Inheritance of a phenotypic characteristic that varies in degree and can be attributed to the interactions between two or more genes and their environment are quantitative trait loci (QTLs) or stretches of DNA that are closely linked to the genes that underlie the trait in question. QTLs can be molecularly identified to help map regions of the genome that contain genes involved in specifying a quantitative trait. Initially, a QTL is localized by a genomic scan to a large chromosomal region. The localization is done by linkage analysis using population data on the co-segregation of phenotypes in families. After a QTL is localized to a specific region that chromosomal region is finely mapped and saturated with additional genetic markers.

Genetic analysis of brain structure is complex, involving genetic and environmental components and interactions. Recent studies have pointed to specific genes that have significant influence on variation in the human brain (Evans et al, 2005) but the significance is not quantified.

Single Nucleotide Polymorphisms

A SNP ("snip") is a source of variance in a genome caused by a single base mutation in the DNA sequence. It is the most simple form and most common source of genetic polymorphisms in the human genome (90% of all human DNA polymorphisms). Specifically, there are two types of nucleotide base substitutions resulting in SNPs; a transition substitution that occurs between purines (A, G) or between pyrimidines (C, T)

which constitutes two thirds of all SNPs; and a transversion substitution that occurs between a purine and a pyrimidine. SNPs are not uniformly distributed over the entire human genome, neither over all chromosomes and neither within a single chromosome. There are one third as many SNPs within coding regions as non-coding region SNPs. A SNP in a coding region may have two different effects on the resulting protein either a synonymous/silent mutation or non-synonymous substitution in the amino acid sequence. A SNP in the genetic profile are labeled as the frequent allele (A/A), the heterozygous allele (A/B) or the rare allele (B/B).

In this causal chain from gene to protein to mental function, brain activity is the likely key intermediary that can help bridge the gap between genes and behavior. As mentioned above, a polymorphic site in a gene can encode different gene products and these proteins may function differently, a SNP can have a direct effect on the function of the gene in which it is located. A variant may result in an amino acid change or may alter exon-intron splicing, thereby directly modifying the relevant protein, or it may exist in a regulatory region, altering the level of expression or the stability of the mRNA. This difference in molecular function could be reflected in different levels of localizations of neural activity during a particular disease state, in this case alcohol dependence; these can be measured using neuroimaging techniques and quantified as morphological changes in structure and function. In particular, a relationship between genetic variation and a brain-based phenotype in the absence of a brain-behavior association can be informative. This sort of finding can identify genetic differences on neural processes (efficiency of tracts) that cannot otherwise be observed directly. Overall, it is estimated that each person is heterozygous for 24,000 –40,000 substitutions that alter amino acid (Cargill et al, 1999).

These variants are likely to occur as rare alleles (Sunyaev et al, 2000), with most non-synonymous coding region SNPs having allele frequencies below 5% (Halushka et al, 1999). But there are non-synonymous coding region SNPs that are both common and associated with diseases. This relation forms the basis and motivation for the identification and genotyping of SNPs, which forms the foundation for linkage and association studies described below.

Linkage Studies

The genomes of all individuals within a family of affected members are scanned and multiple microsatellite markers or SNPs that may be associated with a specific disease through out all chromosomes. If the tested markers are in close in proximity to the gene of relevance to the disease, affected siblings are expected to share more identical alleles, resulting in a "marker" for the disease. Parametric, for monogenetic diseases, and non-parametric, for complex diseases such as AD, statistical analysis tests can be used to evaluate a significant linkage between the gene and disease. The advantage is that linkage studies can be used to systematically screen the entire genome.

Association Studies

This study design aims to analyze whether a single gene and its polymorphic structure affects the specific disease involving a sampling strategy of unrelated individuals. These tests are dependent on the sequence variant in question having a true functional effect on the phenotype, or being in linkage disequilibrium (LD) with a functional variant. Here, LD represents the statistical correlation between two sequence variants due to a shared history and, thus, is a stochastic phenomenon. The candidate gene analysis tests if certain alleles of the gene are associated to a disease, a trait or

endophenotype. A "candidate gene" is one whose function is related to the pathophysiology of the disease, or the gene lies in a chromosomal region that has already been linked to the disorder by linkage analysis (Dick DM and Foroud T, 2002). In the pathophysiology of AD multiple neurotransmitter systems are involved and thus numerous genes are stated as candidate genes. For further analysis a population based study is chosen. In this case the polymorphisms of two defined groups are compared with each other. In the genetic research of AD these two groups could include a low AD in one group versus high AD in the other. With multiple genes are involved in the pathogenesis of AD and the effects of a single gene are more than likely to be small, large sample sizes are needed to detect such genes.

Association studies of quantitative endophenotypes, like neuroimaging measures, usually involve simple tests for differences in means between marker genotypes, typically a SNP (Glahn et al, 2007).

1.4.3 Identified Candidate Genes in AD

Despite the complications mentioned in identifying genes involved in complex disorders, recent progress has identified specific genes involved in the predisposition to AD (see **Figure 10**). In 2007, Rodd and colleagues used a comprehensive translational approach for identifying candidate genes for alcoholism. The approach cross-matched animal model brain gene expression data with human genetic linkage data, as well as human tissue data and biological roles data, a method called convergent functional genomics (CFG). A comprehensive microarray analysis of gene expression data from five brain regions (frontal cortex, amygdala, caudate-putamen, nucleus accumbens and hippocampus) revealed identification of high probability candidate genes, pathways and

mechanisms for alcoholism (see **Figure 11**). Specifically, the data revealed that alcohol has pleiotropic effects on multiple systems. Pleiotropy occurs when a single gene influences multiple phenotypic traits and a new mutation in the gene may have an effect on some or all traits simultaneously. Consequently, a new mutation in the candidate gene may have an effect on some or all traits simultaneously. Pathways identified by Rodd et al included cell adhesion signaling, iron-heme metabolism, cardiovascular regulation, stress response, and cell proliferation. SNPs that have consistently associated with AD are polymorphisms in the alcohol metabolizing enzymes such as the alcohol dehydrogenase (ADH) class I isozymes (Shen et al, 1997).

Several lines of evidence also implicate γ-aminobutyric acid (GABA), the major inhibitory neurotransmitter in the central nervous system, is involved in many if the behavioral effects of alcohol, including withdrawal signs and ethanol preference (Grobin et al., 1998). Most of the $GABA_A$ receptor genes are organized into clusters on chromosomes 4, 5 and 15 and have emerged from numerous genome wide linkage scans of AD (Long et al., 1998; Covault, et al., 2004). Specifically, a systematic investigation of markers identified a significant association of multiple SNPs between a cluster on chromosome 4 and alcohol dependence and it's electrophysiologic endophenotype (Edenberg et al, 2005).

Opioidergic neurotransmission has been implicated in the reinforcing effects of several drugs of abuse, including AD (Dick and Bierut, 2006). Specifically, the gene coding for the opioid receptor (OPRM1) displays functional polymorphisms and a number of studies have reported an association between OPRM1 and substance dependence (Wagner et al., 2004).

Another gene recently implicated in association with alcoholism is a cholinergic muscarinic receptor, CHRM2, pointing to a region on chromosome 7 when identified during linkage analysis. An association with CHRM2 was also observed with electrophysiologic endophenotypes, an example of how endophenotypes lead to gene identification and associate to a diagnosis.

The dopamine system is known to play an important role in reward behavior and the effects of alcohol are mediated through this pathway in the mesolimbic pathway. Specifically, systemic genotyping across the DRD2/ANKK1 region suggests evidence of an association between SNPs in the region and severe alcohol dependence and antisociality (Dick and Bierut, 2006).

Genes involved in the regulation of the serotonin system are also candidates for involvement in the AD pathophysiology. Serotonin (5-HT) is involved in many aspects of alcohol consumption, abuse, and dependence. The gene encoding the 5-HT transporter (5-HTT) exhibits a functional polymorphism in which the shorter allele has lower transcriptional efficiency. A meta-analysis of this variant demonstrated a significant association between AD and the short allele (Fein et al, 2005).

Current research focuses on genes identified in association with alcohol dependence in the context of several major neurobiological pathways including alcohol metabolism and neurotransmitter systems.

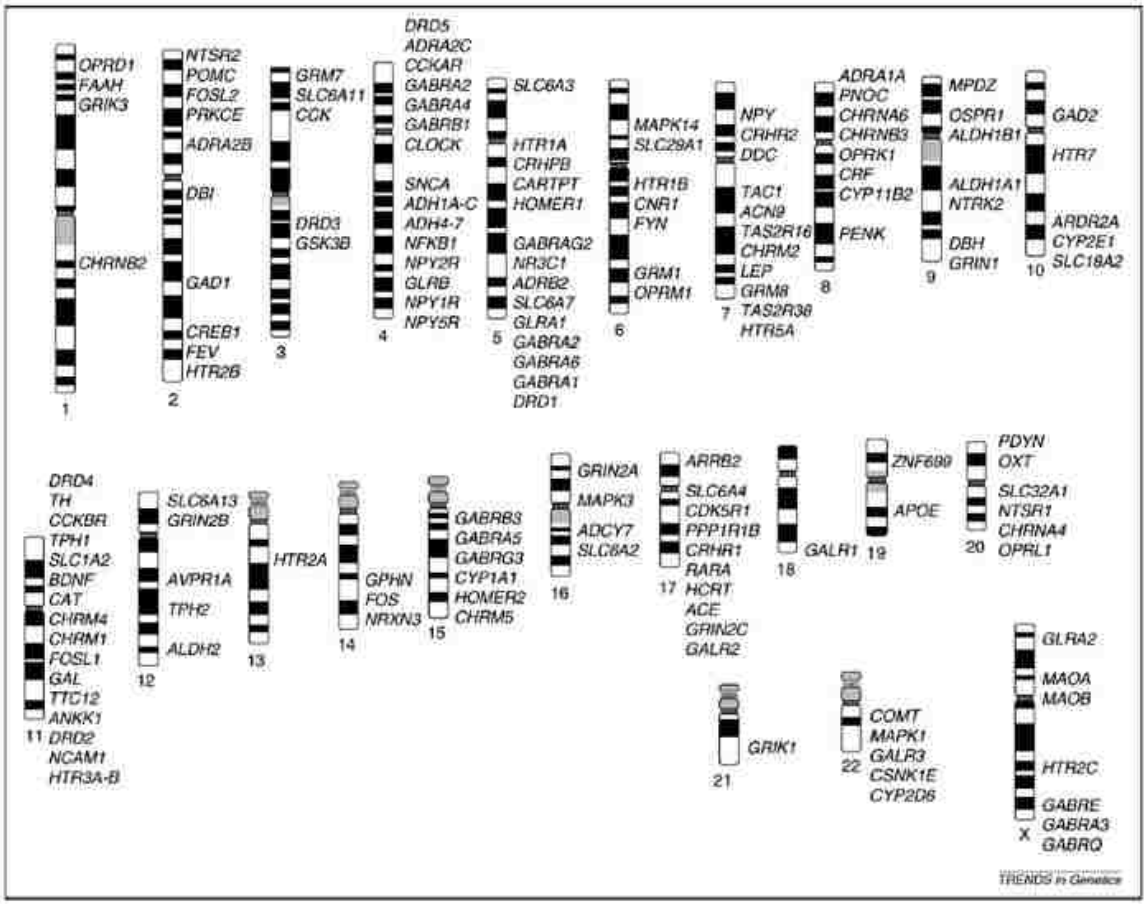

Figure 10. List of candidate genes involved in AD and alcohol related phenotypes. The list was compiled from published reports of candidate genes in human studies and the list of candidates on the 'addictions' array chip (Hodgkinson CA et al, 2008). Human chromosome ideogram from Dept. of Pathology, Univ. of Washington (www.pathology.washington.edu) (Kalsi G et al., 2008).

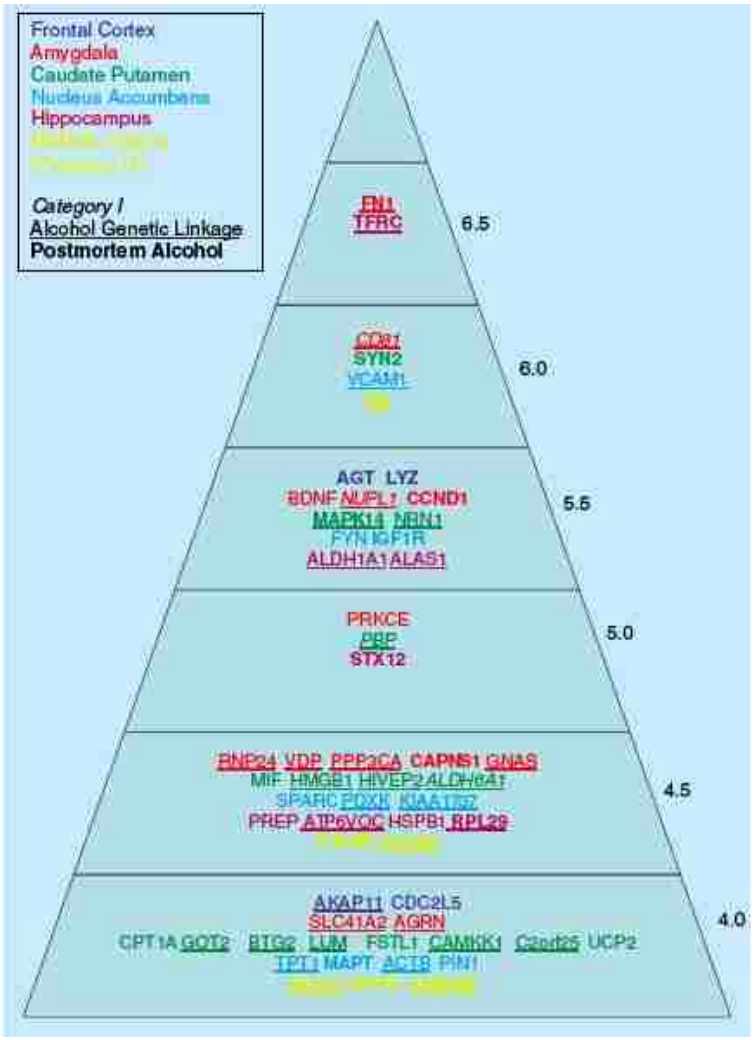

Figure 11. Top candidate genes. Pyramid generated by the tabulation of independent converging lines of evidence, the CFG method. (Rodd ZA et al., 2007).

CHAPTER 2: RESEARCH PROPOSAL

2.1 Rationale

Chronic alcoholism has been associated with global changes in brain morphology and is a complex, multi-factorial disorder resulting from the interplay between genetic and environmental factors. Chronic ingestion of alcohol adversely impacts brain systems involved in cognition and alters sensitivity to the rewarding effects of alcohol. This breakdown of the "reward cascade," includes insensitivity to natural rewards, increased sensitivity to alcohol and repeated cycles of abuse and eventually, an alcohol use disorder (AUD). A well-known target of damage is the frontal cortex of the brain and the circuitry of the mesolimbic pathway, linking the thalamus, the caudate putamen, the nucleus accumbens, the amygdala, and the hippocampus—the seat of the modulation of reward and punishment in addiction (see **Figure 12**). The cortical and sub-cortical limbic aspects are connected and modulated by several white matter tracts, specifically the cingulum bundle (gyrus and hippocampal aspects), the uncinate fasciculus, the inferior fronto-occipital fasciculus, the inferior and superior longitudinal fasciculus, the forceps minor and major, the anterior thalamic radiation and the corticospinal tract (see **Figure 13**). Furthermore, these combined cortical and sub-cortical regions overlap brain regions involved in memory, emotion, and reinforcement, which are adversely affected by damage to gray matter regions and/or by degradation of interconnecting white matter tracts. This damage can be traced using non-invasive in vivo neuroimaging techniques such as Magnetic Resonance Imaging (MRI) and Diffusion Tensor/ Diffusion Weighted Imaging (DTI/DWI) which characterizes neuronal dysfunction. Previous researchers have reported alcoholism related damage in several cortical and sub-cortical structures

using MRI and previous DTI studies have shown several damaged white matter tracts in alcoholic subjects seen by widespread low fractional anisotropy (FA) values (Brewer and Perrett, 1971; Cala et al, 1985; Pfefferbaum et al, 2004; Pfefferbaum et al, 1992; Agartz et al, 1999; Pfefferbaum et al, 2008).

AD is a complex disorder with multiple genetic backgrounds. The susceptibility genes that are the focus of the present study, were chosen because they are known to encode for underlying mechanisms that are linked to the pathophysiology of alcoholism. These postulated candidate genes and genetic studies of AD examine the metabolism of alcohol and the dopaminergic, GABAergic, glutamergic, opioid, serotonergic and cholinergic neurotransmitter systems. Genes typically have multiple functional polymorphisms and affect neural networks globally, not just isolated brain regions and only alcohol metabolism and neurotransmitter systems. For this reason, several SNPs in genes involved in growth and myelination have been chosen to focus on morphological changes in the cortical and subcortical regions of the brain involved in alcohol dependency. The combination of neuroimaging data (which may represent candidate endophenotypes or disease vulnerability markers of AD) with genetic information appears to be a valuable way to study a particular subset of polymorphisms which may have functional consequences. Recent studies demonstrate that specific polymorphisms in genes associated with myelination and synaptic plasticity are associated with subtle alterations in the white matter connectivity and structures of the cortical and sub-cortical regions (Agartz et al., 1999). Furthermore, some of these polymorphisms correlate with alterations in sub-cortical structures of the limbic pathway associated with cognitive

dysfunctions and symptoms of alcoholism (Puls et al., 2008). These findings suggest that these specific SNPs may influence the deleterious effects of alcohol on brain structure.

Studying a group of anatomic regions, which are components of structural and functional circuits, is an important avenue in identifying a biomarker for a disease. Here we will use fiber tracking to examine the variation in the effects of low and high alcohol dependence on fiber quality of multiple major association, projection tracts and structures involved in vulnerability to the effects of chronic alcohol use. It has been previously reported that long-term alcohol consumption leads to degeneration of white matter and grey matter structures in cortical and sub-cortical regions of the brain. Previous research has shown a reduction of hippocampal volume in alcoholics (Kurth et al., 2004) and changes in white matter (Harding et al., 1997). Quantitative morphometric studies show brain volume shrinkage that relates to a reduction in the volume of the white matter in the cerebral hemispheres rather than volume changes in the cerebral cortex. MRI studies have reported that the greatest cortical and sub-adjacent white matter loss occurs in the frontal lobes (Pfefferbaum et al., 1997). However, the characteristics of morphological changes within most of the structures in the sub-cortical regions, including the limbic loop, specifically, have not been reported and are poorly understood. In addition to previously published data on the hippocampus and amygdala, morphological changes in the caudate-putamen and the nucleus accumbens have yet to be quantified. As for white matter tracts between and around these primary structures of the limbic pathway the cingulum bundle (gyrus and hippocampal aspects), the uncinate fasiculus, the inferior fronto-occipital fasciculus, the inferior and superior longitudinal fasciculi, the uncinate

fasiculus, the forceps minor and major, the anterior thalamic radiation and the corticospinal tract must also be quantified in alcohol dependent individuals.

Like brain regions, genes do not operate in isolation. In lieu of this, analysis of connections among regions can be used to identify brain networks that are affected by genetic variation. Regions of interest (ROIs) are identified based on a priori hypotheses and brain alterations assessed by MRI or DTI. Individuals are then genotyped for candidate alleles yielding two or more different genotype groups to compare. By examining the strength of correlation between the morphological changes (from Specific Aim 1) and the genetic profiles of the alcohol dependent individuals, we can indicate what genotype influences certain phenotypes, predisposing certain tissue to early damage or resiliency. The ultimate directive is to integrate genes and their products with brain-based intermediate/structural phenotypes of clinical disease, alcoholism, producing a biomarker or susceptibility marker for disease progression.

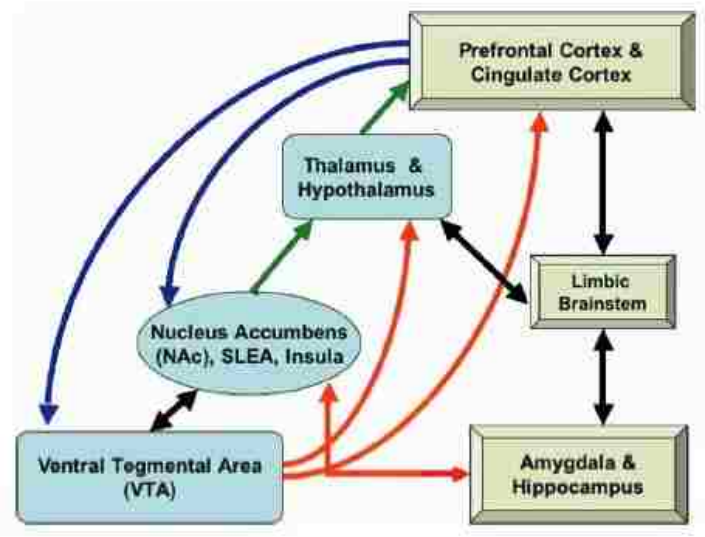

Figure 12. Brain regions involved in the extended reward system. Prefrontal and cingulated regions connect to the nucleus accumbens (NA), the midbrain ventral tegmental area (VTA), and reciprocally with other limbic system structures (amygdala and hippocampus). The VTA projects to the NA, to the thalamus and hypothalamus and to the prefrontal cortex (Makris N et al., 2008).

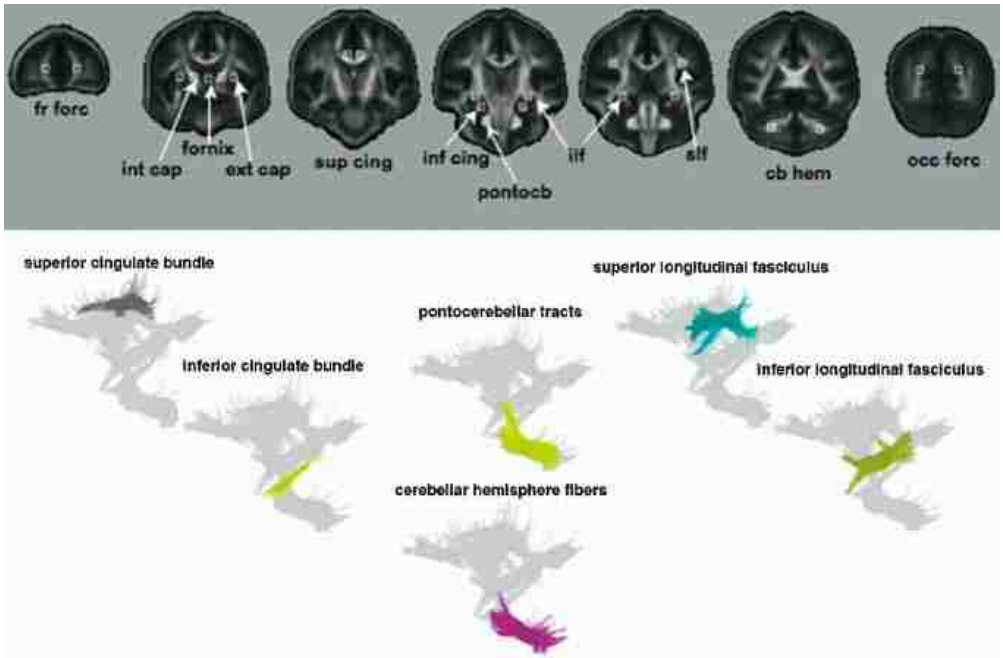

Figure 13. DTI target locations of 6 of the 11 bilateral fiber bundles identified on coronal images of the population-average FA template and representative colorized fiber bundles superimposed on a composite saggital image of six fiber bundles (Makris N et al., 2008).

2.2 Hypothesis And Specific Aims

The experiments in this proposal utilized MRI to determine whether alcohol dependence is associated with structural brain changes and to determine whether specific SNPs, previously linked to structural changes, are associated with the brain changes that may result from chronic exposure alcohol. The hypotheses and specific aims are:

2.2.1 Hypotheses

We hypothesize that a level of alcohol dependence is associated with alterations in gray matter volume and white matter coherence and that specific SNPs in genes involved in growth & plasticity and myelination will be associated with the alterations in gray matter volume and white matter coherence.

2.2.2 Specific Aim 1

Determined whether white matter connectivity and cortical and sub-cortical grey matter volumes are different in individuals with high levels of alcohol dependence versus those with low levels of dependence. Their scale score on the Alcohol Dependence Scale behavioral test determined the low and high alcohol dependent individuals. Low and high alcohol dependent subjects had been scanned in a 3-Tesla scanner to obtain whole brain MRI images. We used DTI fiber tractography software to measure tract length and volume and analyzed using IDL software to determine white matter tract integrity/coherence of low and high alcohol dependent subjects. The obtained fractional anisotropy (FA) measurements should show greater demyelination in the cingulum bundle (gyrus and hippocampal aspects), the uncinate fasiculus, the inferior fronto-occipital fasciculus, the inferior and superior longitudinal fasciculus, the uncinate fasiculus, the forceps minor and major, the anterior thalamic

radiation and the corticospinal tract regions of high alcohol dependent subjects versus low alcohol dependent subjects. We also determined changes in volume of cortical and sub-cortical structures—the thalamus, the nucleus accumbens, the caudate-putamen, the amygdala, and the hippocampus, in low versus high alcohol dependent subjects, using the same MRI whole brain scans and FreeSurfer software for analysis.

2.2.3 Specific Aim 2

Tested whether single nucleotide polymorphisms (SNPs) in genes related to myelination and growth are associated with differences in the structural measures described in Specific Aim 1. For these association studies we used genes with SNPs that have been previously known to show dysfunction in disease states such as alcoholism, schizophrenia, and depression. These predisposed genes for white matter tracts are SNPs in Myelin Associated Glycoprotein (MAG) functionally known to initiate and maintain the myelin sheath and Oligodendrocyte Transcription Factor 2 (OLIG2), a transcription factor of myelin-specific genes. The predisposed genes for cortical and sub-cortical structures are SNPs in Brain Derived Neurotrophic Factor (BDNF), Nuclear Factor of Kappa Light Polypeptide Gene Enhancer in B-cells 1 (NFKB1) and Neurotrophic Tyrosine Kinase, Receptor, Type 2 (NTRK2), all involved in development/growth, immune response, and learning and memory. The genetic profiles of low and high alcohol dependent subjects were obtained in reference to the specified SNPs using BeadStudio. The percentages of frequent, heterozygous and rare alleles were mapped with FA and MD values of white matter coherence and cortical and sub-cortical grey matter volumes (obtained in Specific Aim 1). An association analysis, with the integration of an alcohol dependent individuals' genetic information with their white and

grey matter damage, was performed to uncover an invariant and interactive relationship between a SNP predisposing tissue to damage or an exacerbation or protection of this tissue due to an endophenotype of alcohol dependence.

CHAPTER 3: RESEARCH AND EXPERIMENTAL METHODS

3.1 Introduction

In general, the volume, FA, MD, AD and RD values were obtained for ten major, well-documented, white matter tract bundles from low and high alcohol dependent individuals whole brain DTI images (n=36). The ten major ROIs tracked were the right and left of each of the following: the cingulum (gyrus and hippocampal aspect), the inferior fronto-occipital fasciculus, the inferior and superior longitudinal fasciculus, uncinate fasiculus, the forceps minor and major, the anterior thalamic radiation and the corticospinal tract. In addition to this, the volumetric measurements of nine cortical and subcortical structures—the cortex, thalamus, caudate, putamen, hippocampus, amygdala and accumbens were also obtained from the MRI full brain scan.

Candidate genes were then selected that had been previously indicated to show SNPs that are associated with a disease, such as schizophrenia, depression as well as alcoholism. The saliva samples from the low and high alcohol dependent individuals scanned provided the genetic profiles and SNP distribution. The genetic profiles were correlated with gray matter structures and white matter tracts showing significant differences to demonstrate an interaction of AD with a specific phenotype and genotype.

3.2 Demographics and Subject Selection

A total of 45 individuals will be included in the final cohort of 21-30 years of age for gray matter alterations and 36 individuals for white matter alterations. Participants were recruited through flyers, mass emails, and newspaper advertisements. Individuals were screened on the phone for specific drinking criteria (see **Table 1**). Individuals who met these criteria were scheduled for a subsequent screening session during which they

provided a DNA sample. The genotype profile was assayed using the procedures described below (Section 3.5 Genotyping). Because sample characteristics could increase error variability, the criteria for inclusion per participant were tightly controlled.

Table 1. Required criteria for inclusion in current study.

TABLE Criteria for Inclusion in Study
1. Age *21-30yrs*
2. Alcohol consumption at least twice per week and at least 3 drinks per occasion during 4 consecutive weeks prior to beginning the study;
3. Breath alcohol level of 0.00 at screening
4. No history of treatment for alcohol dependence
5. No history of severe alcohol withdrawal
6. No history of injury to the brain or brain related medical problems;
7. Not currently taking any psychotropic medications
8. No evidence of recent illicit drug use

In general, study participants were required to complete an Alcohol Use Disorders Identification Test (AUDIT) from which ADS (Alcohol Dependence Scale) number was assigned. The questionnaire discusses loss of behavior control, obsessive drinking style, psychoperceptual and psychosocial withdrawal, setting up a total number for level of dependence (see below for details: Individual Difference Measures). The population was then ranked and set into quartiles with the first quartile defined as low alcohol dependence, and the fourth quartile defined as high alcohol dependence. The 21-30 years of age cohort was used for this study and due to a lack of preprocessing by FSL of the MRI scans of several of the subjects, the cohort was split into gray matter and white matter subgroups for ease of analysis (**Table 2**).

Depression, taken into account by the BDI-II that was administered to the subjects, showed a significant correlation with ADS and was taken into account as a co-variant in all analyses (**Graph 1**).

Table 2. Demographics of ADS individuals between 21-30 years of age. Number of men and women is indicated as well as the average age. Average maximum drinks are within the past week. Quartiles were set based on an original date set of 192 individuals for ADS and BDI-II.

Demographics and Clinical Characteristics of Individuals Grey Matter Cohort

	Low ADS	High ADS
men/women	18/8	17/2
Age (years)*	24	26
Avg. Max Drinks	13	18
Smoker/Non-Smoker	7 19	9 10
ADS Score	5	18
BDI-II* Score	4	11

Q1=Low ADS (< 7)
Q4=High ADS (> 16)

Q1=Mild Depression (< 3)
Q4=Severe Depression (> 14)

*Avg. Age = 25y
**Beck's Depression Inventory-II

Demographics and Clinical Characteristics of Individuals White Matter Cohort

	Low ADS	High ADS
men/women	15/6	13/2
Age (years)*	23.9	25.9
Avg. Max Drinks	13.7	15.6
Smoker/Non-Smoker	5 16	6 9
ADS Score	5	17
BDI-II* Score	4	12

Q1=Low ADS (< 7)
Q4=High ADS (> 16)

Q1=Mild Depression (< 3)
Q4=Severe Depression (> 14)

*Avg. Age = 24.9y
**Beck's Depression Inventory-II

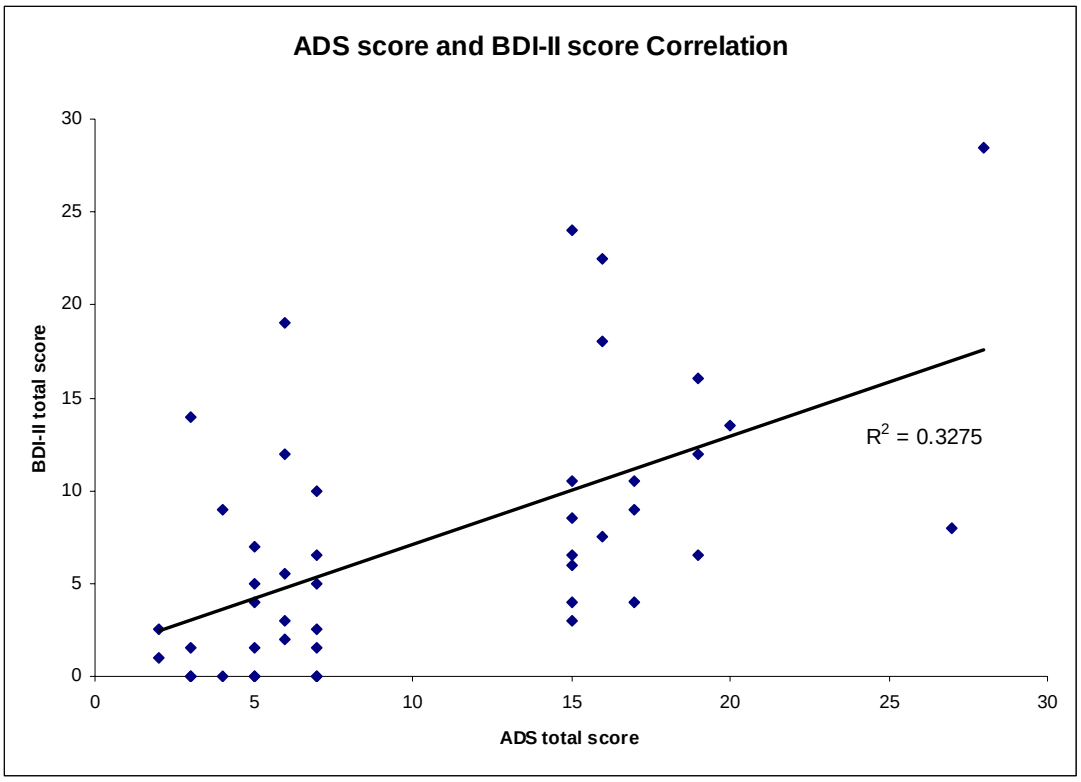

Graph 1. ADS scale score showed a significant correlation with BDI-II score. For this reason BDI was accounted for in all analyses as a co-variant.

3.2.1 Pre-Procedure

Drinking alcohol within 24 hours of the experimental session was prohibited. Each subject was tested using a breathalyzer to insure that no alcohol had been consumed and only subjects with a breath alcohol concentration of zero were allowed to participate in the scan session. After being tested for alcohol in the system (using a brethalyzer), subjects completed a *DSM IV interview for alcohol dependence* and the measures related to personality, drinking history, drinking problems, and family history of alcohol problems prior to scanning (Individual Difference Measures, see below for explanations: DQ, TLFB, TPQ, ADS, ADD and BDI-II). These tests were administered by Julie

McCollough and Flora Soto-Endicott. After the individual difference measures were completed (approximately 1.5 hours), the participant was prepared for the imaging part of the experiment. Once subjects were comfortable with the procedures they were inserted into the bore of the magnet for a high-resolution 3D spoiled gradient echo T1-weighted image that is collected for image registration and normalization.

Individual Difference Measures.

The following questionnaires were given to subjects who meet the criteria for inclusion in order to examine variables that may mediate or moderate the effects of alcohol.

1. A Demographics Questionnaire was used to collect information on age, sex, marital status, SES, occupation, income, education, and race/ethnicity.
2. A Time Line Follow Back (TLFB) interview (Sobell, 1980) was used to assess the quantity and frequency of drinking within the past month. The TLFB is a calendar assisted structured interview that provides the subject with temporal cues to increase the accuracy of recall. This interviewer-administered instrument has demonstrated test-retest reliability and validity (Sobell & VanderSpek, 1979).
3. The Tridimensional Personality Inventory (TPQ) is a 100-item questionnaire with good reliability and validity (e.g., Cloninger, 1987). The TPQ consists of three main scales that include Harm Avoidance, Reward Dependence, and Novelty Seeking.
4. The Alcohol Dependence Scale (ADS) was used to collect information on the severity of alcohol symptomatology within the last year. The ADS has proven to

be a valid and reliable measure of the severity of alcohol dependence (Skinner & Allen, 1982).

5. Alcohol Dependence Diagnosis was derived from the alcohol portion of the Structured Clinical Interview for DSM-IV, Nonpatient Version (SCID-IV).
6. The Beck's Depression Index-II is a 21-item self-report instrument intended to assess the existence and severity of symptoms of depression as listed in the American Psychiatric Association's Diagnostic and Statistical Manual of Mental Disorders Fourth Edition (DSM-IV; 1994). BDI has been used for 35 years to identify and assess depressive symptoms, and has been reported to be highly reliable regardless of the population. It has a high coefficient alpha, (.80) its construct validity has been established, and it is able to differentiate depressed from non-depressed patients (Beck et al, 1974).

3.3 Neuroimaging: Magnetic Resonance Imaging (MRI) and Diffusion Tensor Imaging (DTI)

The project utilized the facilities of the University of Colorado Brain Imaging and Drug Abuse Center. A GE 3T whole body MRI scanner provides an increased signal-to-noise ratio. With the increased signal-to-noise reduced pixel size and slice thickness were obtained. The enhanced gradient coils in the 3T scanner allow much faster acquisition time as well. Data was collected with a 64x64 matrix over a 200mm x 200mm FOV (in-plane resolution of 3.125mm x 3.125mm) with TE = 30 ms and TR = 2500 ms. Each data set consisted of 40 oblique slices, 3 mm thick with a 1 mm gap, angled parallel to the planum sphenoidale. The inversion-recovery SPGR sequence was used to acquire an axial 3-D anatomical image volume with optimal T1 contrast (TI=500 ms, FA=7

degrees, slice thickness=1.5mm, 256x256 matrix, 200mm x 200mm FOV, bandwidth =15.6kHz, 124 slices). The imaging time for the 3-D anatomical volume is about 10 minutes. The EPI images, the inversion-recovery SPGR sequence will be used to acquire an axial 3-D anatomical image volume with optimal T1 contrast (TI=500 ms, FA=7 degrees, slice thickness=1.5mm, 256x256 matrix, 200mm x 200mm FOV, bandwidth =15.6kHz, 124 slices). At the beginning of the experiment, a T1-weighted spin echo data set (40 axial slices of part head, matrix = 512 x 512) was acquired using the same slice angles, thickness, and gap as the EPI images. The purpose of the T1 spin echo data set is to optimize co-registration of functional images to volumetric T1 data set.

DTI data were acquired using a single-shot echo-planar imaging with sensitivity encoding (SENSE, parallel-imaging factor, 2.5) (Prussmann et al, 1999). The imaging matrix was 96x96 with a field view of 240x240 mm (nominal resolution, 2.5mm), zero filled to 256x256 pixels. Transverse sections of 2.5 mm thickness were acquired parallel to the anterior commissure/posterior commissure line. Diffusion weighting was encoded along 30 independent orientations (Jones et al, 1999) using *b*-value of 700mm2/s. The scanning time per dataset was approximately 6 min including 2 min image reconstruction delay (see **Figure 14** for general representation).

In general, DTI datasets were processed using the analysis software DTIStudio (developed and distributed by Johns Hopkins University, http://lbam.med.jhmi.edu). Images were first realigned using the AIR program (Woods et al, 1998), in order to remove any potential small bulk motions that occurred during the scans. The six elements of the diffusion tensor were calculated for each pixel using multivariate linear fitting. After tensor diagonalization, three eigenvalues and eigen vetors were obtained and

fractional anisotropy were calculated (Wakana et al, 2007). The eigenvector associated with the largest eigenvalue was used as an indicator for fiber orientation. DTIStudio, in the color maps, colors were assigned to specific directions of fibers: red, green and blue were right-left, anterior-posterior, and superior-inferior, respectively.

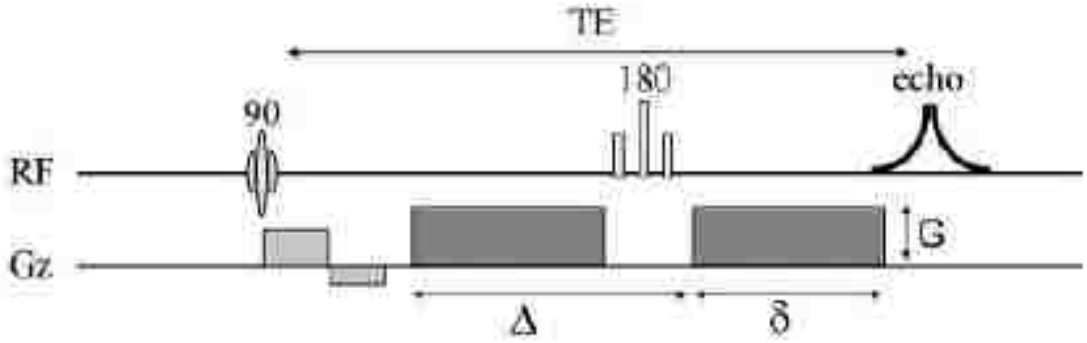

Figure 14. Pulse sequence diagram for a diffusion-weighted acquisition shows that 2 diffusion sensitizing gradients (dark gray) are added to a spin-echo sequence, 1 before and 1 after the 180 degree refocusing pulse. The diffusion weighting factor depends on the amplitude of the diffusion gradient (G), the duration of each diffusion gradient (δ), and the interval between the onset of the diffusion gradient before the refocusing pulse and that following the refocusing pulse (Δ). RF indicates the radiofrequency pulses and the readout of the water molecules, Gz, gradient pulses. (Mukherjee P et al., 2008).

3.4 Quantification

3.4.1 FreeSurfer and Gray Matter Volumes

FreeSurfer is an MRI brain imaging software package developed by the Athinoula A. Martinos Center for Biomedical Imaging at Massachusetts General Hospital with support from CorTechs Labs, Inc, La Jolla, CA. A functional tool in brain mapping, it facilitates the visualization of the functional regions of the highly-folded cerebral cortex. It contains both volume based and surface based analysis, which primarily use the white matter surface (Dale, A. M., B. Fischl, et al, 1999). FreeSurfer includes tools for the reconstruction of topologically and geometrically accurate models of both the gray/white

and pial surfaces, for measuring cortical thickness, surface area and folding, and for computing inter-subject registration based on the pattern of cortical folds. In addition to this, the software contains an automated labeling of 35 non-cortical regions.

With respect to preprocessing of the MRI data, the images in each participant's time series were motion corrected using MCFLIRT module of FSL (FMRIB's Software Library) package (created by Image Analysis Group in FMRIB, Oxford University). Images in the data series were **(1)** spatially smoothed with a 3D Gaussian kernel (FWHM = 6 x 6 x 6 mm^3), **(2)** intensity normalized for all volumes by the same factor and **(3)** temporally smoothed using a high-pass filter. The FEAT (FMRIB's Easy Analysis Tool) module of FSL package will be used for these steps and later statistical analysis. After statistical analysis for each subject's time series, statistical maps were warped into the common MNI stereotaxic space before random effect group analysis is performed. To do so, **(1)** An average EPI volume will be registered to a high resolution partial head volume taken at the same orientation and with an equal number of slices. **(2)** This same partial head volume will be registered to a high-resolution full head volume. **(3)** Last, this full head volume will be registered to an average brain in MNI space. Transformation matrices generated were used to register the final statistical results into the average MNI space. Coordinates were reported in both MNI and Taliarach space (T-space). This processing used the FLIRT (FMRIB's Linear Image Registration Tool) module of the FSL package.

The FreeSurfer processing stream is controlled by a shell script called *recon-all*. The script calls component programs that organize raw MRI images into formats easily usable for morphometric and functional MRI statistical analysis with the FS-FAST

package. Freesurfer uses a morphed spherical method to average across subjects for a GLM group analysis with the QDEC tool. FreeSurfer automatically segments the volume and parcellates the surface into standardized regions of interest (ROIs) that the Center for Morphometric Analysis has developed.

The volume-based stream is designed to preprocess MRI volumes and label subcortical tissue classes. The stream consists of five stages (fully described in Fischl, et al, 2002, 2004b). The first stage is an affine registration with Talairach space specifically designed to be insensitive to pathology and to maximize the accuracy of the final segmentation. This is followed by an initial volumetric labeling. The variation in intensity due to the B1 bias field is corrected. Finally, a high dimensional nonlinear volumetric alignment to the Talairach atlas was performed. After the preprocessing, the volume is labeled (see below). The volume-based stream has evolved somewhat independently from the surface-based stream. The volume-based stream only depends upon the skull stripping to create a mask of the brain in which the labeling is performed.

The final segmentation is based on both a subject-independent probabilistic atlas and subject-specific measured values. The atlas is built from a training set, i.e., a set of subjects whose brains (surfaces or volumes) have been labeled by hand. These labels are then mapped into a common space (Talairach space for volumes and spherical space for surfaces) to achieve point-to-point correspondence for all subjects. Note that a "point" is a voxel in the volume or a vertex on the surface. At each point in space, there exists the label that was assigned to each subject and the measured value (or values) for each subject. Three types of probabilities are then computed at each point. First, the probability that the point belongs to each of the label classes is computed. The second

type of probability is computed from the spatial configuration of labels that exist in the training set, which is termed the neighborhood function. The neighborhood function is the probability that a given point belongs to a label given the classification of its neighboring points. The neighborhood function is important because it helps to prevent islands of one structure in another at the structure edges. Third, the probability distribution function (PDF) of the measured value is estimated separately for each label at each point. For volume-based labeling, the measured value is the intensity at that voxel.

The classification of each point in space to a given label for a given data set is achieved by finding the segmentation that maximizes the probability of input given the prior probabilities from the training set. First, the probability of a class at each point is computed as the probability that the given class appeared at that location in the training set times the likelihood of getting the subject-specific measured value from that class. The latter is computed from the PDF for that label as estimated from the training set. The probability of each class at each point is computed. An initial segmentation is generated by assigning each point to the class for which the probability is greatest. Given this segmentation, the neighborhood function is used to re-compute the class probabilities. The data set is re-segmented based on this new set of class probabilities. This is repeated until the segmentation does not change. This procedure allows the atlas to be customized for each data set by using the information specific to that data set. Once complete, not only is there a label for each point in space, but there is also the probability of seeing the measured value at each voxel. The product of this probability over all points in space yields the probability of the input. This procedure has been shown to be statistically indistinguishable from manual raters (Fischl, et al, 2002) and relatively insensitive to

changes in acquisition parameters (Fischl, et al, 2004a). The results are shown in **Figure 15**, the volumetric labeling shows several subcortical structures (putamen, hippocampus, ventricles, etc). In FSL all white matter is considered a single label, and so another program is used for tracking white matter from the DTI image obtained.

For this project, the automated pipeline and script obtained values for cortical and subcortical volumes for cortex, thalamus, caudate, putamen, hippocampus, amygdala and accumbens.

(A) (B)

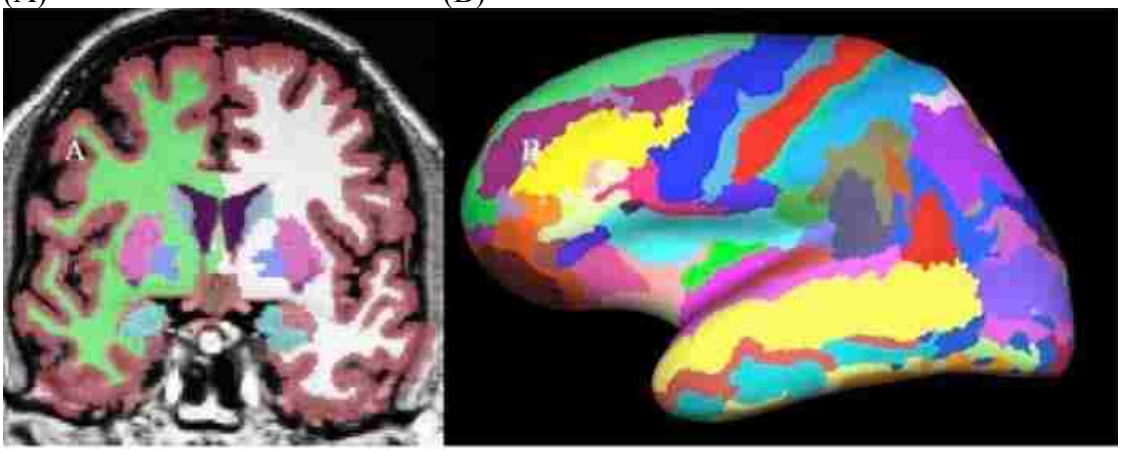

Figure 15. Volume based labeling. (A) Volume-based labeling. Note that cortical gray matter and white matter are represented by single classes. Also note that there are separate labels for the structures in each hemisphere. (B) Surface-based labeling. (FreeSurferAnalysisPipelineOverview, http://surfer.nmr.mgh.harvard.edu/fswiki/).

3.4.2 DTIStudio and White Matter Tractography

DTIStudio is a program developed for diffusion tensor image (DTI) computation and fiber tracking. The software reads data formats from a variety of MR scanners. Tensor calculation is performed by solving an over-determined linear equation system using least square fitting. Various types of map data, such as tensor elements,

eigenvalues, eigenvectors, diffusion anisotropy, diffusion constants, and color-coded orientations can be calculated. The results are visualized in orthogonal views and in a three-dimensional mode. Three-dimensional tract reconstruction is based on the Fiber Assignment by Continuous Tracking (FACT) algorithm and a brute-force reconstruction approach (Mori et al, 1999; Xue et al, 1999). To improve the time and memory efficiency, a rapid algorithm to perform the FACT is adopted (for a complete overview from voxel to tract please see **Figure 16**). An index matrix for the fiber data is introduced to facilitate various types of fiber bundles selection based on approaches employing multiple regions of interest (ROIs). The program is developed using C++ and OpenGL on a Windows platform (Jiang et al, 2006).

In general, for 3D tract reconstruction, fiber assignment by FACT method was used with FA threshold 0.2 and an inner product threshold of 0.75, which prohibited angles larger than 60 degrees during tracking. A multi ROI approach was used to reconstruct tracts of interest. Tracking was performed from all pixels inside the skull (brute force approach) (Conturo et al, 1999) and results penetrating manually defined ROIs. When multiple ROIs were used for a tract of interest, three types of operations were employed, “AND”, “CUT”, and “NOT” (see **Figure 17**), the choice of which depends on the characteristic trajectory of the WMT (Wakana et al, 2007).

For this project, the chosen tracts in question that were tracked using DTIStudio were the cingulum (gyrus and hippocampal aspect), the inferior fronto-occipital fasciculus, the inferior and superior longitudinal fasciculus, uncinate fasiculus, the forceps minor and major, the anterior thalamic radiation and the corticospinal tract (see Appendix I for tracking reconstruction).

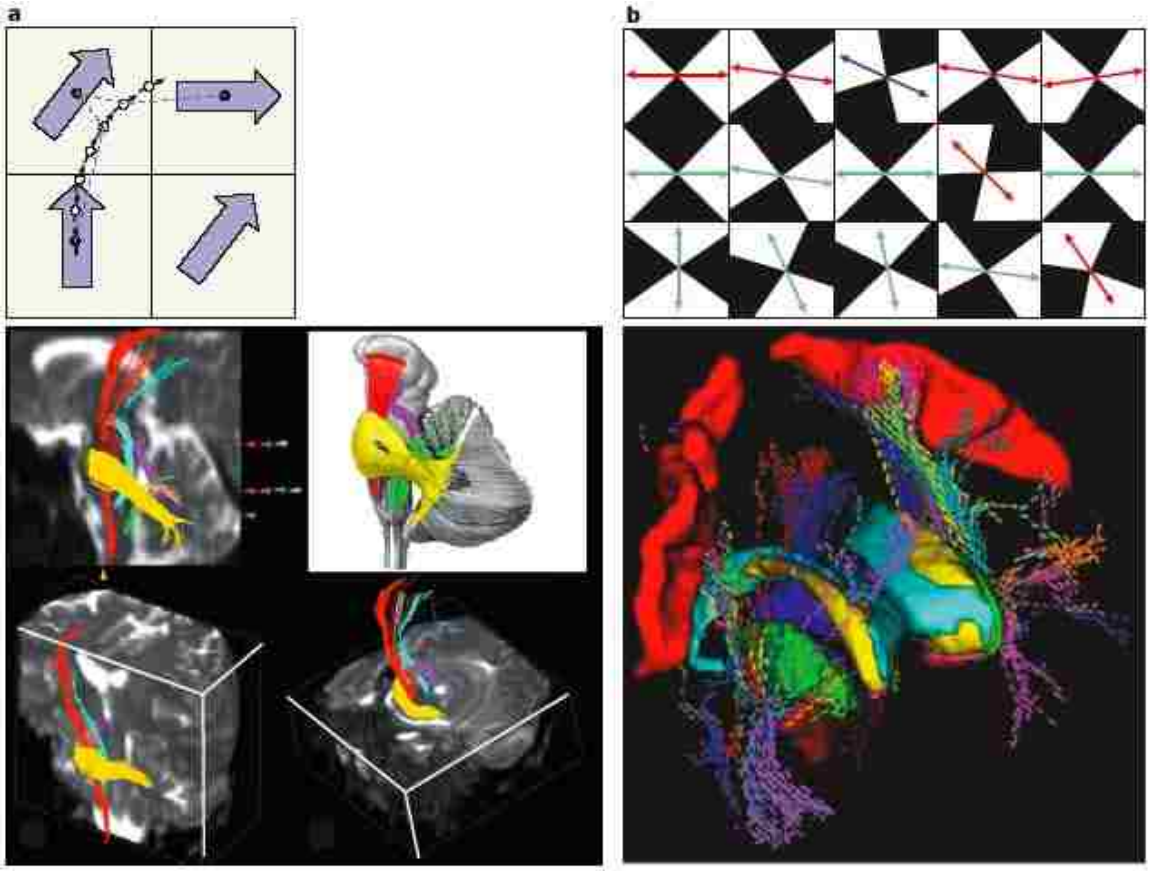

Figure 16. Fiber tracking: connecting voxels. Several approaches together connect voxels after white matter fibers have been identified and their orientation determined. (a) With the FACT algorithm, tracking is performed on a voxel-by-voxel basis. The overall track is determined from a seed point, following successive orientations associated with adjacent voxels (Mori S et al., 1999) (b) Regularization methods allow local patterns fiber stiffness to be taken into account. Voxels with uncertain orientation (blue) can then be included or excluded from tracts, depending on the allowed degree of curvature of the tracks (Poupon C et al., 2000).

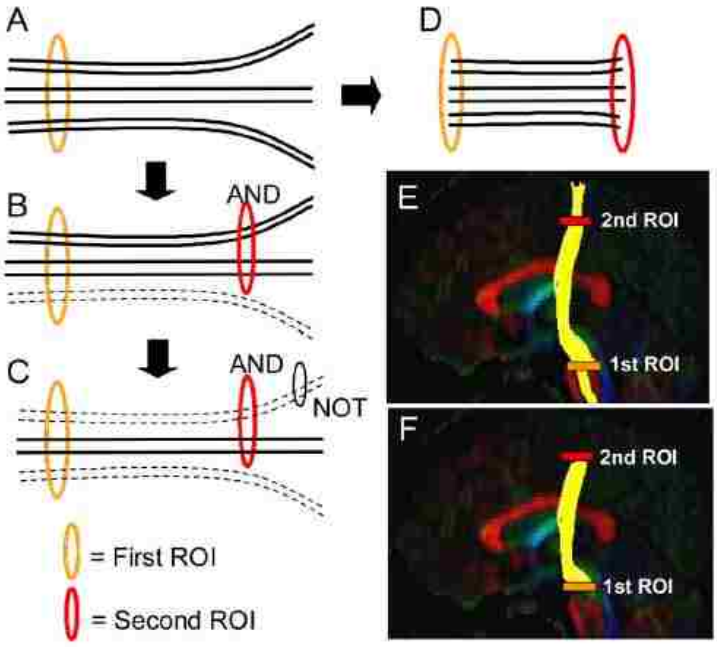

Figure 17. A schematic diagram of 3 types of ROI operations; AND, NOT , and CUT. After the first ROI is drawn, all tracts that penetrate that ROI are retrieved (A). When the second ROI is applied as an "AND" operation, the fibers that penetrate both ROIs are retained (B). Fibers leading to other pre-determined tracts may be deleted from the ROI using the "NOT" operation (C) leaving the ROI in question (D). For example, for the corticospinal tract we see the first ROI above the decussation (E) "AND" the second ROI below the pyramidal cells of the motor cortex (E) leaving the ROI and the fibers to be tracked (F). (Wakana S et al, 2007).

3.5 Genotyping

3.5.1 Whole-genome Genotyping & CNV analysis on the Illumina® Infinium® Assay Platform using the Human1M-duo V3 BeadChip

DNA Collection, Extraction, and Storage:

Participants were instructed to generate and deliver 5 ml of saliva in to a sterile 50 ml conical centrifuge tube. The saliva sample was then placed in the refrigerator and lysis buffer was added within 24 hours. Tris-HCl, pH 8; EDTA, pH 8; SDS and NaCl were added at 100 mM, 20 mM, 0.5% and 125 mM final concentrations; respectively. The tubes are refrigerated until the DNA is extracted, usually within 48 hours. Proteinase K

(0.2 mg/ml) is added and the tubes are incubated at 65°C for 60 minutes. An equal volume of isopropyl alcohol is then added to each tube, the contents are mixed, and the DNA is collected by centrifugation at 3,500 x g for 10 minutes. The DNA pellet is rinsed once with one ml of 50% isopropyl alcohol and allowed to air dry. For RNase treatment, 20 ug/ml RNAse A and 50 U/ml RNase T1 were added and incubated at 37^{o}C for 30 minutes. To precipitate the DNA, two volumes of 95% ethanol was added and mixed by gentle inversion then collected by centrifugation at 3,500 xg for 15 minutes. The samples were allowed to air dry followed by re-suspension in 1 ml of 10 mM Tris-HCl, 10 mM EDTA buffer, pH 8.0, and placed in a 1.8 ml cryovial. The concentration of DNA is calculated from the absorbance at 260 nm analysis and then adjusted to a concentration of 10 ng/μL.

Protocol:

The DNA is then purified and quantified in preparation for whole genome amplification, followed by fragmentation and ethanol precipitation. The DNA is then re-suspended in hybridization buffer and applied to the bead chip array for an overnight incubation. The amplified and fragmented DNA samples anneal to locus-specific 50-mers (covalently linked to one of over 1,000,000 beadtypes) during the hybridization step. Following hybridization, the arrays are washed to eliminate unhybridized and non-specifically hybridized DNA. One bead type corresponds to each allele per SNP locus. The samples then undergo single base extension and staining followed by more washing. The arrays are allowed to dry and then scanned using the Illumina iScan system and in turn analyzed using Illumina's software for automated genotype calling performed by Marilee Morgan.

Data Analysis:

Analysis of the scanned results was achieved using Illumina's BeadStudio software in conjunction with the BeadStudio genotyping module. BeadStudio Software is a modular analysis tool for genotyping, gene expression, and methylation applications. The data is then filtered in BeadStudio for call rate, call and minor allele frequency to remove bad samples and bad SNP's. BeadStudio comes equipped with several plug-ins to generate compatible files for further analysis using third party and/or custom software packages.

3.5.2 Candidate Gene Identification

Haploview: Statistical analyses for linkage disequilibrium, single SNP association, and haplotype-based association

Linkage disequilibrium was estimated based on the formula: D = Pab-Pa•Pb. D is LD (normalized by the maximum value of possible D); Pab is the haplotype expectation frequency at loci A and B. The terms Pa and Pb are allele frequencies at two loci. LD was estimated using the Haploview program (Barett et al., 2005). If D′ values are ≥ 0.98, there is little evidence for historic recombination. Thus, the two markers are considered to be in "strong LD" (Gabriel et al., 2002). An LD block was defined according to Gabriel's definition that less than 5% of comparisons among informative SNP pairs show strong evidence of historic recombination.

Gray Matter Candidate Genes

Growing evidence from neuroimaging, histological, and gene expression studies suggests that volumnar deterioration in limbic structures may contribute to the development of alcoholism. Genetic studies have identified polymorphisms in several

genes important in growth, BDNF and its binding receptor NTRK2, also known as TRKB. Linkage findings in the addictions, particularly cigarette smoking with or without alcohol dependence, have been reported for loci on chromosomes 9 and 11, corresponding to the locations of TRKB and BDNF, respectively. In addition to this, the Collaborative Study on the Genetics of Alcoholism (COGA) performed whole-genome linkage analysis in a sample of families that include alcoholic first-degree relatives (Nelson et al, 1995). A broad region on chromosome 4q was found linked to the phenotype of alcohol dependence in these families (Reich, 1996). Located on this chromosome at 4q24 is NFKB1 and appears to affect the risk of alcoholism, particularly contributing to an earlier onset of the disease (Rodd ZA et al., 2008). We then correlated these SNPs with DTI data and other neuroimaging information in high and low dependence alcoholic subjects.

BRAIN DERIVED NEUROTROPHIC FACTOR (BDNF)

GENE: BDNF LOCATION: CHRM. 11

Candidate gene studies and linkage-based genome scans have identified multiple chromosomal regions as sources of susceptibility to AD, showing some convergent findings. Previous research concurrent with the present study, has shown that cigarette smoking with or without AD, has been linked to broad regions of chromosomes 9 and 11. Among candidate addiction susceptibility genes defined by these linkage signals are those that encode the neurotrophin, brain derived neurotrophic factor (BDNF, chrm. 11), and its cognate receptor, neurotrophic tyrosine kinase receptor B (TrkB, NTRK2, chrm. 9). Several polymorphisms in the gene for brain-derived neurotrophic factor (BDNF) might play a role in the development of or vulnerability to alcoholism and/or clinical

characteristics of alcoholic individuals. The gene maps to chromosome 11p13-15 and a quantitative trait loci study has indicated that there is a gene localized to 11p13 that increases the risk for severe alcohol withdrawal (Buck et al., 1997). Furthermore, a linkage study to alcohol dependence suggested that the BDNF locus (Uhl et al, 2001) and chromosome 11p15.5 were included in loci that a pooled-sample microarray showed an association with drug abuse. More than 40 SNPs have been described in the BDNF gene (Sklar et al, 2002) and among these is a SNP frequent in humans producing a nonconservative amino acid substitution of a valine at codon 66 for a methionine (Val66Met, dbSNP number rs6265), see **Figure 18**.

The distribution of the Met substitution is approximately 30%-50% of people worldwide are heterozygous (Val/Met) or homozygous (Met/Met) for the methionine substitution (Shimizu, Hashimoto & Iyo, 2004). Carriers of the Met allele make up about 30% of the U.S. population (Shimizu, et al, 2004), with the most commonly affected individuals of Indo-European descent and of this only 4% in the U.S. are carriers of the homozygous Met allele (Met/Met). An association study of BDNF gene polymorphism and alcoholism has also demonstrated that the Val66Met polymorphism may play some role in the course of the disease of alcoholism, rather than the development of vulnerability to alcoholism (Matsushita et al, 2004). In this study the frequencies of Met/Met genotype and the Met allele of the Val66Met polymorphism were significantly higher in alcoholic subjects who had a history of alcoholism with deliriem tremens and the Met allele advanced the onset of the disease (Matsushita et al, 2004).

The variant sequence is located in the 5' pro-BDNF region, which encodes for the precursor peptide (pro-BDNF) that is proteolitically cleaved to form the mature protein

(Seidah et al., 1996). Although this polymorphism doesn't affect the protein function of mature BDNF, the Met allele has been shown to alter intracellular trafficking and packaging of pro-BDNF, and thus the secretion of the mature peptide. This was demonstrated by Egan et al in 2003 in which rat hippocampal neurons transfected with the Met allele exhibited abnormal intracellular trafficking and altered BDNF secretion versus those cells transfected with the Val allele. Specifically, depolarization dependent secretion of BDNF was significantly impaired when Met-BDNF failed to localize to secretory granules or synapses (Egan et al, 2003). This study also employs in vivo approaches - cognitive testing, and fMRI, to demonstrate that BDNF plays a role in healthy human verbal episodic memory. Egan M.F., et al demonstrates the feasibility of studying, in vivo, the effects of specific genes on hippocampal biology and memory and implicates a specific genetic polymorphism as a factor of altered human hippocampal function, which is likely to have an impact on susceptibility to illnesses. Hariri, A.R., et al showed the contribution of the Val66Met allele to memory-related hippocampal activity in healthy volunteers using blood oxygenation level dependent fMRI (BOLD fMRI) during declarative hippocampal formation dependent memory tasks. Results indicated that Met carriers exhibited decreased hippocampal engagement in comparison with Val homozygotes during both encoding and retrieval processes. This interaction between the Val66Met and the hippocampal response accounted for 25% of the total variation in the recognition memory performance (Hariri A.R., 2003). These data implicate a genetic mechanism for variation in normal human declarative memory.

Evidence supporting a role for BDNF signaling in mechanisms of alcohol dependence has been well documented in humans as well as animal models. For example,

Joe et al., demonstrated that the mean plasma BDNF level was significantly lower in alcohol dependent patients than in normal controls. In animal studies, McGough et al, has shown that in BDNF-deficient mice, decreased levels of BDNF lead to increased ethanol sensitization and increased voluntary ethanol consumption after a two week withdrawal compared to wild-type animals. In addition, this group showed that when wild-type C57BL/6 mice were allowed to self-administer ethanol, having unlimited access to both water and a 10% ethanol solution for four weeks, *BDNF* mRNA levels were significantly increased in dorsal striatum, a brain region associated with motor control. These results suggest that BDNF signaling is part of regulatory pathway that may offset the development of dependence by limiting alcohol intake. This concept was supported by a previous report where rats received an infusion of BDNF into the ventral tegmental area (VTA), preventing drug-induced adaptations in a brain region known to be involved in drug reinforcing behavior (Berhow et al, 1996).

Alcoholics frequently suffer from comorbid psychiatric disorders as well, making elucidation of the underlying motivation to drink difficult. Anxiety, depression, PTSD, bipolar disorder and schizophrenia all predispose patients to alcohol abuse (Goldstein, et al, 2006). Studies have linked the Val66Met allele with altered neuropsychiatric disorders such as schizophrenia (Varnas et al, 2008), depression (Sen et al, 2003), and bipolar disorder (Neves-Pereira et al, 2002; Sklar et al, 2002). Studies in schizophrenic subjects have demonstrated that Met carriers perform worse in working and episodic memory tests than Val carriers along with reduced grey matter (GM) volumes within brain regions participating in verbal memory and visuospatial abilities (Ho, B. et al, 2006). In the Ho, et al study, carriers of the Met allele, regardless of whether healthy

volunteers or schizophrenic patients, had smaller occipital and temporal lobe volumes versus Val homozygotes.

A loss of BDNF-mediated signaling is also thought to play a role in major depression (Duman et al, 1997). Neuroimaging data consistent with this demonstrates reduced hippocampal volumes, among other regions, associated with depressed patients compared with controls (Manji et al, 2003). Trait depression, has been found to moderate the effects of the BDNF genotypes on hippocampal volumes with Met carriers with high depression showing a reduction in GM volume of the mean hippocampus versus Val homozygotes (Joffe et al, 2008). Studies using MRI have shown that Val/Met healthy individuals have smaller hippocampal volumes relative controls homozygous for the Val allele (Pezawas et al, 2004; Szeszko et al, 2005). Differences in cortical and hippocampal morphology are one of the most reliable effects observed in carriers of the Met allele. Thus, this polymorphism could be very informative to interpret the neuroimaging data of the structures involved in addiction obtained on high and low alcohol dependence subjects.

(A)

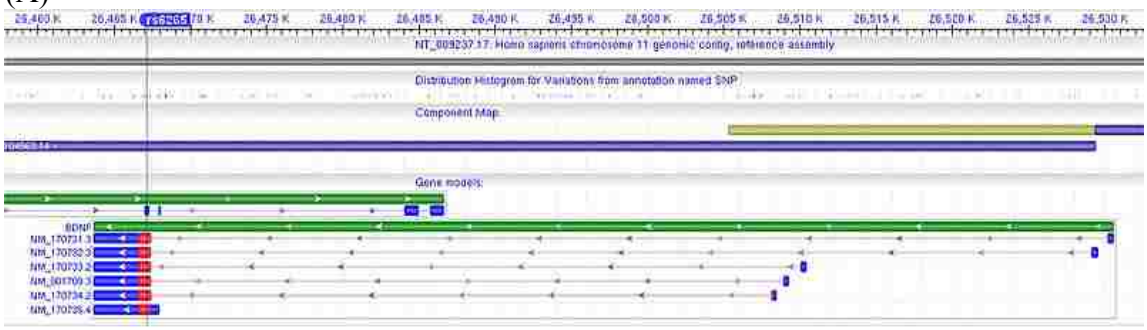

(B)

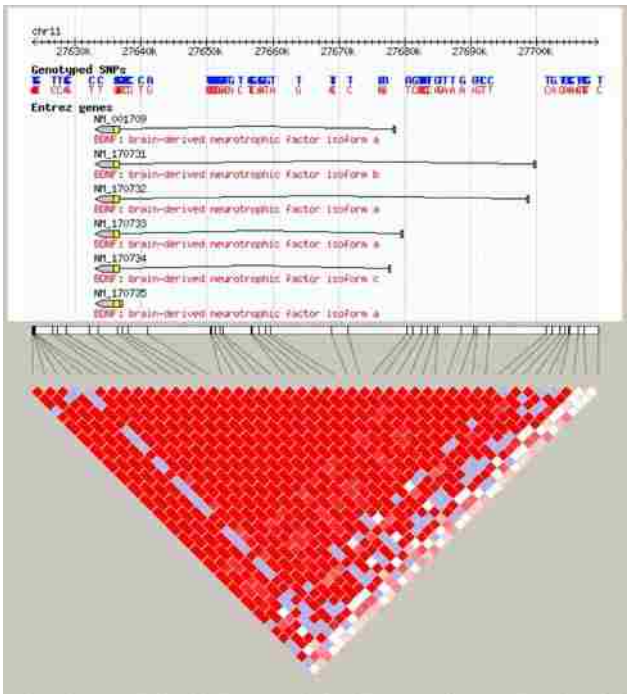

Figure 18. View of BDNF gene and SNP. (A) NCBI EntrezNucleotide View of BDNF gene and mRNA transcripts. Markers indcate location of SNP: Purple: rs6265 (Val66Met). The variant sequence is located in the 5' pro-BDNF region, encoding the precursor peptide (pro-BDNF) proteolitically cleaved to form the mature protein (Seidah et al, 1996). (B) Haploview generated LD map of the BDNF region in HapMap CEU population. Regions of high LD (D=1 and LOD>2) are shown in bright red. Markers with lower LD are shown in red (with D value indicated as a percentage) through pink (decreasing color intensity indicates decreasing D value). Regions with high D values but low informativeness (LOD>2) are shown in light blue. Regions of low LD and low LOD scores are shown in white.

NEUROTROPHIC TYROSINE KINASE RECEPTOR B (TRKB)

GENE: NTRK2 LOCATION: CHRM. 9

As stated previously, candidate gene studies have identified multiple chromosomal regions as sources of susceptibility to AD and previous research has shown that cigarette smoking, with or without AD, has been linked to broad regions of chromosomes 9 and 11. Among candidate addiction susceptibility genes, brain derived neurotrophic factor (BDNF, chrm. 11), and its cognate receptor, neurotrophic tyrosine kinase receptor B (TrkB, NTRK2, chrm. 9) have been implicated.

Neurotrophins, a family of developmentally regulated proteins, are critical for differentiation and survival of post-mitotic neurons and in the process of synaptic plasticity. The Trk family of receptors mediate the biological activity of neurotrophins by intrinsic protein-tyrosine kinase activity (Greene et al, 1995), but with different binding affinities for neurotrophins. The extracellular domain of the receptor contains two cysteine rich regions separated by a leucine rich domain. Between those domains and the plasma membrane are two IG like regions that are followed by the transmembrane domain. Intracellularly, the receptor contains the Shc-binding site, a tyrosine kinase domain and a tail region containing a PLC□ binding site (Stoilov et al, 2002). Specifically, TrkB receptor activation is mediated by high-affinity binding by BDNF that results in receptor dimerization and trans-autophosphorylation of tyrosine residues in the carboxyl-terminal intracellular domain that is required for activation of signaling cascades. This activation also includes transcriptional activation of the BDNF gene (BDNF) (Saarelainen, et al, 2001).

At least three protein isoforms of TrkB are produced by alternative splicing of *NTRK2* pre-mRNAs. These isoforms are the full-length tyrosine kinase receptor (TrkB.FL), an isoform lacking the tyrosine kinase domain (TrkB.T1), and an isoform lacking the tyrosine kinase domain but containing a Shc binding site (TrkB.T2.Shc) (Stoilov et al, 2002, see **Figure 19**). All three isoforms are expressed in brain, TrkB.T1 being the major isoform expressed in the adult brain in mostly glia and the somatodendritic and axonal compartments of hippocampal and motor neurons (Haapasalo et al., 2001) whereas TrkB.T2.Shc is neuron specific (Stoilov et al., 2002). Postulated roles for these truncated isoforms include facilitation or inhibition of neuronal signaling, ligand clearance or sequestration, and cell-cell adhesive effects, axonal outgrowth and synaptic plasticity (Klein et al., 1990). The T1 and T2.Shc isoforms have dominant inhibitory effects blocking BDNF signaling by sequestering full-length trkB receptors within non-functional heterodimers preventing autophosphorylation (Eide et al., 1996). The functions of the truncated TrkB isoforms are not known (Hartmann et al., 2004). However, there is accumulating evidence that truncated TrkB isoforms have a paradoxical role,--dominant-negative inhibitory activity on full-length TrkB receptors versus mediating signal transduction independent of full-length TrkB receptors (Haapasalo et al., 2001; Hartmann et al., 2004).

The essential functional role of BDNF-TrkB-mediated signaling was demonstrated in a model of neurodegeneration, where survival of hippocampal neurons in culture derived from trisomy 16 mice, which produce the truncated kinase deficient isoform, Trk-T1, that would have been destined to die were restored by introduction of exogenous full-length TrkB (Dorsey et al., 2002).

A role for TrkB linked to AD in humans has been reported once before which found evidence for allele, genotype, and haplotype-based association of *NTRK2* with AD, antisocial personality disorder type, in a Finnish population providing evidence for a new role of TrkB in addictive disorders (Xu et al., 2007). Xu et al, showed a strong significant allelic association between three markers and AD, SNPs (4, 5, and 30) were represented more frequently in the AD group than in the controls, suggesting that these SNPs were associated with AD in the Finnish population.

Xu et al used publicly available genotyping data from HapMap Public Release #20 to compare patterns of LD between the CEU panel (90 individuals [30 trios] from Utah), and the Finnish sample from their study. A total of 511 SNPs from *NTRK2* were genotyped by the HapMap project. Of these, 96 SNPs were selected from HapMap and pairwise measures of LD determined for the *NTRK2* region. Linkage disequilibrium of the NTRK2 gene showed five LD blocks (**Figure 19**) and although only 43 SNPs were used in this study, this suggested that the 43 SNPs selected were sufficient to represent the "true" LD structure in this region. Block 3, which contained SNP 30, contained six SNPs (SNP26 to SNP33), which covered exons 17 to 19. Ten SNP pairs were in complete LD, producing D′ values > 0.99. In the present study, Illumina 1M Duo contained SNP 27 (rs1822420), 30 (rs10780691) and 33 (rs4304401), being in complete LD, all in complete LD (Xu et al, 2007).

A haplotype based association with AD produced four, seven-locus, haplotypes in block 3, which accounted for 94% of chromosomes in the controls and 95% of chromosomes in the alcoholic group. Within block 3, haplotype 3A contained the major allele of SNP 30 and was at slightly higher frequency in the control group (0.503) than in

AD subjects (0.424) (r^2 = 5.858, *P* = 0.015, corrected *P* = 0.062), while haplotype 3B, which included the minor allele of SNP 30, was more abundant in the AD group than the control group, supporting the single allele association with SNP 30 that Xu, et al suggested previously.

Xu et al.'s study provides supportive evidence for an association between variation at *NTRK2* and AD. Evidence of association between *NTRK2* gene and AD used both single locus and haplotype-based approaches. It is the long term remodeling of neuronal circuitry that is thought to underlie development of addictive behaviors, including AD (Nestler et al., 2005).

BDNF is well known to be essential for neuronal survival, protection, and activity-dependent synaptic remodeling. BDNF signaling, via TrkB, may alter the expression of target genes related to limiting alcohol of AD (McGough et al, 2004). Global levels and region specific levels of trkB (rat TrkB) mRNA following chronic alcohol exposure were determined and levels of trkB mRNA levels were increased in the hippocampus of rats exposed to chronic ethanol, as determined by an RNase protection assay (Tapia-Arancibia et al., 2001). Future studies are required to refine treatment conditions and expression assays. With these issues in mind, Tapia-Arancibia et al. observed an increase in trkB mRNA levels in the hypothalamus from chronic alcohol exposed rats, a brain region known to be associated with satiety (Tapia-Arancibia et al, 2001). Increased TrkB expression or TrkB-mediated signaling may serve as a negative regulatory pathway that acts to regulate ethanol intake. This concept is supported by recent findings showing that *NTRK2* was associated with increased risk to eating disorders and personality traits related to anxiety (Ribases et al., 2005). Variation in

NTRK2 affecting expression of full-length or truncated isoforms or their stability could significantly affect this negative regulatory pathway. Thus, during chronic alcohol exposure, individuals with decreased TrkB-mediated signaling may be at greater risk of AD.

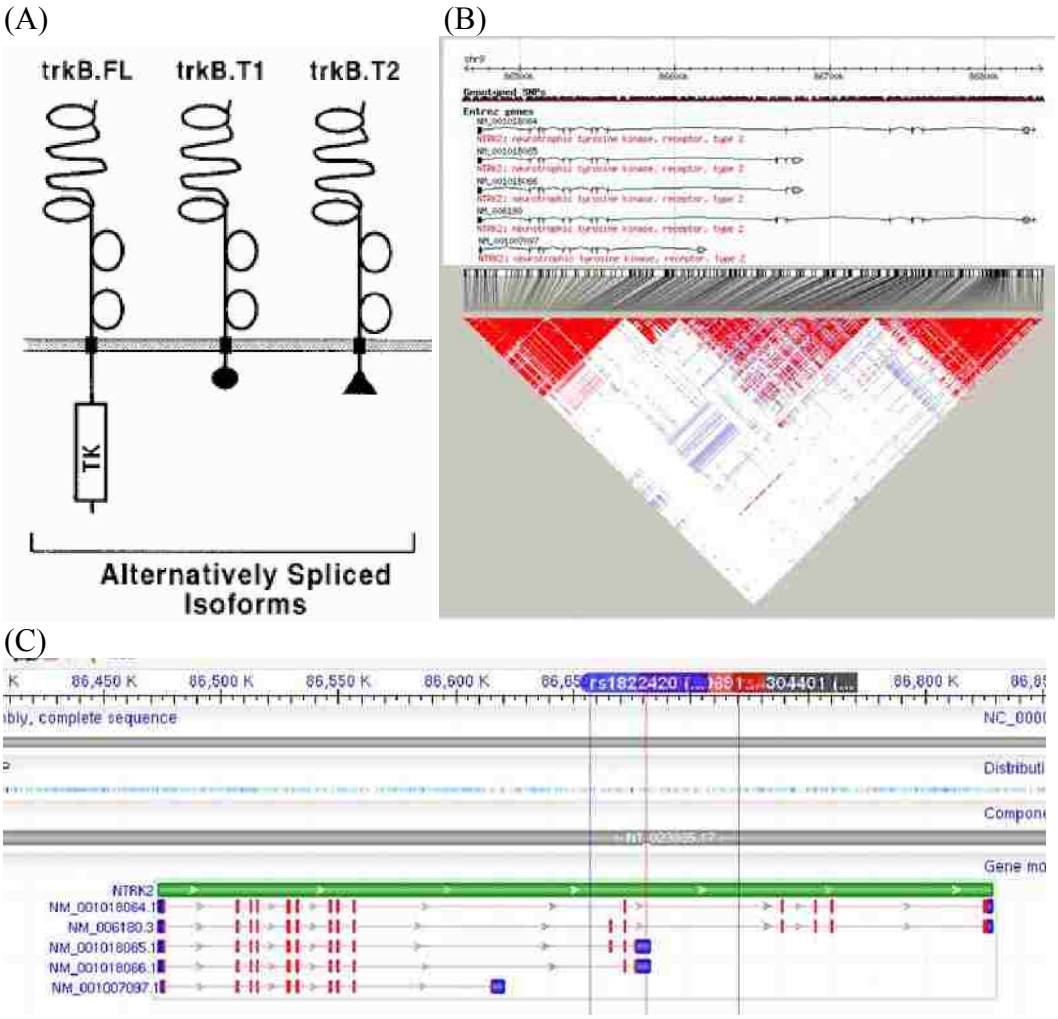

Figure 19. View of NTRK2 gene and SNPs. (A) Schematic of TrB.FL, TrkB.T1 and TrB.T2.Shc (Baxter et al., 1997). (B) Haploview generated LD map of the NTRK2 region in HapMap CEU population. Regions of high LD (D=1 and LOD>2) are shown in bright red. Markers with lower LD are shown in red (with D value indicated as a percentage) through pink (decreasing color intensity indicates decreasing D value). Regions with high D values but low informativeness (LOD>2) are shown in light blue. Regions of low LD and low LOD scores are shown in white. (C) NCBI EntrezNucleotide View of NTRK2 gene and mRNA transcripts. Markers indcate location of SNP: Purple:rs1822420 (SNP27), Red:rs10780691 (SNP30), Slate:rs4304401 (SNP33). Full

length TrkB receptor contains all three SNPs. Truncated form TrkB.T1 and TrkB.T2 contain only SNP 27 and SNP30, which falls in the 3'UTR.

NUCLEAR FACTOR-*KAPPA*B (NFκB)

GENE: NFKB1 LOCATION: CHRM. 4

NFKB1 extends 116kb along chromosome 4q24 and encodes a 105kDa Rel Family protein. In its full-length form, it is an inhibitor of transcription, which is cleaved to 50kDa DNA-binding subunit of NFκB, a ubiquitous transcriptional activator in mammalian cells (Meffert et al., 2003, 2005). NFκB has since been found in the brain and is expressed in neurons, glia and Schwann cells of the central and peripheral nervous systems (Bakalkin et al., 1993; Kaltschmidt et al., 1994; and Meberg et al., 1996). The NFKB1 gene is auto-regulated by NFκB and also regulates BDNF (Marini et al, 2004). Marini et al identified an NFκB binding site within promoter III of the BDNF gene that is regulated by NMDA receptors and contributes to NMDA mediated neuroprotection.

NFκB is important in NMDA-mediated neuroprotection, possibly by increasing the expression of BDNF (Lipsky et al., 2001); NFκB expression may in turn be activated by BDNF in an autocrine loop (Lipsky et al., 2001; Jiang et al., 2005). Ethanol attenuates the NMDA-mediated increase in BDNF (Bhave et al., 1999). Recently, it was found that in rats treated for 4 days with high levels of ethanol (to model binge drinking), NFκB binding to DNA in rat brains increased, and substantial brain damage occurred (Zou et al., 2006).

A broad region on chromosome 4q was found linked to the phenotype of alcohol dependence in at least three alcoholic first degree relatives from the Collaborative Study

on the Genetics of Alcoholism (COGA) (Williams et al., 1999). In 2007, Edenberg et al, tested the association of NFKB1 with alcoholism. Nineteen SNPs in and near NFKB1 were analyzed in 219 multiplex alcoholic families of European descent. Family based association analyses detected significant evidence of association with eight SNPs and marginal evidence for five more with an association driven by the affected individuals with earlier onset alcoholism (55% of the sample population with onset >21 years). Further analysis of the age of onset has also provided evidence for the association of 12 more SNPs in this gene (Edenberg et al., 2008). From the Edenberg et al study 3 of the 12 SNPs showing an association with earlier onset of alcohol dependence (rs980455, rs230530, rs1609798) were chosen for this particular study due to their appearance as markers on the Illumina Array (see **Figure 20**). Although numerous SNPs have been identified the functional impact of these SNPs on NFKB1 is unknown.

(A)

(B)

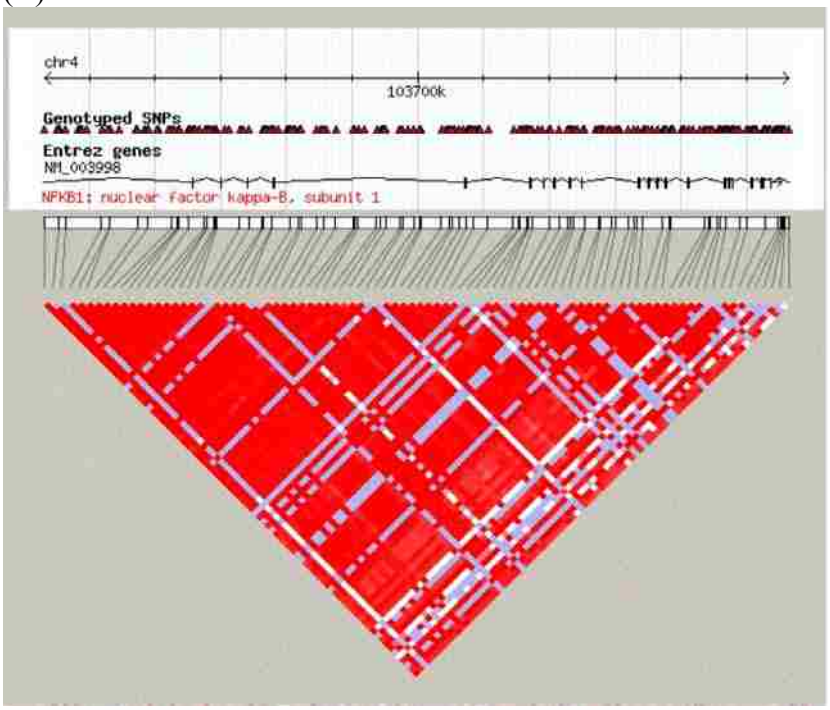

Figure 20. View of NFKB1 genes and SNPs. (A) NCBI EntrezNucleotide View of NFKB1 gene and mRNA transcripts. Markers indcate location of SNP: Purple:rs230530, Red:rs160798. (B) Haploview generated LD map of the NFKB1 region in HapMap CEU population. Regions of high LD (D=1 and LOD>2) are shown in bright red. Markers with lower LD are shown in red (with D value indicated as a percentage) through pink (decreasing color intensity indicates decreasing D value). Regions with high D values but low informativeness (LOD>2) are shown in light blue. Regions of low LD and low LOD scores are shown in white.

White Matter Candidate Gene

Neuroimaging, histological and gene expression studies suggest that myelin and oligodendrocyte dysfunction contributes to the development of alcoholism. Genetic studies have identified polymorphisms in several important regulators on myelination, initiator of myelination MAG, and the transcription factor OLIG2, which are involved in transcriptional and post-transcriptional regulation of the expression of multiple myelin genes, respectively.

Myelin Associated Glycoprotein

GENE: MAG LOCATION: CHRM. 19

Myelin associated glycoprotein is a myelin specific transmembrane protein believed to be important for the initiation and maintenance of the myelin sheath (Schachner and Bartsch, 2000) as well as for maintaining oligodendrocytes and axons, i.e. for synaptic stabilization (Davis et al., 2003). Several studies have reported that the transcriptional regulatory elements are located in introns (Beohar and Kawamoto, 1998). The gene consists of 14 exons within a span of 21.67kb and maps to chromosome 19q13.1 Studies have shown that postnatal ethanol exposure reduced the expression of MAG isoforms in the cerebellum of animals in adulthood (Zoeller et al., 1994). This data demonstrates that ethanol exposure, especially during the period of rapid myelination, has selective effects on mRNA isoforms encoding MAG. Although numerous SNPs have been identified, the functional impact on MAG is unknown (see **Figure 21**).

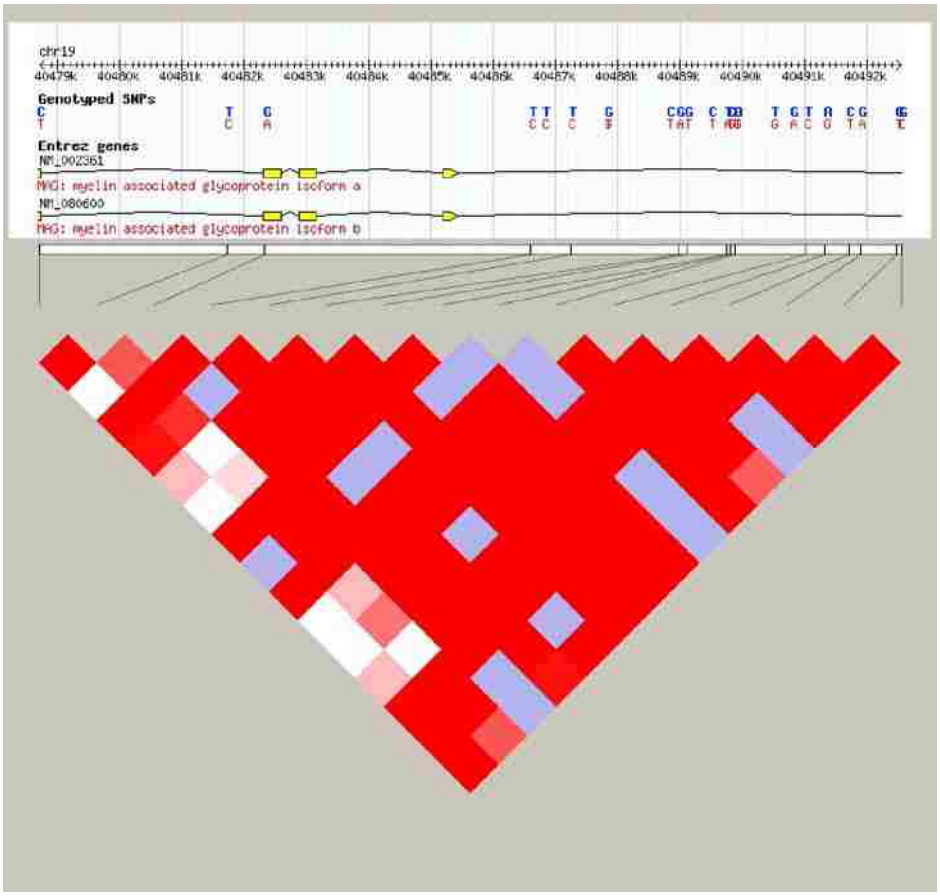

Figure 21. Haploview generated LD map of the MAG region in HapMap CEU population. Regions of high LD (D=1 and LOD>2) are shown in bright red. Markers with lower LD are shown in red (with D value indicated as a percentage) through pink (decreasing color intensity indicates decreasing D value). Regions with high D values but low informativeness (LOD>2) are shown in light blue. Regions of low LD and low LOD scores are shown in white.

Oligodendrocyte lineage transcription factor 2

Gene: OLIG2 Location: 21

Oligodendrocyte lineage transcription factor 2 is a basic helix–loop–helix transcription factor and alcohol dependence might affect the expression of many other OMR genes because it influences precursor (Lu et al., 2000) as well as fully matured (Gokhan et al, 2005) oligodendrocytes and is both necessary and sufficient for the genesis

of oligodendrocytes and myelination (Rowitch et al., 2002). Given its role as a master regulator of oligodendrocyte lineages (Marshall et al., 2005), OLIG2 is a prime candidate for hosting susceptibility SNPs with wide-ranging secondary effects on gene expression. Although numerous SNPs have been identified the functional impact of these SNPs on OLIG2 is unknown (see **Figure 22**).

(A)

(B)

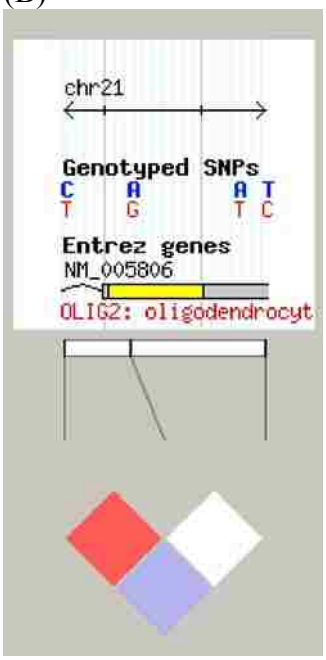

Figure 22. View of OLIG2 genes and SNPs. (A) NCBI EntrezNucleotide View of OLIG2 gene and mRNA transcripts. Markers indcate location of SNP: Purple:rs762178 (B) Haploview generated LD map of the OLIG2 region in HapMap CEU population. Regions of high LD (D=1 and LOD>2) are shown in bright red. Markers with lower LD are shown in red (with D value indicated as a percentage) through pink (decreasing color intensity indicates decreasing D value). Regions with high D values but low informativeness (LOD>2) are shown in light blue. Regions of low LD and low LOD scores are shown in white.

3.6 Statistical Analyses

3.6.1 Morphological Statistics

All gray matter volumes and white matter tract quantitative data was measured for significance using a General Linear Model ANCOVA weighted by maximum drinks and co-varied with the BDI-II score on SPSS. Graphing was completed using Graphpad software for ease of editing and imaging.

3.6.2 Genotype Statistics

Genotypes of all subjects were identified using BeadStudio software. Calculations of minor allele frequency (MAF) and Hardy Weinberg Equilibrium (HWE) were also calculated using BeadStudio software. ADS L and ADS H individuals were compared to one another in a 2 (ADS Group: Low vs. High) x 1(ROI) x 3 (Genotype: AA, AB, BB) mixed factorial design. Significant interactions/correlations between significant ROIs identified in Specific Aim 1 and 2 were found using Univariate Analysis of Variance on SPSS.

CHAPTER 4: RESULTS

4.1 Morphological Alterations in Gray Matter

Significant alterations in gray matter were seen between high and low AD individuals. Specifically, the right caudate (F(1,39)=4.109, p=0.05, **Figure 23**) and the right putamen (F(1,39)=5.199, p=0.028, **Figure 24**) of high AD individuals showed a significantly larger volume than those of the low AD individual cohort. A significantly smaller volume was seen in the left hippocampus (F(1,39)=5.786, p=0.021, **Figure 25**) and left amygdala (F(1,39)=6.048, p=0.018, **Figure 26**) of high AD individuals, whereas the left accumbens showed a significantly larger volume in high AD individuals (F(1,39)=4.111, p=0.049, **Figure 27**).

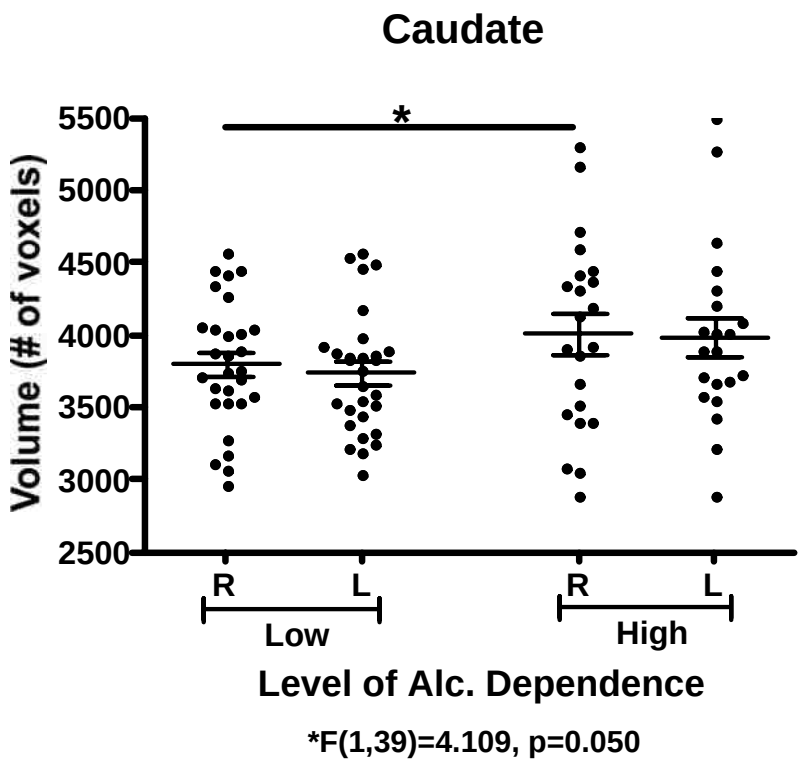

Figure 23. The right caudate of high AD individuals showed a significantly larger volume than low AD individuals, (F(1,39)=4.109, p=0.05).

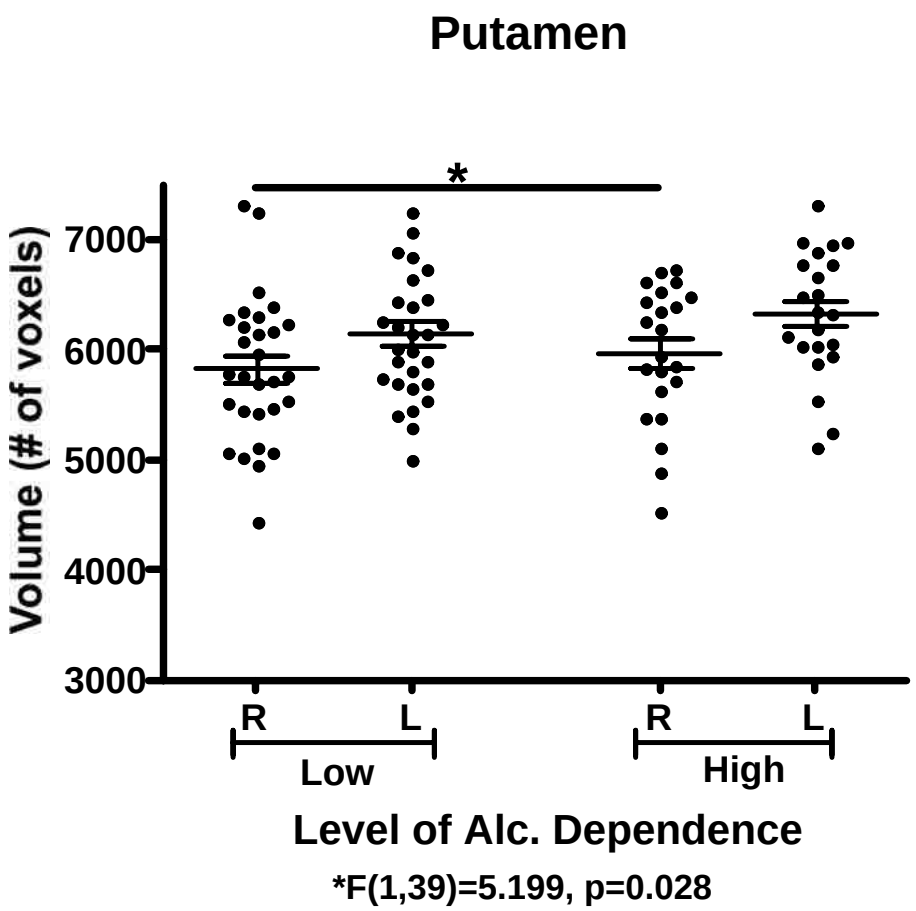

Figure 24. The right putamen showed a significant larger volume in high AD individuals than low AD individuals, (F(1,39)=5.199, p=0.028).

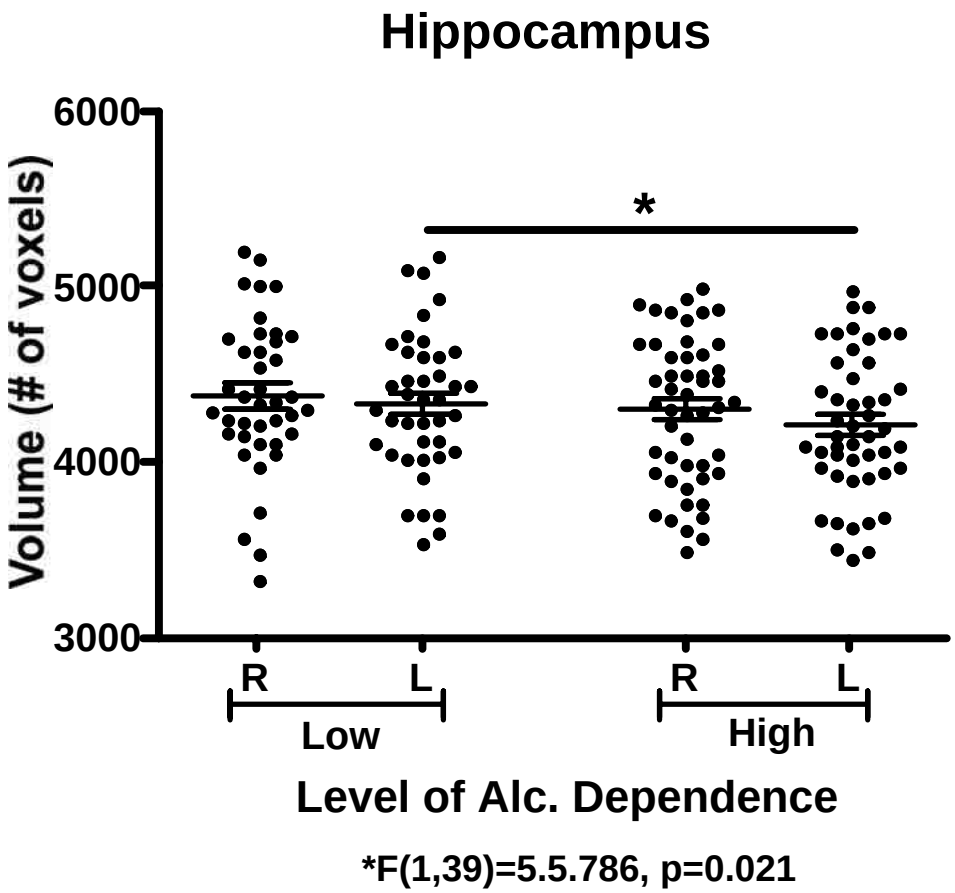

Figure 25. The left hippocampus of high AD individuals showed a significantly smaller volume than in low AD individuals, (F(1,39)=5.786, p=0.021).

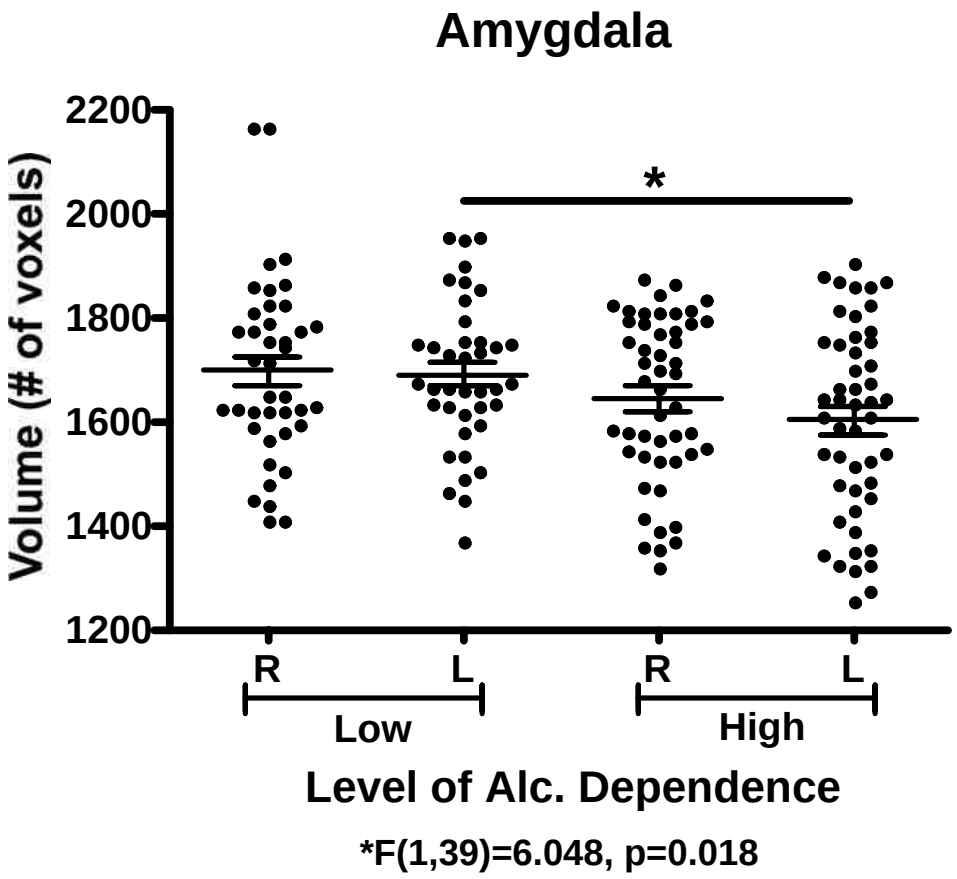

Figure 26. The left amygdala showed a significantly smaller volume in high AD individuals than low AD individuals, (F(1,39)=6.048, p=0.018).

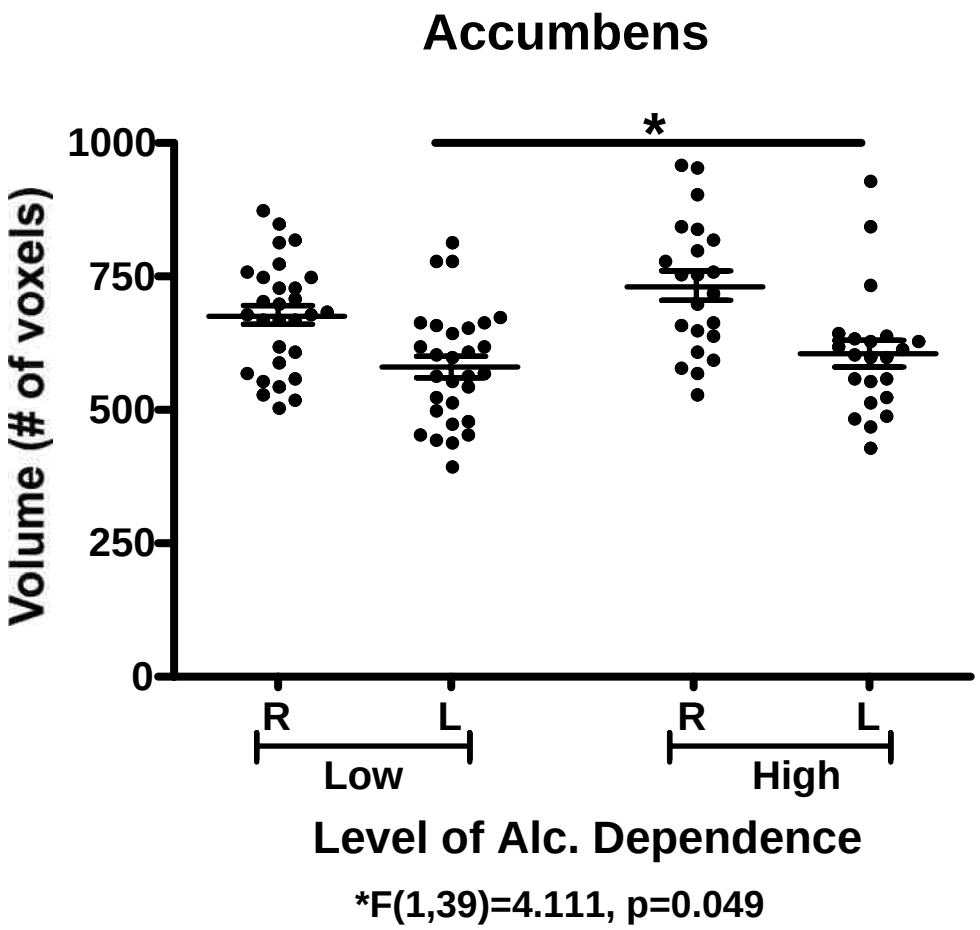

Figure 27. The left accumbens showed a significantly larger volume in high AD individuals than low AD individuals, (F(1,39)=4.111, p=0.049).

4.2 Morphological Alterations in White Matter

Changes in the white matter of low and high AD individuals involved alterations in volume and mean diffusivity. Specifically, the cingulum bundle (gyrus aspect) [F(1,32)=6.791, p=0.014, **Figure 28**] showed a significantly larger volume where as the left corticospinal tract [F(1,32)=9.868, p=0.004, **Figure 29**] showed a significantly smaller volume in high AD individuals. There was significantly lesser mean diffusivity (MD), axial diffusivity (AxD) and radial diffusivity (RD) in the right uncinate fasciculus

[$F(1,32)=7.071$, $p=0.012$, $F(1,32)=6.676$, $p=0.015$, and $F(1,32)=4.120$, $p=0.050$, respectively, **Figure 30**] indicating a putative measure of better axonal integrity.

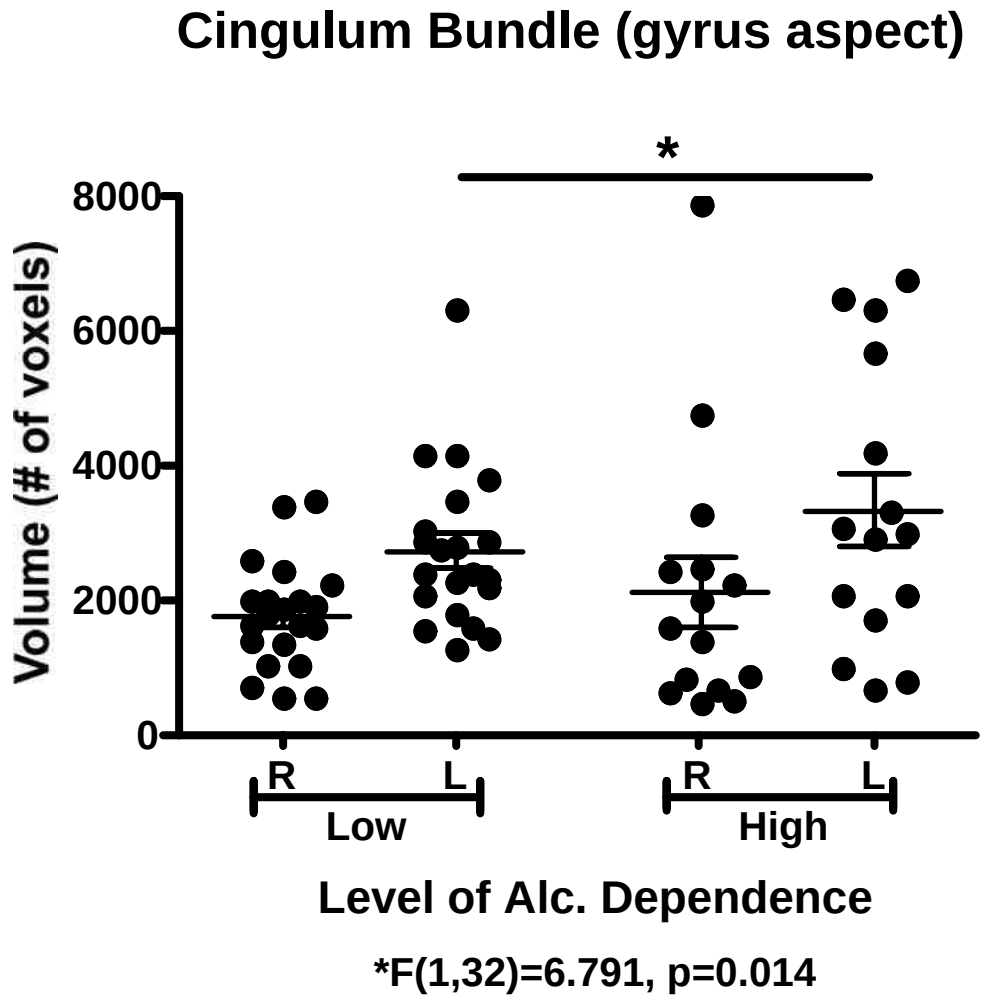

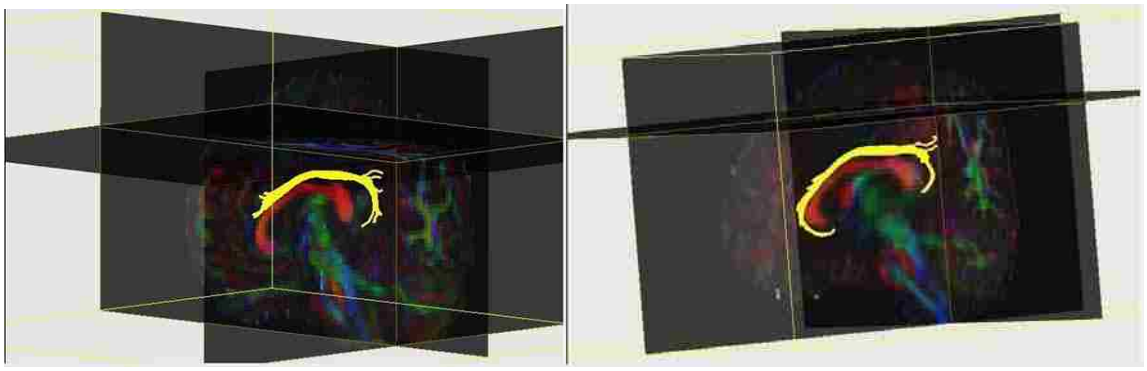

(B) Cing. Bundle (gyrus) LOW AD **(C) Cing. Bundle (gyrus) HIGH ADS**

Figure 28. (A) Left cingulum bundle (gyrus aspect) showed a significantly larger volume in high AD individuals than low AD individuals. Images of a randomly chosen low AD (B) and high AD (C) individual's cingulum bundles (gyrus aspects) after DTI tracking in DTIStudio.

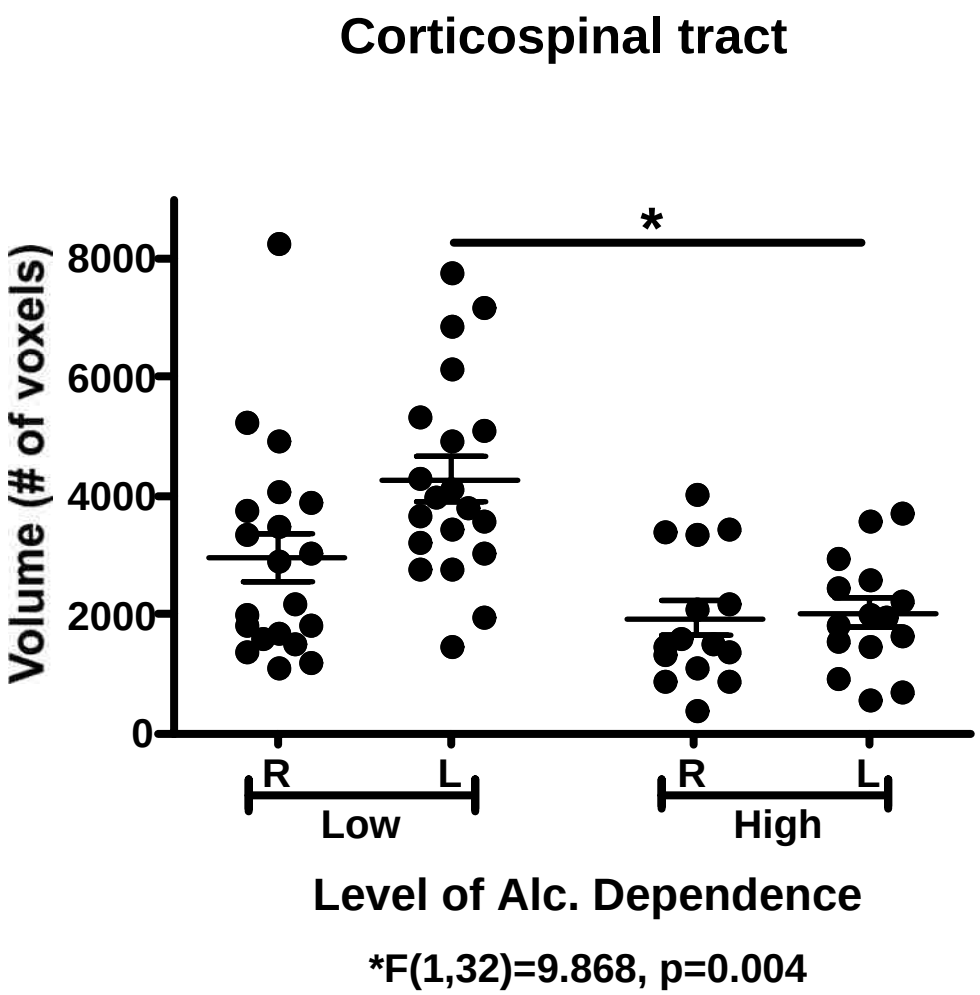

Figure 29. Left corticospinal tract showed a significantly smaller volume in high AD individuals than low AD individuals (F(1,32)=9.868, p=0.004).

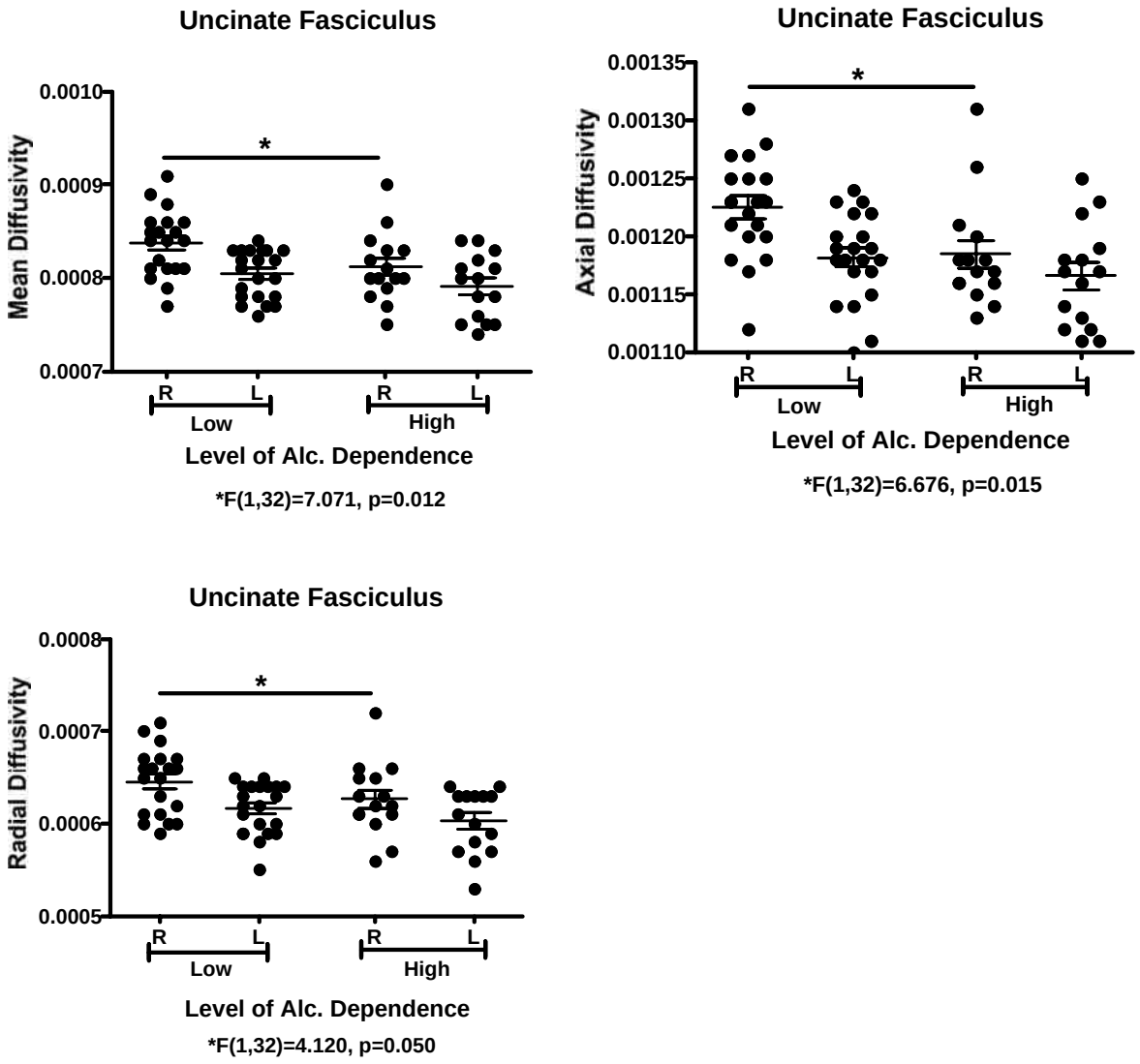

Figure 30. Right uncinate fasciculus showed less mean diffusivity (MD), axial diffusivity (AxD), and radial diffusivity (RD) in high AD individuals than in low AD individuals.

4.3 Candidate Gene Information and AD Individual Genotypes

The current study, using previously published genetic studies identified polymorphisms in several genes important in neuronal growth and myelination. Specific SNPs from GM and WM genes were chosen, resulting in the **Table 3** and **Table 4** which

include SNP ID, location, alleles, minor allele frequencies, pathophysiologies and the epidemiology with the AD cohort from the current study.

The genotype output from BeadStudio is also shown below with the major, minor, and heterozygous allele count. It is interesting to note that for the rs6265 BDNF SNP, 41 of the 44 subjects carry the Met allele, see **Table 5**.

Table 3. List of Genes and candidate SNPs chosen for the current study.

List of Genes and SNPs					
	Gene ID/ Chromosome	**SNP ID**	**Location**	**Alleles*/ Function**	**SNP Related Pathophysiology**
GREY MATTER SNP	BDNF/11p13	rs6265	CR	A/**G** Val66Met	Protein encoded member of the nerve growth factor family. Induced by cortical neurons, necessary for survival of striatal neurons, and hippocampal development and function. Mutation associated with BDNF distribution, packaging, trafficking and secretion malfunction. May play a role in the regulation of stress response and mood disorders.
	NTRK2/9q22.1	rs10780691 rs1822420 rs4304401	3' UTR intron intron	**C**/T **C**/T C/**T**	Cognate receptor for BDNF, signalling through this kinase leads to cell differentiation. Mutations in this gene have been associated with obesity and mood disorders, functional impact unknown
	NFKB1/4q24	rs980455 rs230530 rs1609798	intron intron intron	A/**G** C/**T** **C**/T	Encodes Rel protein-specific transcription inhibitor that undergos cotranslational processing to produce a 50 kD protein that is a DNA binding subunit of the NF-kappa-B (NFKB) protein complex, transcription regulator activated by cytokines, oxidant-free radicals. translocates into the nucleus and stimulates the expression of genes (BDNF). Incorrect activation associated with inflammation, persistent inhibition associated with delayed cell growth
WHITE MATTER SNP	MAG/19q13.1	rs720308 rs2301600 rs3746248	intron CR CR	**A**/G **C**/T A/**G**	Protein encoded is a type I membrane protein, member of the immunoglobulin superfamily. Mutation associated with process of myelination, initiation and maintenance of myelination, synapse stability via myelin-neuron cell-cell interactions
	OLIG2/21q22	rs762178	CR	A/**G**	Gene encodes basic helix-loop-helix transcription factor expressed in oligodendroglial cells. Mutation is associated with decreased transcription of myelin-specific genes.
* Bold letters indicate major allele, CR: Coding Region					

Table 4. List of Genes and candidate SNPs chosen for the current study including the minor allele frequency from the CEU database versus the AD cohort and the Hardy-Weinberg Equilibrium statistics from the CEU database versus the AD cohort.

	Gene ID/ Chromosome	SNP ID	MAF CEU**	HWP***	LD#	MAF##	HWE P###
GREY MATTER SNP	BDNF/11p13	rs6265	0.175	1.00	NA	0.182	0.13
	NTRK2/9q22.1	rs10780691 rs1822420 rs4304401	0.397 0.167 0.100	1.00 1.00 0.05	no	0.443 0.114 0.170	0.77 1.00 0.32
	NFKB1/4q24	rs980455 rs230530 rs1609798	0.458 0.364 0.331	0.439 0.527 1.00	no	0.443 0.109 0.330	0.77 0.22 0.49
WHITE MATTER SNP	MAG/19q13.1	rs720308 rs2301600 rs3746248	0.217 0.342 0.183	0.584 0.273 0.403	no	0.182 0.318 0.227	0.13 0.73 0.66
	OLIG2/21q22	rs762178	0.375	0.403	NA	0.5	0.36

** MAF: Minor Allele Frequency, CEU: Utah residents with Northern and Western European ancestry

***HWP: Hardy-Weinberg Probability

#LD: Linkage Disequilibrium

##MAF: Minor Allele Frequency of study population

###HWE P: Hardy-Weinberg Equilibrium Population of study population

Table 5. Individual Genotypes of AD Individuals. This includes the low AD (blue), high AD (orange), major, heterozygous, minor allele count, as well as total allele counts (green).

		Gene, SNP ID, Genotype										
		BDNF	NTRK2			NFKB1			MAG			OLIG2
		rs6265	rs10780691	rs1822420	rs4304401	rs980455	rs230530	rs1609798	rs720308	rs2301600	rs3746248	rs762178
AD Individuals	M87189298	G G	C T	C C	T C	G G	T T	T T	A A	T C	A G	A G
	M87114670	G G	T T	C C	T C	A G	T T	T C	A A	C C	G G	A A
	M87109984	A A	C T	C C	T T	A G	T C	C C	A A	C C	A G	A A
	M87120980	G G	T T	T C	T T	G G	T T	T C	A A	T C	G G	A G
	M87196594	G G	C T	C C	T T	A G	T T	T C	A A	T C	G G	A G
	M87151676	G G	C T	C C	T C	A A	C C	C C	A A	C C	G G	A G
	M87185249	G G	C C	C C	T T	A A	T C	C C	A A	C C	G G	G G
	M87169984	A G	C T	C C	T T	A G	T C	T C	A A	C C	G G	A G
	M87115517	A A	C T	C C	T C	A G	T C	T C	A A	C C	A G	A G
	M87198790	G G	T T	T C	T C	A G	T C	T C	A G	T C	G G	A G
	M87150951	G G	C C	C C	T T	A G	T C	T C	A A	C C	A G	A G
	M87189597	G G	C T	T C	T T	A G	T C	T C	G G	T T	G G	A G
	M87188301	G G	C C	C C	T T	A G	T C	T C	A G	T C	G G	A A
	M87182832	G G	T T	C C	T C	G G	T T	T T	A A	T T	G G	A G
	M87181072	G G	C T	C C	T T	A A	C C	C C	A G	T C	G G	A A
	M87136065	G G	C T	T C	T T	A G	T C	T C	A A	C C	A G	G G
	M87118004	A G	C T	C C	T C	A A	T C	C C	A A	C C	G G	G G
	M87137660	G G	T T	C C	T T	A A	T C	T C	A G	T C	A G	A G
	M87157736	G G	C C	C C	T T	A A	C C	C C	A A	T C	G G	G G
	M87147975	G G	C C	C C	T T	G G	T T	T T	A A	C C	G G	A G
	M87180947	A A	C T	C C	T T	A A	C C	C C	A A	C C	G G	G G
	M87129006	G G	T T	C C	T T	A A	T C	C C	A G	T T	G G	A A
	M87144978	A G	T T	T C	T T	A G	T T	T C	A A	C C	A G	A G
	M87195743	G G	C T	C C	T T	A G	T T	T C	A A	T C	A G	G G
	M87131456	G G	T T	C C	T C	G G	T T	T T	G G	T T	G G	A G
	M87109470	G G	C T	C C	T C	A G	T C	T C	A A	C C	A A	G G
	M87148033	G G	T T	C C	T T	A G	T T	C C	A G	T C	G G	G G
	M87122697	G G	C T	C C	T T	G G	T T	T T	A G	T C	G G	A A
	M87148957	G G	T T	C C	T C	A A	T C	C C	A A	T C	G G	G G
	M87113317	A G	C T	C C	T C	A A	T C	C C	A G	T C	A G	A G
	M87180407	G G	C T	C C	T T	A G	T C	C C	A A	C C	A G	A G
	M87112783	G G	C T	T C	T T	A A	C C	C C	A A	T C	G G	A G
	M87119370	A G	C C	C C	T T	A G	T C	C C	A A	C C	A G	A G
	M87177119	G G	T T	T C	T T	A A	T C	C C	A A	T C	G G	A A
	M87118605	A G	C C	C C	T T	A G	T C	T C	A A	C C	A A	A A
	M87173074	G G	C T	T C	T T	A G	T C	C C	G G	T T	G G	A G
	M87182419	A G	C T	C C	T T	A G	T C	T C	A A	C C	G G	A G
	M87165919	G G	T T	C C	T C	A G	T C	C C	A A	C C	G G	A G
	M87146401	G G	C T	T C	T T	A A	T C	C C	A A	T C	A G	A G
	M87117785	G G	C T	C C	T C	G G	T T	C C	A A	C C	G G	A A
	M87123990	A G	C C	C C	T T	A G	T C	C C	A G	T C	A G	A G
	M87120670	A G	C T	T C	T T	A G	T C	C C	A A	C C	A G	A G
	M87144991	G G	C T	C C	T C	G G	T T	T T	A G	T C	G G	A G
	M87146463	A G	T T	C C	T C	A G	T C	T C	A A	C C	A A	A G
Low AD Alleles	Major	15	3	20	17	6	8	12	18	12	15	4
	Heterozygous	7	14	5	8	11	16	9	6	10	10	17
	Minor	3	8	0	0	9	2	5	2	4	1	4
High AD Alleles	Major	16	5	14	12	2	5	9	13	9	12	5
	Heterozygous	3	9	5	7	12	10	8	4	8	4	8
	Minor	0	5	0	0	4	3	1	1	1	2	5
Alleles	Major	31	8	34	29	8	13	21	31	21	27	9
	Heterozygous	10	23	10	15	23	26	17	10	18	14	26
	Minor	3	13	0	0	13	5	6	3	5	3	9

4.4 Associations

Exploratory associations found significant associations between two gray matter structures and two SNPs was observed after univariate analysis of variance was performed on gray matter structures that had significant alterations in volume and the AD individual's genotype (significance reported for ADS*SNP association, $p<0.05$). As seen in the **Figure 31**, for Low ADS ("0" subgroup) to High ADS ("1" subgroup), carriers of Val/Met genotype of the rs6265 BDNF SNP ("0") show an association between level of dependence [ADS*rs6265, $F(1,43)=5.503, p=0.024$] for the right amygdala volume, whereas those individuals of the Val/Val ("1") or Met/Met genotypes ("-1") show no effect of an association with level of AD. No significant association or conclusion can be drawn about the Met/Met ("-1") population because only three of the 44 subjects were Met/Met. Also, for the right amygdala, an association is seen between low and high ADS individuals that are T/T genotype ("-1") of rs4304401 of the NTRK2 gene, [ADS*rs4304401, $F(1,43)= 5.343, p=0.026$, **Figure 32**.] Note that there was a significant trend towards an alteration in the right amygdalar volume between low and high ADS subjects (**Figure 26**). Another significant association occurred in relation to the level of dependence where major allele carriers of the SNP rs4304401 of the NTRK2 gene who were high AD individuals had larger right accumbens volumes ADS*rs4304401, $F(1,43)= 5.324, p=0.026$, **Figure 33**. Note that there was a significant trend towards an alteration in the right accumbens volume between low and high ADS subjects (**Figure 27**).

Although not significant, the results for rs6265 in the ROIs of the right accumbens and left hippocampus and left caudate all show main effects of level of dependence, an increase in volume and interestingly, being a Val/Met genotype, **Figure 34**.

White matter tract associations focus on the uncinate fasiculus radial diffusivity as the significant ROI that shows a significant association in high AD individuals that are G/G genotype, but no association was seen to the radial diffusivity in high AD individuals who are A/G or A/A genotypes of the SNP rs3746248 of the MAG gene (ADS*rs3746248, F(1,33)= 3.265,p=0.050), **Figure 35**.

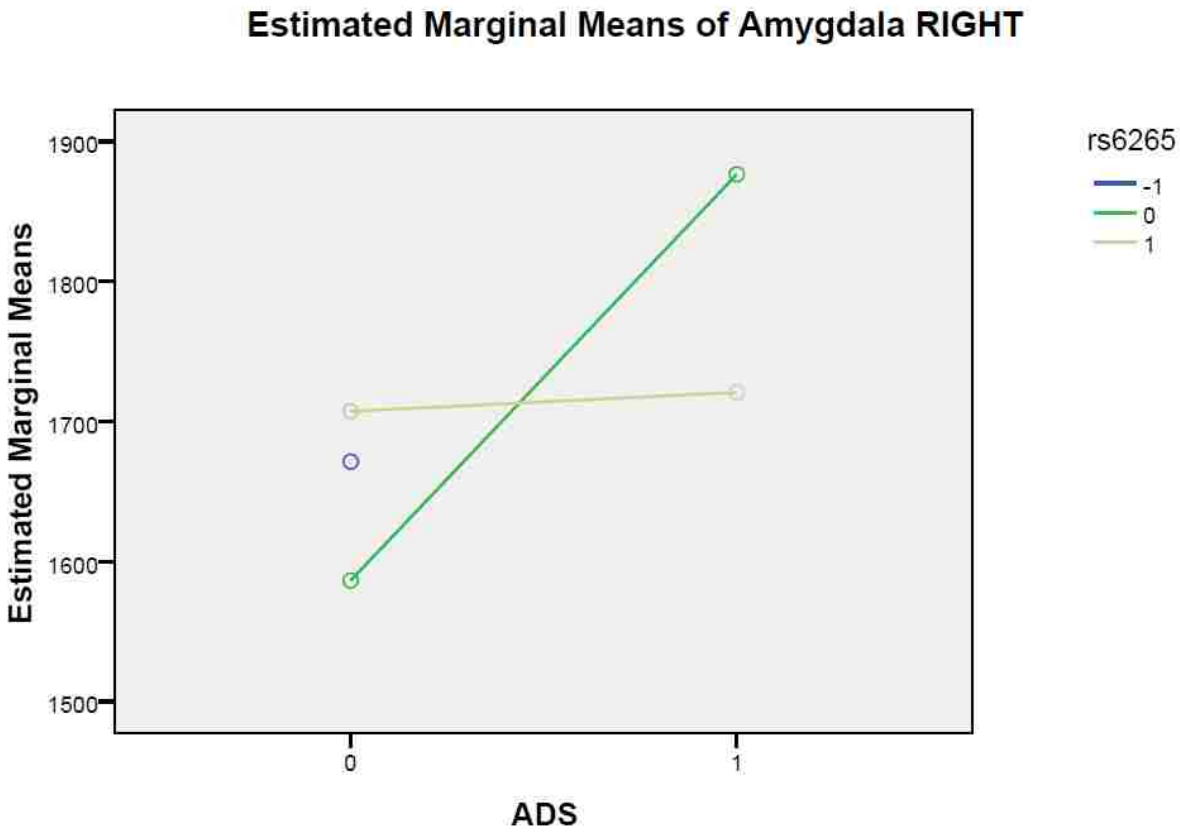

Figure 31. Association of Amygdala X ADS level X SNP rs6265. An association was indicated for heterozygous Val/Met carriers between low to high individuals amygdalar volumes, (F(1,43)=5.503,p=0.024). "1"= Val/Val, yellow line, "0"= Val/Met, green line, and "-1"= Met/Met, blue circle. X-axis, "0" indicates low AD, "1" indicates high AD.

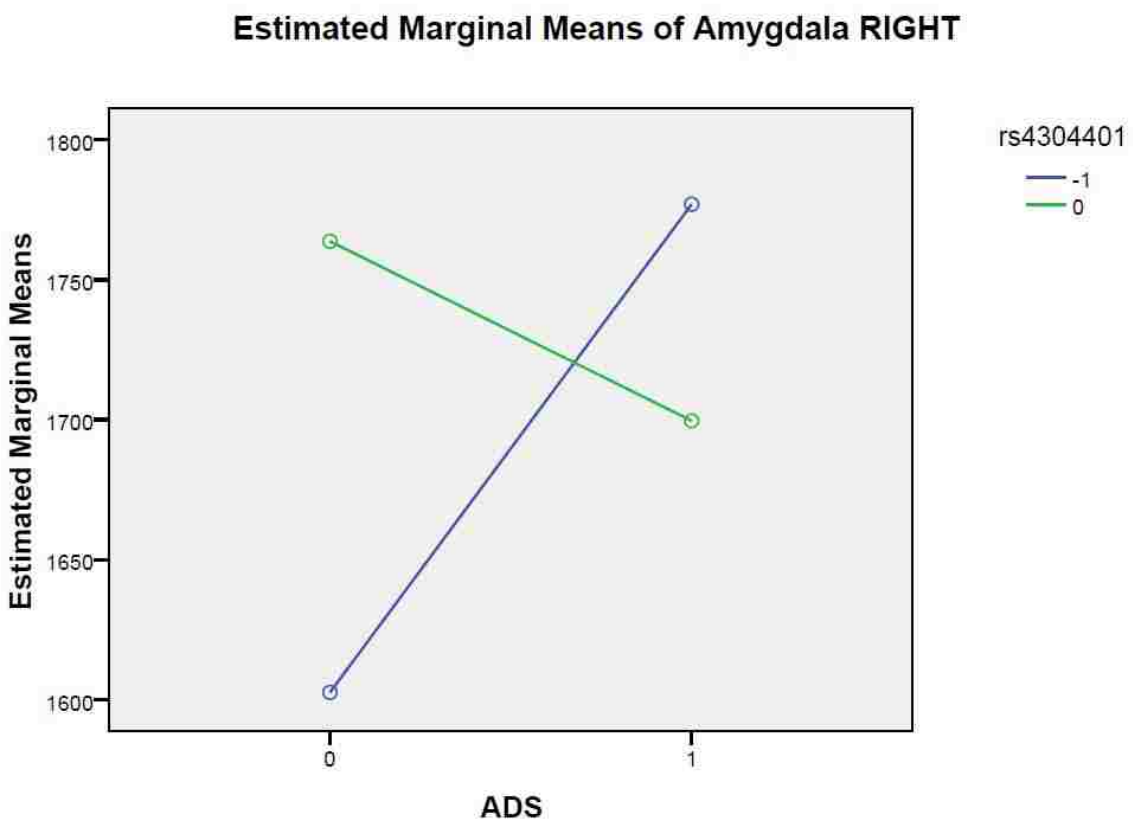

Figure 32. Association of Amygdala X ADS level X SNP rs4304401 in NTRK2. An association was indicated for homozygous allele carriers between low to high individuals amygdalar volumes, F(1,43)= 5.343,p=0.026. "-1"= T/T, blue line, and "0"= C/T, green line. This population contained no C/C individuals. X-axis, "0" indicates low AD, "1" indicates high AD.

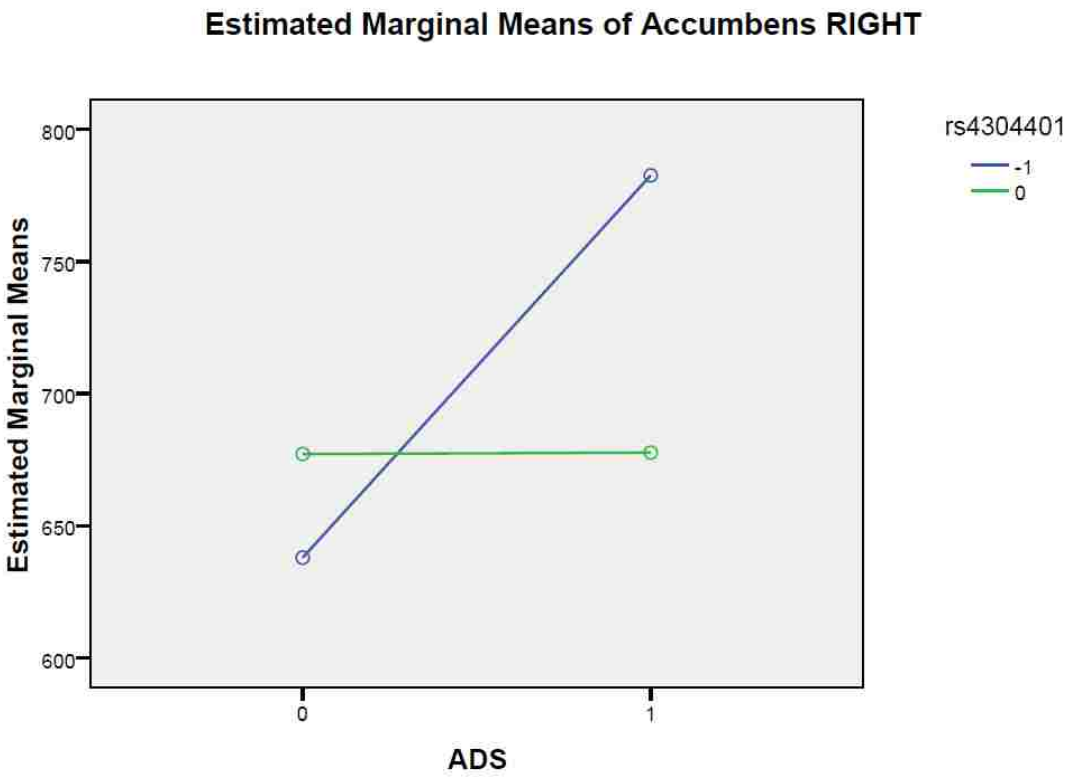

Figure 33. Association of Accumbens X ADS level X SNP rs4304401. Positive correlation indicated for heterozygous allele carriers between low to high individuals accumbens volumes, $F(1,43)= 5.324, p=0.026$. "-1"= T/T, blue line, "0"= C/T, green line. This population contained no C/C individuals. X-axis, "0" indicates low AD, "1" indicates high AD.

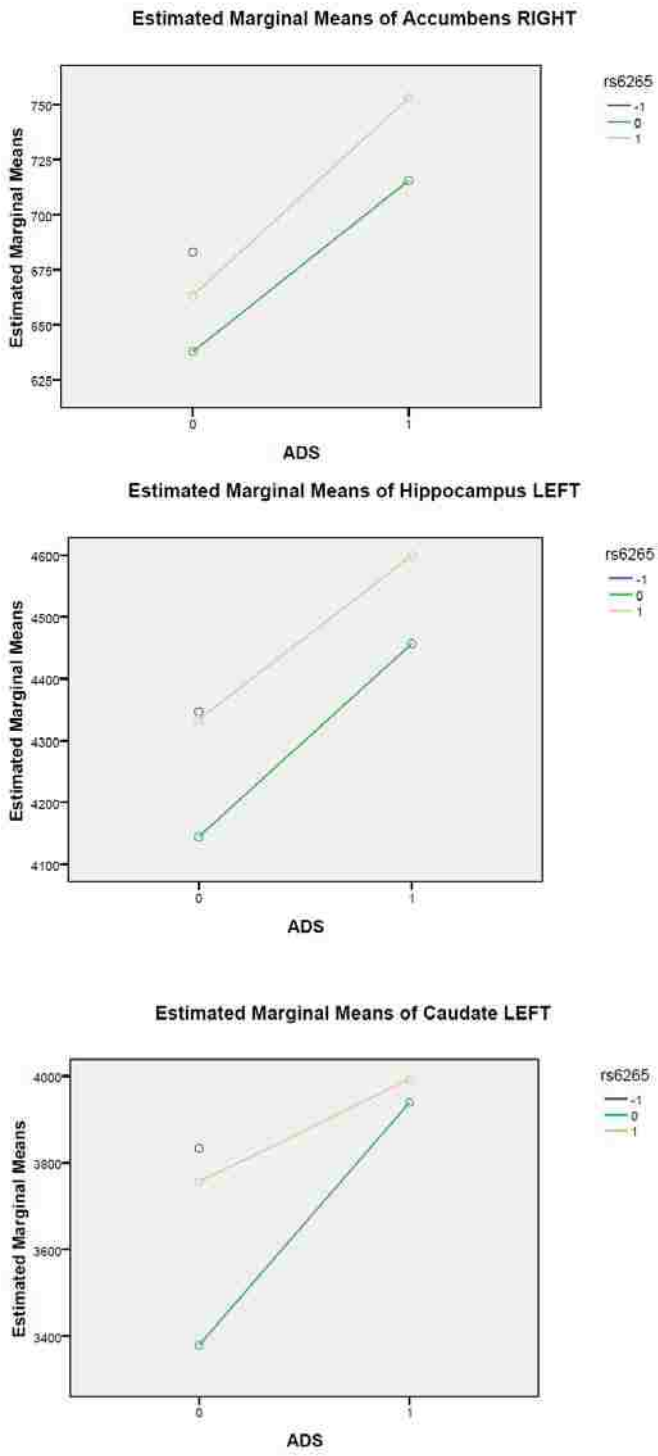

Figure 34. Main effect of alcohol dependence and rs6265 of BDNF, not significant. "-1"= Val/Val, blue line, "0"= Val/Met, green line, and "1"= Met/Met, yellow line. X-axis, "0" indicates low AD, "1" indicates high AD.

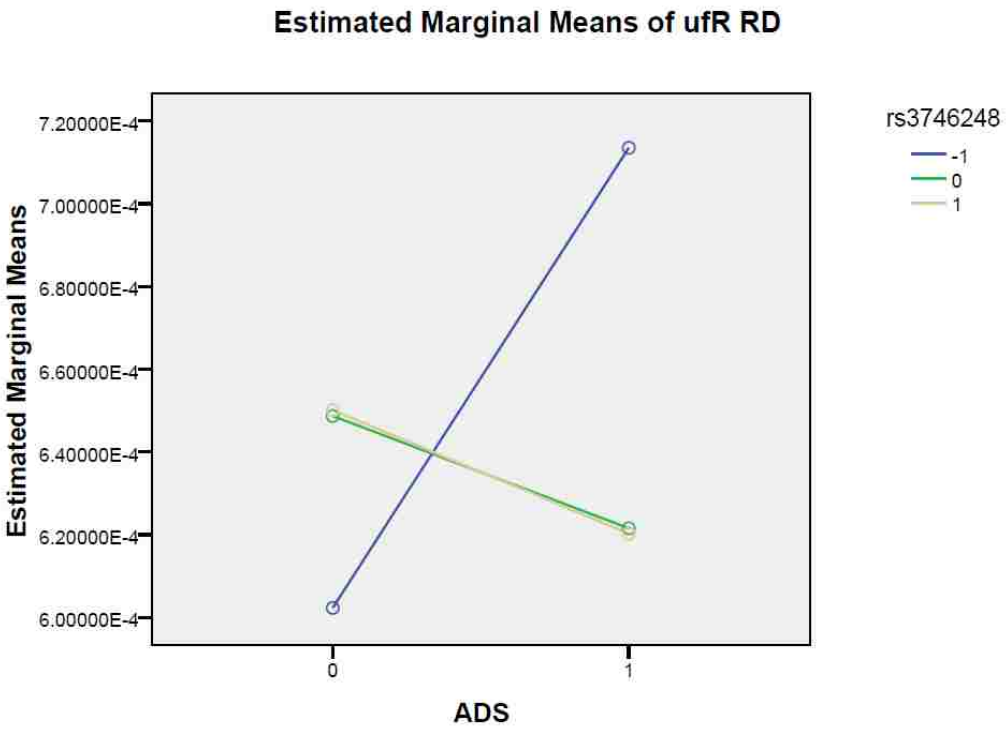

Figure 35. Association of Uncinate Fasciculus X ADS level X SNP rs3746248 of MAG. An association was indicated for homozygous G/G allele carriers between low to high individuals UF radial diffusivity, F(1,33)= 3.265,p=0.050. "-1"= G/G, blue line, "0"= A/G, green line, and "1"=A/A, yellow line. X-axis, "0" indicates low AD, "1" indicates high AD.

CHAPTER 5: GENERAL DISCUSSION

5.1 Overview of major research findings

In this study, we used MRI and DTI to measure alterations in neuroanatomy of alcohol dependent individuals and associated these findings with an individual's genotype for candidate SNPs to obtain information on biomarkers or susceptibility markers for AD. It is well known that alcohol consumption has deleterious effects on the human brain in older alcohol dependent individuals. In a younger cohort of individuals, our analyses suggested an association between gray matter volumes and alcohol dependence. Given the young age of the cohort, this suggests that either alcohol produces alterations early in the trajectory of dependence or it suggest that differences in gray matter volumes may precede heavy drinking. In other words, some gray matter volume differences may be a risk factor for alcohol dependence rather than a consequence of alcohol dependence.

The limbic system consists of a network of cortical and subcortical regions that mediate the effects of positive and negative reinforcement in addiction. And as such, the system is central for sensory processing, stimulus reward associations, memory and mood (Fuster et al, 2006; Goldman-Rakic et al, 1987). In this study, we used FSL based MRI morphometry to measure volumetric brain alterations of numerous structures in low and high alcohol dependent individuals. We tested the hypothesis that the gray matter within certain regions of the reward network would be altered volumetrically in low versus high AD individuals linking a behavioral category with an endophenotype. We observed that several GM structures were significantly altered in volume between low versus high AD individuals. These alterations were: in the high AD cohort, a significantly larger caudate

putamen; a significantly smaller left hippocampus and amygdala; and in the low AD cohort a significantly larger left accumbens.

DTI anisotropy and diffusivity measures derived from fiber tracking of selected white matter fiber tracts and bundles enabled in vivo examination of the effect of low versus high alcohol dependence on the microstructural integrity of major fiber bundles. These data did not replicate earlier reports of macrostructural and microstructural vulnerability of frontal regions to alcohol dependence by assessing FA of specific white matter tracts and bundles (Pfefferbaum et al, 2008).

However, results showed a larger volume of the left cingulum bundle (gyrus aspect) and a smaller volume of the left corticospinal tract of high AD individuals. The most interesting finding, not previously published, was smaller values of the MD, AxD and RD of the right uncinate fasciculus, which usually indicates better axonal integrity.

The results of Specific Aim 2 were exploratorty at best. With its multifactorial design of 1 ROI X 2 levels of AD X 1 SNP, results demonstrated significant positive and negative correlations between significant morphological alterations, level of AD and specific SNP carriers. Specifically, in reference to right amygdalar volume, individuals with the Val/Met genotype of the rs6265 BDNF SNP showed a positive correlation with level of AD. Also, for the right amygdala, a positive correlation was seen between level of dependence and individuals with the T/T genotype of the rs4304401 of the NTRK2 gene. Another significant positive correlation occurred in relation to the level of dependence and individuals with the T/T genotype of the rs4304401 SNP of the NTRK2 gene for the right accumbens. Interestingly, the rs6265 SNP of the BDNF gene showed a trend of a main effect within the low and high AD cohorts in several ROIs; right

accumbens, left hippocampus and left caudate and an individual's Val/Met or Met/Met genotype..

White matter tract associations focused on the uncinate fasiculus as the significant ROI in which a significant positive correlation was seen level of dependence and an individual of the G/G genotype of the rs3746248 SNP found in the coding region of the MAG gene. However this SNP, in which both forms G/G or A/A lead to the same polypeptide sequence, is synonymous (silent mutation) resulting in the same amino acid sequence of the MAG protein.

5.2 Interpretation of Results

5.2.1 Gray Matter Alternations

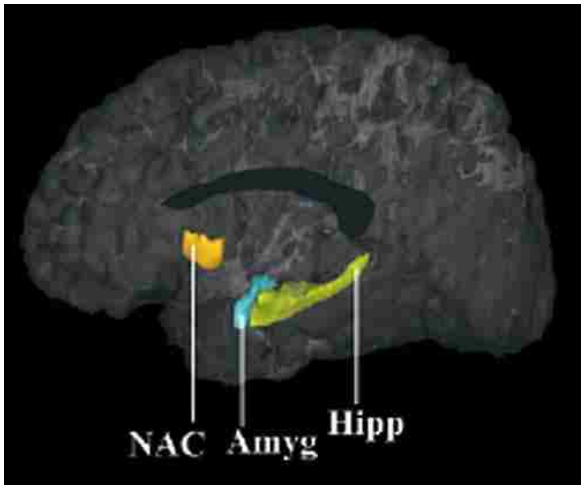

Prior structural neuroimaging studies in alcoholism have focused primarily on global alterations in cerebral cortex, white matter and cerebellum, and additionally in the hippocampus, demonstrating reductions in volume in older alcoholics (Sullivan 2000; Moselhy et al, 2001; Makris et al, 2008). There is extensive connectivity among the amygdala and adjacent structures within the nucleus accumbens region, structures that are part of the same neural system and these centers are involved in associations between stimulus cues and reward (De Olmos et al, 1999). Therefore, structural alterations in the caudate putamen, the accumbens and the amygdala could influence the processing of rewarding stimuli, which is a central feature of alcohol dependence (Kalivas & Volkow, 2005).

We found a significant reduction in the volume of the amygdala of high AD in relation to the low AD cohort, but an increase in the volumes of caudate-putamen and accumbens in the high AD cohort supporting the claim that there may be a alterations in the processing stream between the amygdala and the nucleus accumbens and the limbic brainstem which then connects to the prefrontal cortex and cingulate cortex. The increase in the volume of the caudate-putamen and accumbens is likely to influence connections within this "stimulus/cue" or "reward system" of alcohol dependence.

Hippocampal and amygdala volume reductions have been previously reported in alcoholics (Agartz et al, 1999) and reduced amygdala volumes were seen in adolescents of high-risk alcoholism families (Hill et al, 2001). In our study, analysis of these critical structures indicated that the left hippocampus and left amygdala were significantly smaller in volume in those individuals that had a high level of AD, validating the study of Makris et al, 2008. The fact that reduced volumes were observed in adolescents as well as our younger cohort suggests the possibility that smaller amygdala volumes may precede or develop very early in the trajectory of dependence. The connections of the amygdala with other structures in this network, such as the prefrontal cortex, hippocampus and accumbens are through its basolateral nucleus while the central nucleus is associated with behavior modulating motivational influence of reward-related events (Swanson et al, 2003). It is unknown if the reduction was within the basolateral or central nucleus at this time, but previous findings have indicated a loss of volume in the basolateral nucleus (Makris et al, 2008) incriminating the reward-network. The brain reward system implicated in the development of alcoholism comprises key elements of a basal forebrain macrostructure, the amygdala, that includes the central nucleus of the amygdala, the bed

nucleus of the stria terminalis, and a transition zone in the medial (shell) part of the nucleus accumbens (Koob, 2003). The left amygdala volumetric decrease is known to account for deficits in performance related to analytical aspects of memory, as well as verbal memory (Aggleton et al 2000).

In 2009 Marinkovic et al., showed in alcoholics a deficient activation of amygdala and hippocampus that underlies impaired processing of emotional faces associated with long-term alcoholism and is a part of the wide array of behavioral problems including disinhibition. In the alcoholic participants, amygdala activity was inversely correlated with an increase in lateral prefrontal activity as a function of their behavioral deficits and prefrontal modulation of emotional function. This inversion was compensation for the blunted amygdala activity during a socially relevant face appraisal task was in agreement with a distributed network engagement during emotional face processing. Marinkovic et al study suggested that alcoholics might rely on prefrontal rather than temporal limbic areas in order to compensate for reduced limbic responsivity and to maintain behavioral adequacy when faced with emotionally or socially challenging situations. In this study the smaller volumes of the amygdala and hippocampus may be reflective of lesser activation demonstrated by alcoholics, suggesting behavioral disinhibition in AD.

It is unclear why the effect was lateralized (please see Appendix III). What is currently known regarding lateralization of this pathway is limited. Structural brain asymmetry and lateralization of functional dominance may result from molecular regulation, neural connections, and plasticity (Anokhin et al, 2006).

This network is an integral part of the neurobiology of drug addiction in general, and AD in particular (Koob et al., 1999). Structural malfunction in this system may

increase risk for alcohol dependence leading to alcoholism and the abnormalities may reflect a genetically influenced alteration in the trajectory of alcoholism (Begleiter et al, 1999). Although genetic factors connecting the asymmetry and functional pathways are supported by this study, molecular correlates of this asymmetry are yet to be identified (Sun and Walsh, 2006).

5.2.2 White Matter Alterations

The mechanism for low white matter FA in chronic alcoholics remains unclear but most likely involves changes in myelination, axonal integrity, and accumulation of extracellular fluid observable best at the microstructural level. FA is a common measure to show WM damage in alcoholics or AD individuals (Pfefferbaum et al, 2008). No significant decrease in FA was seen between low AD versus high AD individuals in the present study, contradicting numerous previous studies that have shown severe damage in the white matter tracts of alcohol dependent individuals. However, previous studies have focused on life time consumption of alcohol with larger sample sizes and an average age between 40-50 years (Pfefferbaum et al, 1992, 2008; Gazdzinski et al, 2005). Our research focused on alcohol dependency in individuals 21-30 years of age, individuals in the first stages of AD, and a quarter of the sample size, n=45. This also suggests that white matter alterations are not likely to represent a premorbid risk factor, but in fact, may be a consequence of long-term alcohol abuse.

Significant results were seen in the more sensitive measure of white matter, mean diffusivity, which can be broken down into axial (AxD) and radial diffusivity (RD). Of great interest was the fact that out of 11 white matter tracts measured, only one tract, the right uncinate fasiculus (UF), showed an alteration in high AD individual cohort. The

UF, which connects the limbic system, such as the hippocampus and amygdala, in the temporal lobe with the frontal lobe such as the orbitofrontal cortex, showed a significant decrease in MD, AxD and RD of high AD individuals. This significant decrease in the MD value means better diffusion of the water molecules along the longitudinal (axonal) axis, indicating better axonal integrity. When looking at the other two measures, the decrease in AxD indicates an increase in the rate of diffusion along the orientation of the fibers in the UF. This decrease in axial diffusivity may be related to the growth of neurofibrils, such as microtubules and neurofilaments, that would increase the tortuosity of the extra-axonal space. Conversely, the destruction of neurofibrils has been found to increase axial diffusivity (Kinoshita et al., 1999). Other factors, which have been proposed to affect axial diffusivity, include fiber coherence (Dubois et al., 2008), and axonal injury, which in animal studies is associated with reduction in axial diffusivity (Kim et al., 2006). The decrease in the RD demonstrates a strengthening in the magnitude of the diffusion in the plane transverse to the axonal bundles and may reflect primarily, but indirectly, the myelination process. Therefore, it is likely that changes in the different measures of diffusivity reflect complex interactions of multiple biological factors that drive it in the direction of better axonal integrity. This suggests that a neuroadaptive effect related to the alcohol dependence may exist in this age group in the right uncinate fasciculus.

Other significant results included a larger volume (number of voxels) of the left cingulum bundle gyrus aspect in high AD individuals in relation to the low AD cohort. The gyrus aspect of the cingulum bundle interconnects parts of the limbic system. It originates within the white matter of the temporal pole, and runs posterior and superior

into the parietal lobe, then turns, forming a belt around the corpus callosum, into the frontal lobe, terminating anterior and inferior to the genu of the corpus callosum in the orbitofrontal cortex (Schmahmann and Pandya, 2006). Functionally, the gyrus aspect is involved in executive control and dysfunction in substance dependent individuals (Verdejo-Garcia, et al., 2006). In this study substance-dependent individuals (SDI) (including alcohol, cocaine, and methamphetamine polysubstance users) were compared with healthy controls on a series of behavioral (Frontal Systems Behavior Scale, FrSBe), cognitive (N-back, Go-No Go, and Wisconsin Card Sorting Tasks), and emotional (International Affective Picture System, IAPS) tasks, each of which was thought to tax a different component of these PFC functional systems. The results indicated that SDI showed greater behavioral problems in the apathy, disinhibition, and executive dysfunction and behavioral deficits were significantly associated with several real-life domains in which SDI typically have problems. Also, SDI also showed poorer performance on cognitive tests of working memory, response inhibition and mental flexibility, and abnormal processing of affective images (Verdejo-Garcia et al, 2006). This study shows evidence that substance-dependent individuals (SDI) are impaired in executive control tasks relying on different systems within the prefrontal cortex (PFC) which consists of three different functional systems: the dorsolateral prefrontal cortex (DLPC), orbitofrontal cortex (OFC), and anterior cingulate cortex (ACC) circuits. Dysfunction within each PFC system is associated with different behavioral, cognitive, and emotional abnormalities. Previous studies have also shown the cingulum bundle to decrease FA (demyelination) in depression and schizophrenia (Kubiki et al, 2003; Wang et al, 2004). In light of the current findings, the significantly larger left gyrus aspect of

the cingulum bundle, running from the genu to the splenium of the corpus callosum, may simply indicate that there is no impairment in executive control tasks within this age cohort although they are dependent on alcohol.

The left corticospinal tract in this study was significantly smaller in the individuals with high AD. Anatomically, the corticospinal tract originates from pyramidal cells in layer V of the cerebral cortex and half of its fibers arise from the primary motor cortex. Other contributions to the tract come from the supplementary motor area, premotor cortex, somatosensory cortex, parietal lobe, and cingulate gyrus. One previous study has shown low FA and high MD in cortico-striatal fibers providing evidence of compromised integrity of the motor circuitry in alcohol use disorders (Yeh et al, 2009). Specifically, we show a smaller volume of the left CST of high AD individuals, this may be a precursor to future motor disabilities that develop with increased substance abuse.

The current results support a ROI specific pattern, rather than a uniform and global distribution, of compromised gray and white matter not seen in previous studies. Within the 21-30 year cohort, it may be possible that the brain is somewhat resilient to the damaging effects of alcohol, but showing the beginnings of neuroadaptive alterations with increased alcohol dependence.

5.2.3 Significant Genetic Associations

In general, there were an insufficient number of subjects to conduct meaningful analyses or correlations of the candidate SNPs. Exploratory analyses on the association between specific SNPs and brain structure were conducted in both the high and low AD groups. A number of significant associations were observed. A significant association

was seen for those individuals that were Val/Met of the rs6265 SNP and level of dependence.

Another significant and interesting association was seen between low and high AD individuals and the T/T rs4304401 SNP found in the NTRK2 gene within the amygdala. This data indicates that the major T/T allele shows a positive correlation with the level of AD as a protective SNP. The same SNP, rs4304401, has an association in the accumbens in which the T/T allele, again, shows a positive correlation with the level of dependence. The SNP is intronic and the gene itself is the cognate receptor for BDNF, the results show a normal distribution of the major T/T allele suggesting normal function of the TrkB receptor protein. Also, these results suggest that as a T/T genotype carrier there is a likelihood of becoming increasingly dependent on alcohol.

The discovery that genetic variation in both the BDNF gene and its cognate receptor TrkB gene show associations with level of AD in the amygdala and accumbens is noteworthy. Main effects of alcohol dependence and being a Val/Met genotype was seen in the associations suggesting that this SNP may influence not only morphology, but also a susceptibility to alcoholism. The BDNF SNP has been implicated in numerous genetic association studies to neuropsychiatric diseases and carries with it a pathophysiology that is damaging to neurons seen in *in vitro* animal studies (Matsushita et al., 2004; Egan et al., 2003; Hariri et al., 2003). Therefore, the Val/Met carrier may have a predilection for altered gray matter volumes, in the amygdala, hippocampus and/or accumbens (Appendix IV). This may indicate a heightened risk or susceptibility to becoming alcohol dependent, although, without a comparison to untreated controls a formal conclusion cannot be drawn.

A significant relationship was also seen in the radial diffusivity of the uncinate fasciculus between level of AD individuals and the SNP rs3746248 found in the coding region of the MAG gene. Specifically, the G/G genotype individuals do not show any amino acid changes associated with the initiation and maintenance of myelination as well as synapse stability. Together this association data from the significant white matter alteration in RD to the SNP to the level of dependence suggests that a carrier of the rs3746248 SNP in the MAG gene may be demonstrating myelination and protection during the neuroadaptation as risk of alcohol dependency increases.

The significant relationships seen in the present study indicate that genetic, endophenotypic and neuroimaging data can be combined to a certain extent in a translational framework. This study differs from prior investigations in three aspects. First, it sees the structures as related to an interconnected system in a "big picture," that treats the gray and white matter structures as a group of regions, but still individually in statistical analyses. Second, several structures in the current study have not been measured or studied in prior neuroimaging studies of alcohol dependent individuals. Third, correlations associating the morphometry defined by behavioral tests and genetic makeup performed were not seen previous studies.

5.2.4 Effect of Age on Nueroanatomical Structures

Brain structural changes become more prominent with aging (Pfefferbaum et al., 2005; Sullivan et al., 1995; Oscar-Bermann et al., 2000), and alcoholism can exaggerate age-related volumetric reductions (Pfefferbaum et al., 1997; Kubota et al., 2001). There is a well-known and well-documented effect of aging and the alteration of volumes of certain structures within the human brain, yet all these studies focus on

affects starting at an average age of 40 years (Pfefferbaum et al., 1997). The original age criteria for our study was a cohort of 192 subjects, 21 to 50 years of age. Upon ranking and defining low and high alcohol dependent individuals, obtaining and analyzing gray matter volumes, a significant positive correlation of age was seen between level of AD and age (**Figure 36**). This suggested that the older an individual the greater the level of dependence on alcohol, which follows a common thread of logic in alcoholism. Due to this positive correlation we proceeded to analyze the individuals by a specific age subset, and for this study we focused on 21-30 years of age. This age group has not been studied in depth and spans a developmental period in which alcohol dependence begins and takes root.

Ge et al. in 2002, show age-associated patterns of change in GM and WM volumes at a global level. The decline in percent of GM starts to occur at a relatively young age (mid-20s), and the decrease is slight, but constant and linear (**Figure 37**). The percent white matter, in contrast, shows a quadratic pattern of change, slightly increasing until an age of approximately 35 years, decreasing quickly thereafter (**Figure 37**, Ge et al., 2002). Adolescent maturational changes in the gray matter occur in spatially and temporally specific patterns, with parietal cortices maturing earlier than frontal cortices (Sowell et al., 1999) and in normal adults, using voxel-based morphometry (VBM), gray matter loss with aging is most prominent in the insula and superior parietal gyri (Good et al., 2001). Longitudinal studies show that gray matter volume increases in early childhood and then declines after puberty (Giedd et al., 1999), and white matter volume progressively increases (Sowell et al., 2002). A decline in gray matter volume is prominent between adulthood and old age, whereas

white matter volume increases between 19 and 40 years, after which it steadily declines (Jernigan et al., 2001). Specifically, in the Sowell et al., 2003 study of 142 subjects scanned for cortical changes across a lifespan, there was a subtle increase in gray matter density until age 30, which remained stable until a precipitous decline in later decades and the cingulate gyrus showed no rapid loss as well. Taking this information into account, our study showed larger volumes in the caudate, putamen, accumbens suggesting that the neuroadaptative phase of alcoholism is working against the effects of aging in the high AD cohort, a preservative effect. Unfortunately, most of these studies focus on decreases in global gray matter and white matter, in the cortical regions, and our study focused on gray matter structures with in the limbic/reward system.

To address controversies regarding the effect of age on the hippocampus, volumes of hippocampus and a control structure, the temporal cortex, were measured on magnetic resonance imaging (MRI) in 128 healthy individuals (20-85 years) (Pfefferbaum et al., 2005). Individuals in this study showed no significant correlations between hippocampal volumes and age, despite significant age-related decline in temporal volumes. A VBM study conducted by Good et al., 2001 of 465 normal adult human brains also demonstrated little or no age effect in the amygdala and hippocampus. The smaller volume of the hippocampus and amygdala of the high AD cohort in our study indicates an effect of AD not of aging.

Cerebral white matter changes throughout the lifespan. It's volume increases from childhood to young adulthood, remains stable during middle age, and shrinks in senescence (Hasan et al., 2008). DTI studies of normal aging show that the

microstructural integrity of WM is also reduced with age, with greater differences observed in the anterior and posterior regions (Pfefferbaum et al., 2000, 2005). Changes of DTI indices were found to continue from late childhood to young adulthood, and were more widespread between early adolescence and young adulthood than between late childhood and early adolescence. Although this difference may be partly accounted for by the smaller age difference between late childhood and early adolescence, than early adolescence and young adulthood, the finding is consistent with a previous report which also showed more widespread FA increase between childhood and young adulthood groups than within the childhood group (Snook et al., 2005). Structural imaging studies have similarly demonstrated prominent brain growth during this period rather than earlier in childhood (Sowell et al., 2001). These findings during the period when complex cognitive functions such as executive function and attention are maturing suggest that these developments may be the neural substrate of maturing cognitive functions. Our study found a larger volume of the cingulum bundle gyrus aspect in high AD cohort suggesting that the morphological alteration may be an effect of aging and/or alcohol dependence, although this cannot be quantified properly. The corticospinal tract showed a smaller volume in the high AD cohort indicating that the alteration was accelerated loss due to alcohol dependence and not aging. The lesser value of the mean diffusivity, axial diffusivity and radial diffusivity, of the right uncinate fasciculus in the high AD cohort, which indicates better axonal integrity or strengthening of the connectivity between the temporal lobe and the posterior orbitofrontal cortex, suggests an effect of aging and maturation that occurs between 21-30 years of age.

Our data provides evidence of effects of aging, although slight, between the ages of 21-30 years, when looking at white matter maturation. The global decrease in gray matter density however does not compare with the larger volumes seen in the high AD cohort.

(A)

Between-Subjects Factors

		Value Label	N
ADS	0	LOW	29
	1	HIGH	39

(B)

Multivariate Tests[b,c]

Effect		Value	F	Hypothesis df	Error df	Sig.
Intercept	Roy's Largest Root	192.709	443.231[a]	20.000	46.000	.000
Age	Pillai's Trace	.553	2.851[a]	20.000	46.000	.002
	Wilks' Lambda	.447	2.851[a]	20.000	46.000	.002
	Hotelling's Trace	1.239	2.851[a]	20.000	46.000	.002
	Roy's Largest Root	1.239	2.851[a]	20.000	46.000	.002
ADS	Pillai's Trace	.267	.840[a]	20.000	46.000	.656
	Wilks' Lambda	.733	.840[a]	20.000	46.000	.656
	Hotelling's Trace	.365	.840[a]	20.000	46.000	.656
	Roy's Largest Root	.365	.840[a]	20.000	46.000	.656

a. Exact statistic

b. Design: Intercept + Age + ADS

c. Weighted Least Squares Regression - Weighted by MaxDrinks

(C)

Correlations

		Age	ADS
Age	Pearson Correlation	1.000	.422**
	Sig. (2-tailed)		.000
	N	84	84
ADS	Pearson Correlation	.422**	1.000
	Sig. (2-tailed)	.000	
	N	84	84

**. Correlation is significant at the 0.01 level (2-tailed).

Figure 36. Age X AD correlation. (A) Population distribution. (B) Multivariate tests performed. (C) Pearson Correlation indicating a significant positive correlation between age and ADS level of dependence, r^2=0.422.

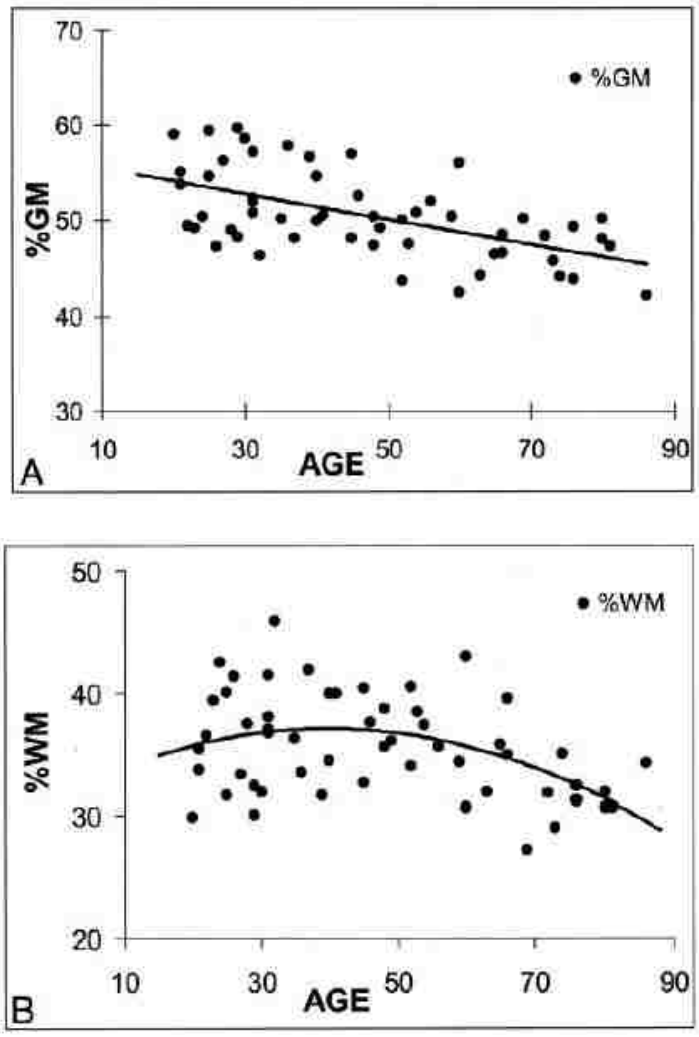

Figure 37. Regression analysis of fractional brain tissue volume estimates on 54 healthy adult subjects. Linear and weighted constrained quadratic models are presented; these indicate the age-related volume estimates throughout adulthood in normal brains. (A) %GM (B) % WM. (Ge et al., 2002)

5.2.5 Lateralization in the Brain of the Young Adult

The hemispheres of the human brain are functionally and structurally asymmetric. The analysis of structural asymmetries is of great use in identifying the neuroanatomical basis of disorders with a presumed developmental etiology, such as dyslexia, autism, and schizophrenia (Crow, 1990; Filipek, 1995). The underlying

assumption in such studies is that abnormal brain development may result in atypical asymmetries, which in turn are related to abnormal functional organization and behavior.

In the Wakana et al., 2008 study, which defined the construction protocols for studying white matter tracts, a normal population was measured in which the averaged sizes of fibers for 10 healthy volunteers can be seen in **Figure 38**. The reconstructed tracts tend to be larger in the left hemisphere and the differences are significant for the cingulum bundle gyrus aspect, superior longitudinal fasiculus temporal, inferior longitudinal fasiculus, and uncinate fasiculus, while no difference is found for the corticospinal tract and inferior fronto-occipital fasiculus. Interestingly, all asymmetric tracts are related to the temporal lobe, but no conclusion was drawn by Wakana et al, 2008 about the asymmetry in the size of the fibers in the temporal lobe, or which regions of the lobe account for the alterations. The asymmetry of the cingulum (Gong et al., 2005) and the superior longitudinal fasiculus (Makris et al., 2005, Nucifora et al., 2005) has been reported in multiple publications.

Our study showed a larger volume of the left cingulum bundle gyrus aspect, and a smaller volume of the left corticospinal in high AD individuals. The current study did not have a "normal, healthy, control" cohort and as such, by comparing to Wakana et al., 2008 data, some conclusions as to lateralization can be drawn even though the scales (mm^3 vs. # of voxels) are different. Looking at the cingulum bundle gyrus aspect (CGC), in normal healthy volunteers the left CGC aspect is significantly larger in volume and in our study both low and high AD individuals show this trend. This suggests that the significantly larger volume of the CGC in high AD individuals

may be linked to neuroadaptive changes occurring due to alcohol dependence. The corticospinal tract (CST) of normal healthy individuals showed no lateralization between right and left, yet in our study low AD subjects showed a larger left CST, which in the high AD cohort was significantly smaller and was the same volume as the right CST. This suggests that low alcohol dependence may be a phase in which neuroadaptation is occurring, and as level of alcohol dependence increases, the CST is subject to degeneration leading it back to the same volume as the right CST as seen in the normal individual. The larger volume of the CST in the low AD cohort may indicate the "neuroadaptation" phase, while the smaller volume of the CST in the high AD may indicate the decrease in motor function seen alcoholic individuals.

In 2001, Watkins et al., measured 142 normal human brains using MRI, with an average age of 24.8 years, that the caudate shows R>L lateralization and the putamen shows L>R lateralization. Although actual data are unknown, in our study the right caudate in both low and high AD individuals showed a trend towards R>L asymmetry. The larger volume of the right caudate between low and high AD individuals, then demonstrates an increase that is not due to lateralization but instead to the effects of alcohol dependence and the neuroadaptation occurring at this time point. Looking at the putamen, in our study, the left putamen reflected the L>R lateralization found in normal control individuals in low and high AD individuals. The significantly larger right putamen in the high AD cohort may be a reflection, again, of some compensatory mechanism of neuroadaptation during the gradually increasing dependence on alcohol.

The hippocampus has been see to have R>L asymmetry in healthy individuals (N=40, average age = 25.5yrs) as does the amygdala (N=20) (Pruessner et al, 2000; Filipek et al, 1994). In our study this asymmetry was not seen in the low AD cohort, where the volume of the right and left hippocampus were very similar. In the high AD cohort, the lateralization was reversed significantly in that the left hippocampus volume was significantly smaller than that of the right. This suggests that that the loss in volume in the left hippocampus is drastic and severely affected by AD. The amygdala also reflects the same path as the hippocampus in that the low AD cohort shows no lateralization, and the high AD cohort has a significantly smaller left amygdala. This suggests, also, that the loss in volume in the left amygdala is large and is affected by AD.

In 1998, Baumann and colleagues, in a preliminary study of eight control post-mortem brains, identified a L>R lateralization of the accumbens. No data could be found on the lateralization of the accumbens in the young adult brain. Based on the Bauman study, our data shows no such lateralization. In the low and high AD cohort, the left accumbens has a smaller volume than the right and the significantly larger volume of the high AD cohort suggests a simple compensatory mechanism of neuroadaptation due to a higher level of AD.

In conclusion, without a control group in our research on which to base these comparisons, no final claims can be drawn as to whether there is an affect of AD on the lateralization of certain structures and whether this emphasis is R>L or L>R. There is in involvement of multiple brain regions in alcohol dependence and a larger

cohort, along with normal healthy control individuals would increase our understanding of the influence AD may have on lateralization.

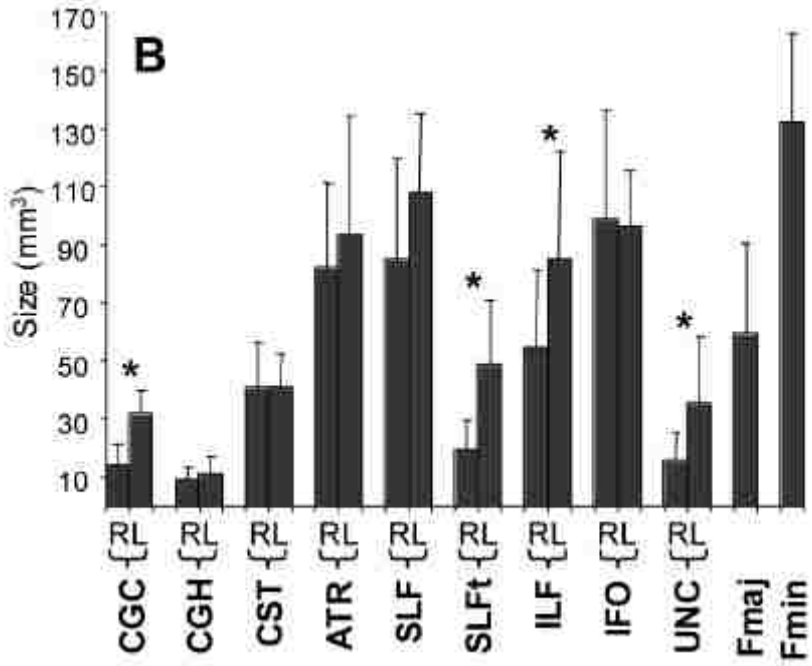

Figure 38. Sizes of white matter tracts of 10 healthy volunteers. Averages and standard deviations shown. Asterisks indicate statistically significant difference with $p<0.05$. R and L indicate right and left hemisphere. CGC, cingulum gyrus; CGH, cingulum hippocampal; CST, corticospinal tract; ATR, anterior thalamic radiation; SLF, superior longitudinal fasiculus; SLFt, superior longitudinal fasiculus temporal; ILF, inferior longitudinal fasciculus; IFO inferior fronto-occipital fasciculus; UNC, uncinate fasciculus; Fmaj, forceps major; Fmin, forceps minor.

5.3 Future Directions

Future studies are being developed to build on the current findings. In order to better understand whether structural differences are a premorbid risk factor versus a consequence of alcohol abuse, a prospective study with longitudinal follow-up measures of structure and alcohol use need to be conducted. Ideally, these studies will examine the progression of structural changes and alcohol use, beginning in adolescent, through mid-life. In addition, the present study only focused on SNPs in candidate genes. With a

sufficient sample size, future studies will be able to conduct genome wide analyses. In addition, other forms of genetic variation should be examined in future studies. Recently, rare structural variants--copy number variants (CNVs)—which correspond to micro duplications or micro deletions of 110kb at least leading to duplicate or disrupted genes, were identified by comparative genomic hybridization in several psychiatric disorders such as schizophrenia (Sebat, 2007; Cantor et al., 2008).

Another developing area of research that should be integrated with brain-based phenotypes is epigenetics. Complex epigenetic mechanisms that regulate gene activity without altering DNA have been shown to produce permanent changes in gene expression, both in cell differentiation and adaptation to environment. Mechanisms such as DNA methylation, post-translational histone modification, nucleosome sliding can cause modifications of chromatin conformation which regulate gene expression (Tsankova et al, 2007). Chromatin remodeling can be studied at the single locus level however, current methods, such as chromatin immunoprecipitation in combination with DNA sequencing (ChIP-seq) allows for genome wide analysis (Ducci and Goldman, 2008). Alcohol exposure has been shown to cause changes in chromatin structure (Mahadev et al, 1998). Recently, an increase in alpha synuclein promoter DNA methylation has been found in patients with alcoholism (Bonsch et al, 2005). Epigenetic variation within the human SNCA gene has been linked to alcohol craving (Foroud et al, 2007) and the gene maps to a QTL for alcohol preference and expression has been seen to increase in different brain areas in rats displaying alcohol preference (Liang et al, 2003) all indicating that DNA methylation also appears to regulate expression of certain genes in alcoholism.

It is important to note that the majority of the studies to date have focused on populations of European ancestry. An additional challenge is to examine AD risk from other population perspectives. There is already considerable data supporting risk differences by population and some risk alleles are known to be population specific (Ducci and Goldman, 2008). Studies on genetically isolated population, such as Native American populations, are very promising due to the high homogeneity of the genetic background, and in this case, high prevalence of alcohol dependence (Compton et al., 2007). Linkage analysis in Native Americans provided evidence for loci on chromosomes 5, 6, 12, 15 and 16 (Ehlers et al., 2004), and allowed the identification of GABA receptor genetic variants as a risk for alcohol dependence (Radel et al., 2005).

Future studies may also need to employ difference approaches to the analyses of the imaging data. Voxelwise analyses based on an initial alignment of the diffusion data to a standard brain image, spatial smoothing and then voxelwise cross-subject analysis of the resulting aligned data is often referred to as voxel-based morphometry (VBM). There has been much debate about the limitations of such an approach, primarily because there can be ambiguity as to whether apparent changes are truly due to change in gray matter density or simply due to spatial misalignment. With the advent of new algorithms, programming, and software, white matter fiber tracking has also advanced in the field of neuroimaging and quantification. Tract-based spatial statistics (TBSS) is an automated observer-independent method of aligning fractional anisotropy (FA) images from multiple subjects to allow groupwise comparisons of diffusion tensor imaging data. The new method, TBSS, aims to solve issues involving misalignment via (a) carefully tuned non-linear registration, followed by (b) projection onto an alignment-invariant tract

representation (the "mean FA skeleton"). It aims to improve the sensitivity, objectivity and interpretability of analysis of multi-subject diffusion imaging studies (Smith SM et al, 2007). The primary advantage of voxelwise analyses compared to tractography-based analysis, used in the current research, is that the entire brain can easily be investigated in a fully automated manner, without having to specify in advance regions of interest or delineate, which done by hand and is time consuming, the specific tracts to measure. However, voxelwise analysis such as TBSS does not directly provide information on long-range structural connectivity in the brain, but is limited to investigating local changes in the white matter structure. It should not, therefore, be used as a replacement for careful tractography-based connectivity analysis of DTI data, which should ideally be used in conjunction with a voxelwise analysis (Smith SM et al., 2007).

Currently there are numerous advances in molecular biology, neuroimaging, genetics and psychopathology, and opportunities arise to study the interplay of genes, brain and behavior within a translational framework. This strategy, in which genetic effects on brain function can be explored using neuroimaging, is somewhat new at present and has been titled "Imaging Genetics (IG)" (Viding et al., 2006). The flow of knowledge within the field of IG includes identifying specific genes that contribute to risk for illnesses that then provide critical information on the causes of these diseases, which then may lead to the development of fresh diagnostic and therapeutic strategies. The present study adds to the mounting evidence that this approach can be an effective means of identifying genetic variation that influences brain based phenotypes which in turn may influence the risk for alcohol dependence.

5.4 Limitations and Critique

In general, there are numerous caveats that exist in a translational framework. The combination of three different fields of science has its advantages and disadvantages. For example, despite the significance of integrating genetic and neuroimaging data, there are several caveats--for a marker to be considered an endophenotype, it must be shown to (1) be highly heritable, (2) be associated with the phenotype, (3) be independent of a clinical state, and (4) impairment must co-segregate with the illness within a family (Gershon and Goldin, 1986; Glahn et al, 2004). Taking all of these categories into account, the current study doesn't demonstrate the heritability of the endophenotypes because the study is not familial but associative.

5.4.1 Depression

In the present study depression, indicated by the BDI-II scale score, was a co-variate during statistical analysis because of its comorbidity to occur along with alcoholism, demonstrated by Merikangas and Gerlernter in 1990. Many people with alcohol problems spend a substantial portion of their lives drinking and thus have less opportunity to demonstrate independent episodes of depression. An alcoholic with true vulnerability for depression may, by natural course of the two illnesses, have no seen independent episodes (Nurnberger JI et al., 2002). Thus, although the interpretation of the linkage results (of the COGA study by Nurnberger JI et al., 2002 in Chapter 2, Section 3.2) in complex diseases is the subject of the ongoing controversy, it appears that a locus on chromosome 1 accounts for some of the familial aggregation of alcoholism and depression. None of the SNPs in this study are located on chromosome 1, where alcoholism and depression co-occur, indicating that there may not have been a need to

co-vary for depression in the statistical analysis, even though a significant positive correlation existed between the ADS scale score and the BDI-II scale score. To follow up on this, both diseases have different underlying mechanisms as well. The findings suggest that one or more genes are associated with different clinical phenotypes, or are pleiotropic. The BDNF gene and its Val66Met SNP rs6265, which causes a dysfunction in protein trafficking, have been implicated in depression and schizophrenia as well. In disorders to which multiple genetic factors contribute but for which no single factor is absolutely necessary, evidence for specific effects can differ among different data sets. A replication study is needed with data sets of a size equivalent to the original data set or the current data set could test depression as its own variable for interactions with morphological alterations and correlations to genotype. The current study suggests a relationship between depression and alcohol dependence in an associative study and is consistent with previous findings (Nurnberger et al., 2002; Merikangas et al., 1994).

5.4.2 Population Stratification

This is the presence of a systematic difference in allele frequencies between subpopulations in a population possibly due to different ancestry, especially in the context of association studies. In this study, AD L and AD H individuals were compared to one another in a 2 (AD Group: Low vs. High) x 1 (ROI) x 3 (Genotype: AA, AB, BB) mixed factorial design. One major concern with this design is that any group differences at the genetic level should not be misinterpreted as a spurious association because the population is stratified into sub-populations (e.g. age, gender, nicotine addiction, BMI, etc) that were not used in the analysis. To reduce this effect, methods can be developed and implemented to test and statistically control for this potential bias. Because the

population stratification may bias the results, and the frequency of the major and minor alleles does not reach Hardy-Weinberg Equilibrium in the current subject population, recent publications suggest methods to control Type I errors due to population stratification (review by Hutchison, Stallings, McGeary, & Bryan, 2004). The proposed method uses extra highly polymorphic markers to generate a generic estimate of population stratification that is then used to adjust the statistical test for association between the candidate marker and the outcome variable. With this in mind, one could use a set number of highly polymorphic markers, compute a χ^2 on each marker, and form a collective χ^2 to test for genetic differences across the ADS individuals (Pritchard & Rosenberg, 1999). If population stratification is seen in the cohort, further analyses of the SNP could be adjusted depending on the direction of the bias.

Sample Size

Genetic studies typically require large sample sizes (200-3000 subjects) and to detect even medium to small gene effects. In contrast, most neuroimaging studies include only 10-20 subjects. Such small studies require a strong prior hypothesis lacking in complex disease genetics and ascertainment strategies to have any chance of detecting a significant correlation. This disparity in sample size is a point of friction between traditional genetics and traditional neuroimaging. Functional neuroimaging data may represent a final common pathway for neuronal activity before it is transformed into a behavior as proposed by Hariri and Weinberger (2003). In this case, functional neuroimaging data could be significantly more sensitive to gene action than over behavior and thus far smaller sample sizes may be needed to detect activity using neuroimaging data than behavioral data. To date, the hypothesis involving AD linking to

a handful of candidate SNPs has only been tested by the present study and showed no conclusive results due to the small sample size. The number of subjects needed for imaging genomic studies is a controversy and an open debate.

Data Complexity

Both imaging and genetic data are complex, each with million of possible variables and the potential for spurious findings. To minimize computational requirements and to limit the number of potential statistical tests, many researchers reduce the imaging data to a small number of scalar values per subject (e.g. hippocampal grey matter density or amygdale activation). This was seen in the current study within Specific Aim 1, dealing with each subjects ROI measurements. Also, a small subset of available genetic information focusing on a single SNP or haplotype was also used in Specific Aim 2. Data reduction procedures are necessary because Type I error control is not yet available. Unfortunately, by significantly reducing one or both types of data, important relationships are lost as seen in the present study. Thus, the development of multi-dimensional procedures to allow whole genome-full brain analyses is necessary.

Measurement Reliability

Large scale genetic studies apply methods to determine the reliability and validity of each sample being processed (e.g. SNP consistency, gender matching) and procedures to minimize potential genotyping error. These methods are not applied in neuroimaging data, though quality and quantification procedures typically reduce error related to data acquisition and analysis. Most neuroimaging studies require significant post-processing to render raw data into behaviorally or genetically meaningful information (e.g. hippocampal demarcation, amygdalar maps of fMRI activation). However, the reliability

of these measures is generally not provided. Many neuroimaging measurements are quite reliable (Specht et al., 2003), nevertheless the relative reliability across individuals or over time of specific dependent measures should be considered when choosing measures to apply in genetic analysis.

5.4.3 Gene-by-Environment (GxE) Interactions and AD

With the heritability of AD in the range of 50-60%, there is considerable environmental influence on the phenotype, which is common for complex trait diseases. However, environmental factors weigh heavily and may be a necessary component of AD, see **Figure 39**. An individual cannot become dependent without exposure to the substance, regardless of genetic makeup. The impact of environmental factors on genetic risk of AD related to alcohol metabolizing enzymes has a very long history. At present, GxE effects can be detected reliably using behavioral assessments and specific candidate loci.

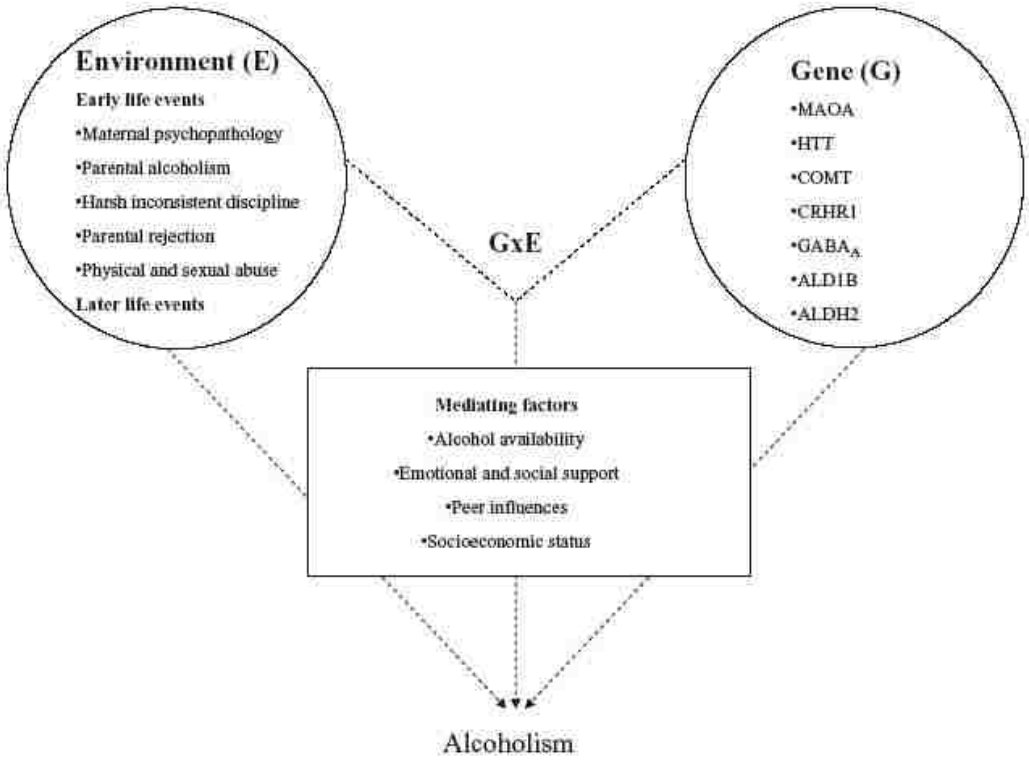

Figure 39. Main and interactive effects of genetics and environmental risk factors for alcoholism (Ducci and Goldman, 2008).

5.5 Summary and Conclusion

Alcohol dependence is a complex addictive disorder, affecting 5.4% of the general population during a lifetime (Kessler, 2005) and represents a complex heterogeneous phenotype, with behavioral, as well as psychological, pharmalogical and genetic components.

This research focuses on a translational framework on current studies of alcohol dependence and the combined fields of genetics and neuroimaging. After assessing the differences between low and high alcohol dependent individuals using ADS scale derived from DSM-IV, morphological changes in the neuroanatomical structures, gray and white matter, were identified. The use of neuroimaging measures as endophenotypes for

psychiatric illnesses could lead to new gene discoveries, and a better understanding of the mechanisms involved in these disorders. The application of imaging measures in molecular genetic investigations could significantly improve our understanding of brain function and structure.

This genomic functional approach was combined with the endophenotypes to narrow the associated gene, or biomarker, identifying a specific step in the pathway to AD. After an overview of genetic research on AD, including genome wide scans and candidate genes analyses, the genotypes of the AD individuals were obtained and correlated.

The study of AD has a long extensive history and has seen new breakthroughs and revisions of previous research in the past decade in the aspect of genetics and environment with the advent of new imaging and genetic analysis techniques.

The present research shows evidence that behavioral diseases are associated with identifiable neuroanatomic alterations, and do form relationships with specific SNPs. Additional information is needed when studying a specific, yet multifactorial disease, such as AD, but nonetheless, we advocate the use of neuroimaging measures in genetic studies. This type of translational research will significantly advance our understanding of systems level neuroscience and brain-related disorders.

APPENDIX I: DTISTUDIO METHODS FOR WHITE MATTER TRACTOGRAPHY

Construction Protocols (Wakana et al., 2008)

Cingulum Bundle Gyrus Aspect

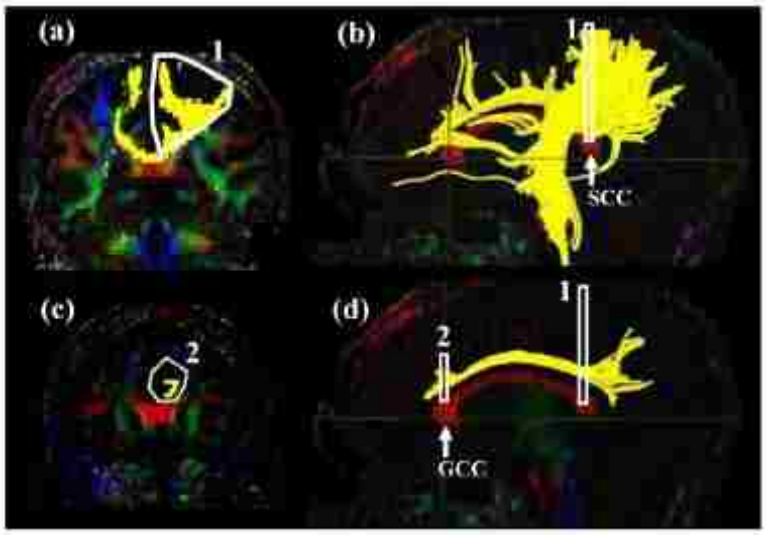

Location of the ROIs for the cingulum in the cingulated gyrus aspect (cgc) on two coronal slices (a and c) and their locations in the mis-sagittal slice (b and d). The SCC and GCC stand for the splenium of the corpus callosum and the genu of the corpus callosum, respectively.

Cingulum Bundle Hippocampal Aspect

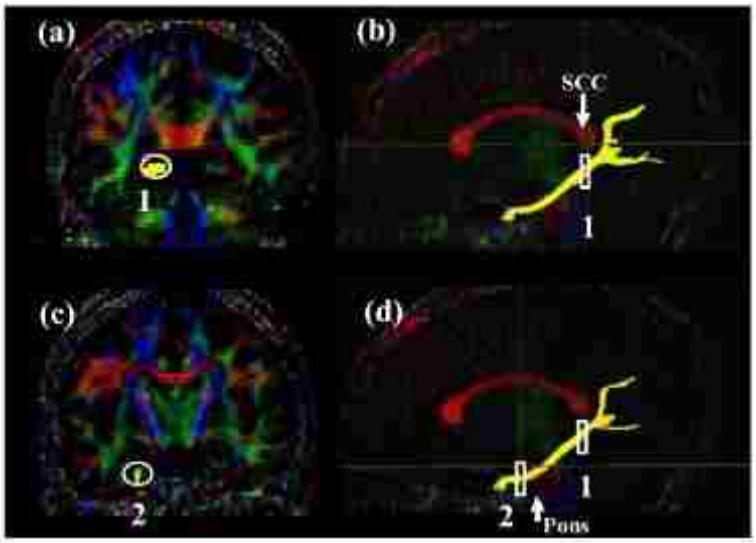

Location of the ROIs for the cingulum bundle hippocampal aspect (cgh) on two coronal slices (a and c) and their locations in the mid-saggital slice (b and d).

Corticospinal Tract

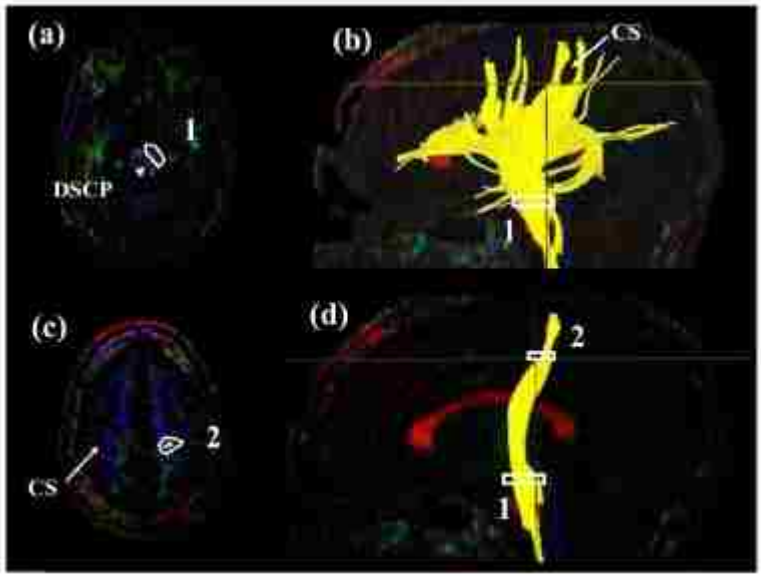

Locations of the ROIs for the corticospinal tract (CST) on two axial slices (a and c) and their locations in the mid- sagittal slice (b and d). The first ROI is drawn on the cerebral peduncle at the level of the decussation of the superior cerebellar peduncle (dscp). From the tracking seen above, the central sulcus (cs) and the projection to the motor cortex is identified. Using the axial slice right after the bifurcation to the motor cortex, the cst is selected.

Anterior Thalamic Radiation

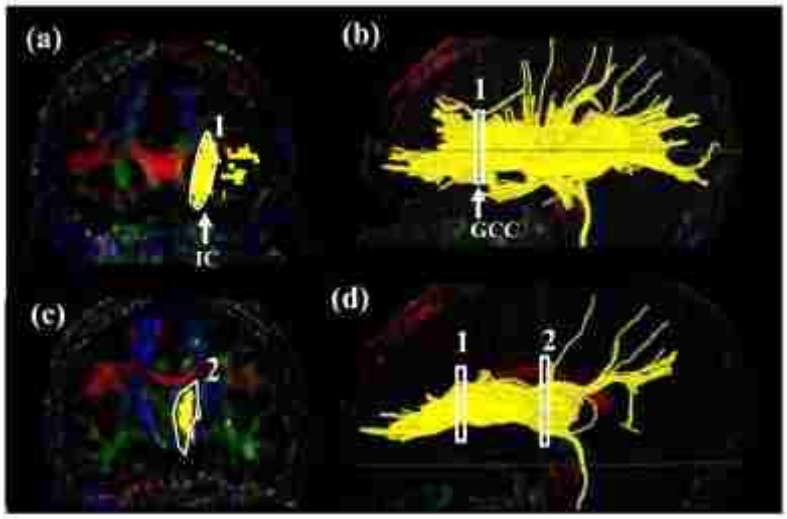

Locations of the ROIs for the anterior thalamic radiation (atr) on two coronal slices (a and c) and their locations in the mid-sagittal slice (b and d). IC, internal capsule.

Superior Longitudinal Fasciculus

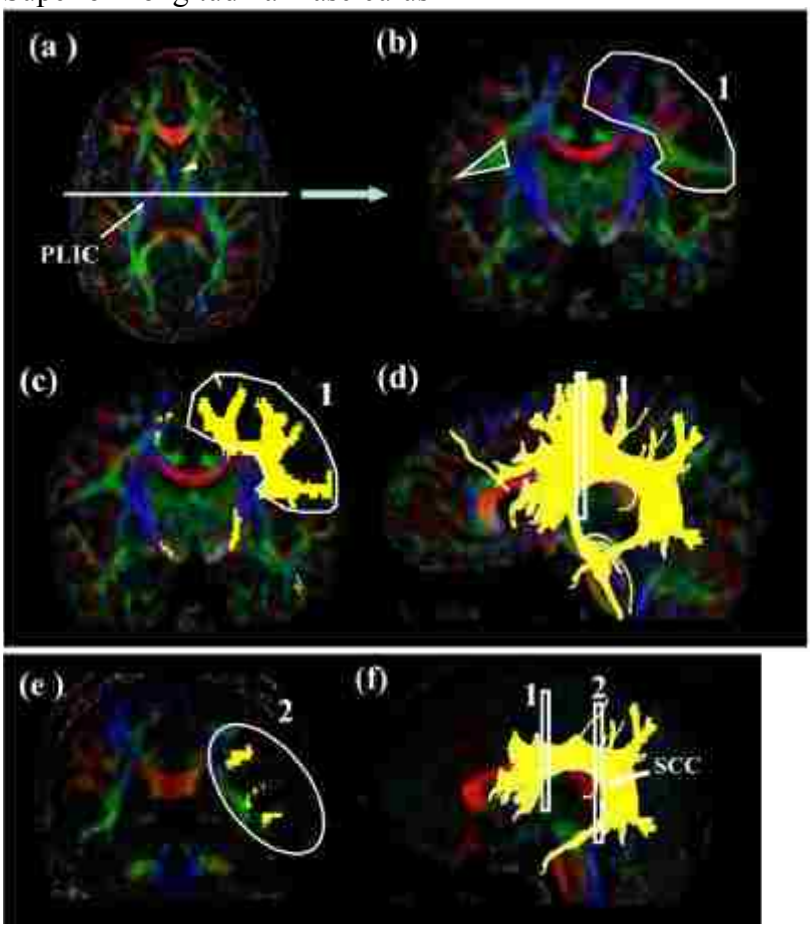

Locations of the ROIs for the superior longitudinal fasciculus (slf). At the middle of the posterior limb of the internal capsule (plic), a coronal slice if selected (b). The slf can be identified as an intense triangle shaped green structure. The first ROI is shown in (c:coronal) and (d: sagittal). For the second ROI, a coronal slice is selected at the splenium of the corpus callosum (f).

Inferior Longitudinal Fasciculus

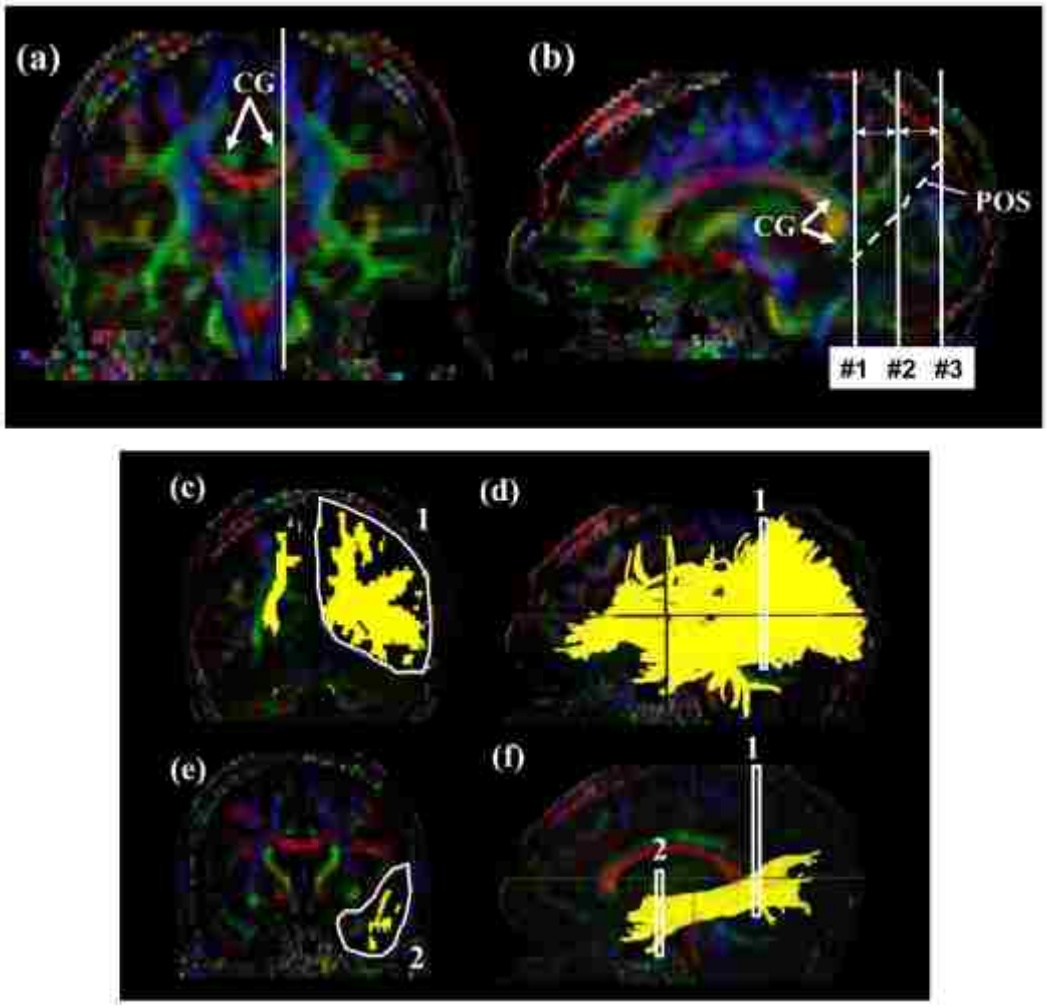

Locations of the ROIs for the inferior longitudinal fasciculus (ilf). First a para-sagittal slice (b) is identified at the level of the cingulum (a, cg). The parieto-occipital sulcus (pos) is identified in the sagittal plane. A coronal slice (c and d) is selected at the posterior edge of the cingulum (slice #1). The second ROI defines trajectories toward the anterior pole of the temporal lobe (e and f).

Inferior fronto-occipital fasciculus

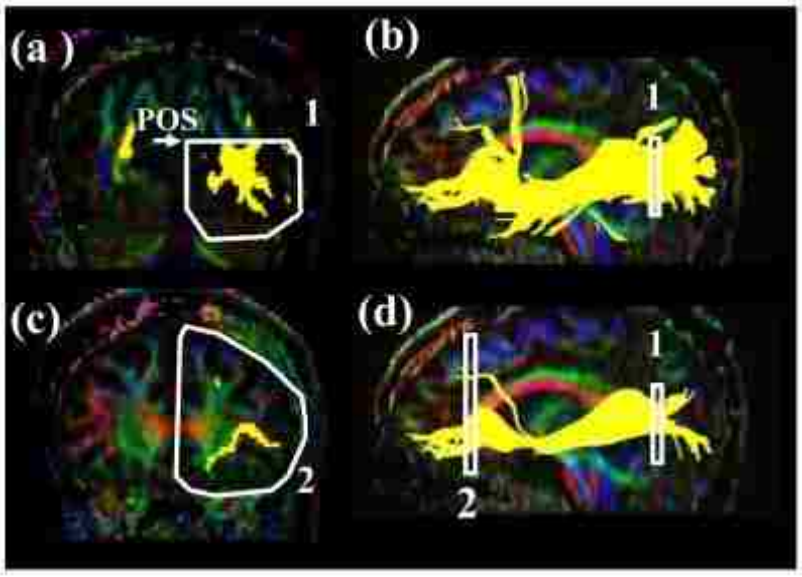

Locations of the ROIs for the inferior fronto-occipital fasciculus (ifo) on two coronal slices (a and c) and their locations in the mid-sagittal slice (b and d). For the coronal slice in (a), the #2 slice in the previous method for the ilf is used.

Uncinate Fasciculus

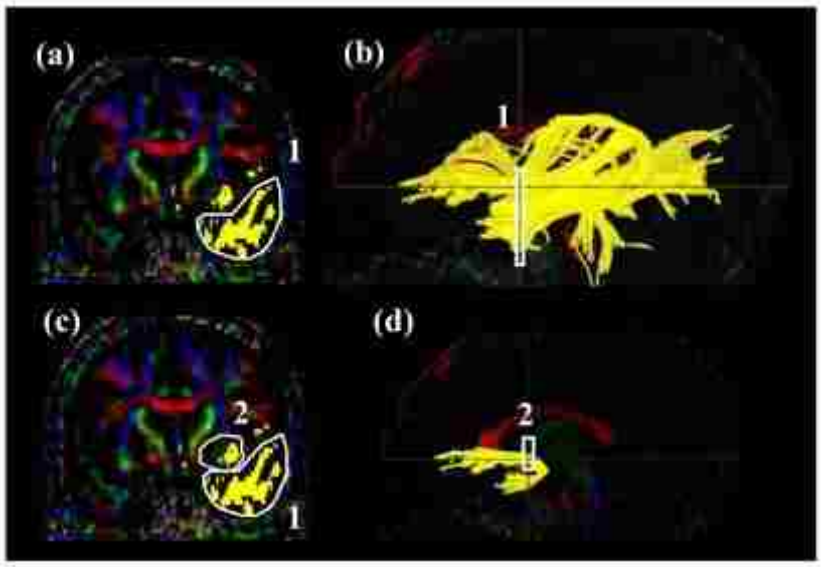

Locations of the ROIs for the uncinate fasciculus (unc) on a coronal slice (a and c) and their locations in the mid-sagittal slice (b and d). The coronal slice (a and c) is the most posterior slice where the frontal and temporal lobe is separated.

Forceps Major

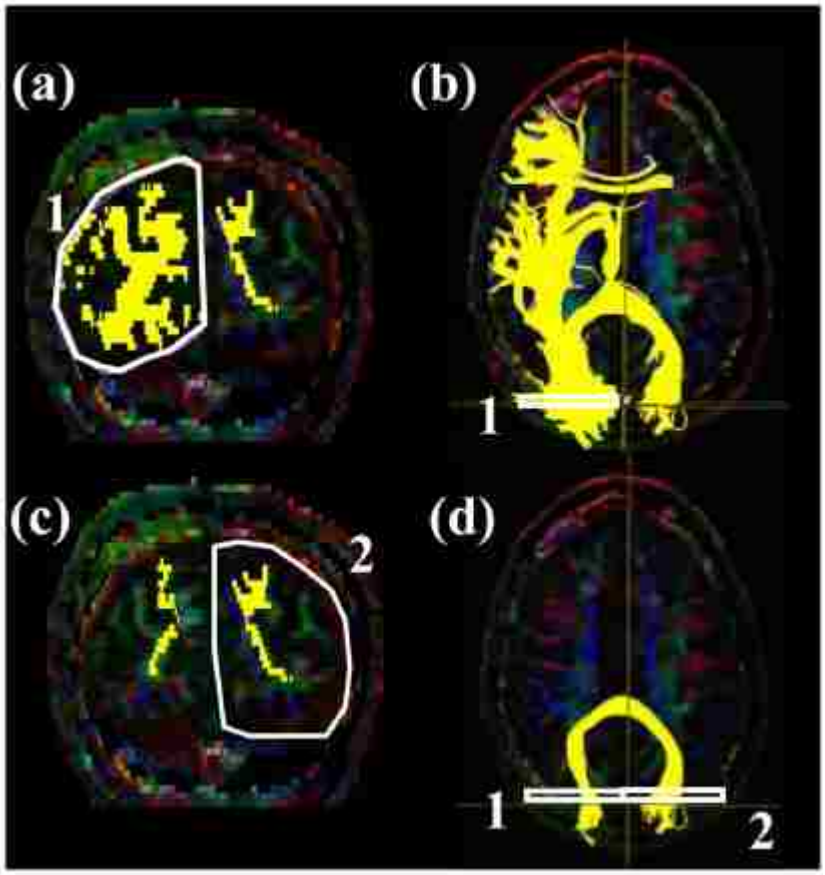

Locations of the ROIs for the occipital projection of the corpus callosum (forceps major) on a coronal slice (a and c) and their locations in an axial slice (b and d). For the coronal slice in (a) and (b), the #3 slice in the ilf is used.

Forceps Minor

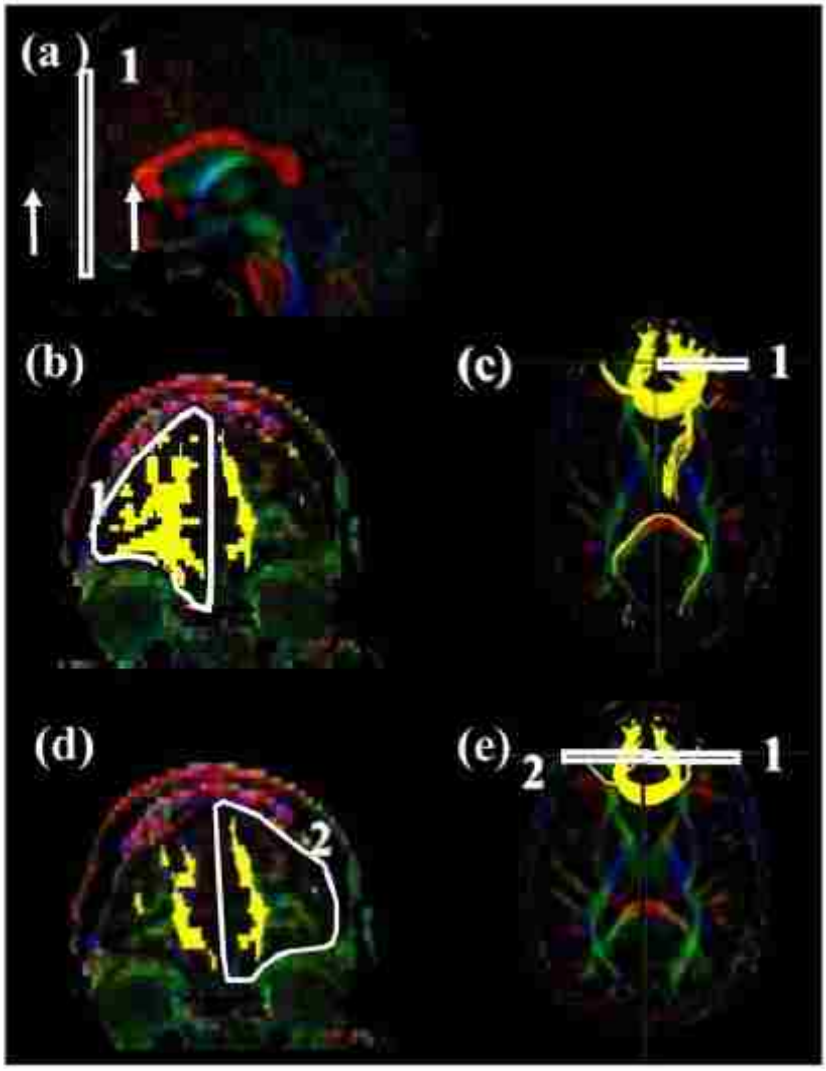

Locations of the ROIs for the frontal projection of the corpus callosum (forceps minor) on a sagittal slice (a), a coronal slice (b and d) and their locations in an axial slice (c and e).

APPENDIX II: BRAIN DERIVED NEUROTROPHIC FACTOR (BDNF) AND GENE X ENVIRONMENT INTERACTION

Looking into gene x environment interactions of human behavior is on the rise. There is great variability in behavioral and biological phenotypes than just genetic factors alone, and these provide clues into the mechanisms modifying genetic risk or resilience in addiction. We describe in brief the impact of the Val66Met polymorphism in alcohol dependence with in this research.

The anatomical information provided by neuroimaging can serve as a convenient link between anatomical alterations seen in human behavioral differences and functional genotype. Alone, each approach is limited in its information on gene function in a complex human disease, but together, a bridge formed links a genotype to a phenotype.

The BDNF gene and its protein are very versatile and vital for neuronal growth and development. BDNF is a molecule that is essential for developmental processes including, neuronal plasticity (Bramham and Messaoudi 2005; Liao et al 2007; Tongiorgi et al 2006), regulation of both short-term synaptic function and long-term activity-dependent synaptic consolidation (Thoenen 1995; Katz and Shatz, 1996), potentiation of synaptic transmission (Lohof et al 1993; Kang and Schuman, 1995; Levine et al 1995), modulation of long-term potentiation (LTP) in vitro and in vivo (Patterson et al 1996) and induction of morphological changes in dendritic spines (McAllister et al 1995). Thus, BDNF has a role in (1) synaptic plasticity; (2) inducing changes in synaptic morphology; and (3) mediating cell survival and cell proliferation

during development. These functions serve to underscore the importance of considering BDNF in any neurodevelopmental disorder of learning.

This research proposed a new direction illustrating the importance of combining genetics, neuroimaging and behavioral studies to define a role for gene x environment interaction. One of the aspects included looking at the BDNF and its impact on behavior and neuroanatomic changes. This line of thought moves us away from the idea of "risk alleles," towards recognizing that an allele may be a risk factor during a period of development and protective factor during another. Specifically, the Met allele shows decreased secretion, and results in functional deficits in learning (Egan et al, 2003). The deficit leads to impaired activity dependent release of BDNF and the expression of the Met allele has been associated with impairment in select forms of learning and memory (Egan et al, 2003) and susceptibility to psychiatric disorders (Neves-Pereira et al, 2002; Sklar et al, 2002; Sen et al, 2003; Ribases et al, 2003, 2004). So, the SNP represents the first alteration in a neurotrophin gene that has been linked to a clinical pathology. As such, the given role of BDNF is promoting learning and memory (Desai et al, 1999), it may be likely that impaired BDNF secretion, due to expression of the Met allele, may have pleiotropic effect in all BDNF-dependent processes and mechanisms.

When BDNF levels peak during adolescence (Katoh-Semba et al, 1997) the trafficking deficit due to the Met may yield only minor differences in measures. Therefore, during this period the increased BDNF expression, and the lower secretion conferred by the Val/Met or Met/Met allele may actually be protective (Gratacos et al, 2007). When BDNF levels are high, carriers of the Val/Val allele may be at greater

risk for psychiatric disorders given that anxiety, depression, and schizophrenia can increase BDNF in the amygdala and ventral striatum, areas implicated in bipolar disorder (Geller et al, 2004) and substance abuse (Matsuhita et al, 2004; Liu, 2005). In humans, BDNF mRNA levels in cortical regions increase approximately one-third from infancy to adulthood. They are relatively low during infancy and childhood, peak during young adulthood, and are maintained at a constant level throughout adulthood. The increase in BDNF at this critical time in human development may have important implications for the etiology and treatment of the severe mental disorders that tend to present during this time (Webster et al 2002). This trafficking deficit may yield only minor genotypic difference in specific types of learning for the Met allele carriers during this period of development, and potentially even be protective against other risk factors (e.g. substance abuse that has been linked to Val allele) (Gratacòs et al., 2007).

The current research provides a new direction for Imaging Genetics and illustrates the importance of examining a gene by environment interaction focusing on a single well-defined gene and SNP in collaboration with a single behavioral disease. We specifically focused on the BDNF gene because of its essential role in synapse formation, learning and development. Such an approach moves us away from "risk alleles," and brings to light the idea that an allele may be protective during one developmental period and a risk factor during another. For example, with the variant Val66Met having decreased regulated secretion, we provide preliminary, exploratory evidence of significant association of level of alcohol dependence and the SNP in morphologically altered volumes of structures involved in the addiction/reward pathway. In this case, BDNF levels peak during young adulthood, and may have a

protective effect on structures in individuals of the Val/Val genotype. Yet, due to a deficit in trafficking of BDNF, Met allele carriers may have deleterious effects on neuroanatomical structures.

With the publication of the human genome, researchers continue to uncover the functions of specific genes. These discoveries will be increased by connecting major avenues of genetic research across disciplines, using different approaches that bridge animal models and human psychiatric disorders, to explain gene–environment interactions across development. Examining how these interactions change during a developmental time period--a single snapshot in time (Viding et al., 2006) may provide a valuable new phenotype trajectory rather than genotype alone. Moreover, such an approach may move psychiatric research closer to preventive strategies for neurodevelopmental disorders with well-defined endophenotypes.

APPENDIX III: RAW GRAY MATTER DATA

Sample ID	Study	adscon	adsobs	adsper	adsphy	adstot	ADS	adsgroup	maxdrinks
M87109984	fMRI	3	0	1	3	7	0		14
M87113317	07-226-352	5	1	1	0	6	0		13
M87115517	fMRI	1	0	1	1	3	0	0	6
M87118004	fMRI	3	1	1	2	6	0		30
M87120980	fMRI	5	1	1	1	7	0		15
M87123990	07226-397	5	0	0	0	5	0	0	15
M87129006	fMRI	5	0	0	2	7	0		12
M87131456	fMRI	3	0	1	3	7	0		18
M87136065	fMRI	5	0	1	0	6	0		15
M87137660	fMRI	1	1	4	1	6	0		16
M87144978	fMRI	5	2	0	2	7	0		10
M87144991	07226-435	3	0	0	3	6	0		13
M87146401	07226-388	4	0	1	0	5	0	0	8
M87146463	07226-441	3	0	0	2	5	0		10
M87147975	fMRI	2	0	1	2	5	0	0	8.5
M87169984	fMRI	5	0	0	2	7	0		21
M87177119	07226-407	3	0	1	0	4	0	0	17
M87178340	07226-395	1	0	0	1	2	0	0	15
M87180407	07-226-354	3	0	1	1	5	0	0	15
M87180947	fMRI	3	0	1	1	5	0	0	10
M87181072	fMRI	3	0	0	0	3	0	0	12
M87182419	07226-413	1	1	1	1	3	0	0	8
M87182832	fMRI	6	0	1	0	7	0		20
M87185249	fMRI	4	1	0	0	4	0	0	10
M87189298	fMRI	1	0	1	0	2	0	0	6
M87196594	fMRI	3	0	0	0	3	0	0	5
M87109470	Tx	16	3	8	4	28	1	1	20
M87112783	07226-384	8	1	2	5	15	1		10
M87114670	fMRI	9	0	2	4	15	1		12
M87117785	07226-432	10	1	1	4	15	1		12
M87118605	07-226-175	9	3	4	4	17	1		21
M87119370	07-226-163	11	3	2	6	19	1	1	30
M87120670	07226-433	8	0	6	5	19	1	1	12
M87122697	Tx	11	2	5	1	17	1	1	12
M87148033	Tx	9	0	1	5	15	1		10
M87148957	Tx	11	0	2	4	17	1	1	7
M87151676	fMRI	11	2	5	4	20	1	1	26
M87157736	fMRI	13	0	9	5	27	1	1	22
M87165919	07-226-199	12	3	1	6	19	1	1	26
M87173074	07-226-183	11	0	2	2	15	1		30
M87188301	fMRI	11	1	2	3	16	1		34
M87189597	fMRI	11	0	1	3	15	1		15
M87195743	fMRI	11	0	2	3	16	1		12
M87150951	fMRI	10	1	3	3	16	1		12
M87198790	fMRI	10	0	3	2	15	1		15

ethnic	gender	cigs	bditot	BDI	bdigroup	age	bmi
latino	male	0	1.5	0		21	26.5
white	male	0	3	0		27	26.63
mixed	female	0	0	0	0	22	22.92
mixed	male	0	12	2		28	26.39
white	male	12	5	2		22	20.22
Latino	male	3	7	2		23	28.06
latino	female	0	0	0	0	21	25.68
Native	male	1	0	0	0	28	71.91
white	female	0	2	0		23	25.02
Asian	male	0	19	1		24	26.57
latino	male	0	10	2		24	25.56
Latino	male	0	5.5	2		23	25.84
0	female	6	5	2		26	27.95
white	female	0	1.5	0		22	24.33
white	male	15	4	2		27	23.37
mixed	male	0	2.5	0		21	20.45
white	male	0	9	2		23	27.13
white	male	0	1	0	0	25	26.57
white	male	2.5	0	0	0	28	25.84
white	male	0	0	0	0	26	25.77
white	male	0	1.5	0		21	21.18
white	female	1	14	1		24	19.77
mixed	male	0	6.5	2		22	25.84
white	male	0	0	0	0	23	25.8
latino	female	0	2.5	0		27	21.08
white	female	0	0	0	0	23	19.74
white	female	40	28.5	1	1	30	22
Latino	female	0	8.5	2		27	21.79
latino	male	0	10.5	2		21	26.63
white	male	2	6.5	2		24	21.97
latino	male	3	9	2		29	28.9
native	male	0	16	1		30	27.6
white	male	0	12	2		29	22.89
latino	male	0	4	2		28	21.3
mixed	male	0	24	1	1	28	31.9
mixed	male	2	10.5	2		25	27.4
mixed	male	0	13.5	2		21	25.37
white	male	1	8	2		25	24.73
white	Male	3	6.5	2		28	26.8
white	male	8	3	0		22	37.4
mixed	male	2	18	1		25	36.87
latino	male	0	6	2		28	25.09
white	male	0	22.5	1	1	22	23.5
white	male	4	7.5	2		30	22.47
mixed	male	0	4	2		22	22.6

Cereb.Cortex RIGHT	Thalamus RIGHT	Caudate RIGHT	Putamen RIGHT	Hippocampus RIGHT
249835	7290	3888	5412	3967
273903	7335	3626	5448	4579
282123	7516	4334	5722	4536
252220	7210	2962	5099	4052
282412	8814	4012	7318	5025
243200	7221	3059	5517	3708
273742	7833	3696	5761	4731
259553	7707	3569	5061	4736
296794	7420	4559	6290	4695
254770	7616	3762	6340	4419
243787	7638	3524	6153	4042
283182	8798	4438	5686	4209
234224	7361	3527	5016	3470
268612	6797	3116	4430	4427
283047	7758	3856	6075	4713
256906	7219	3988	5461	4699
243263	7904	4033	6241	4218
292737	7476	3166	6533	4277
247970	7792	3629	6219	4829
269860	7835	4046	6267	5160
284160	8685	4448	5953	4169
220824	6885	3281	5067	4154
282291	7264	3874	5789	4343
250441	7390	4062	6156	4633
247854	8472	3715	4952	4246
248111	7431	3744	5754	4373
199465	7599	3049	4882	3761
230154	6547	3521	5108	4058
255342	7217	3073	5376	4290
264433	7776	4449	5833	4024
258257	7031	2891	5704	4305
269102	7649	4347	6335	4471
298019	8447	5297	6380	4901
247962	7768	3926	5626	4468
286551	7954	4183	6722	4612
266754	7333	3397	5937	3980
296024	8131	4719	5843	4874
272228	8194	3660	6606	4693
267616	8355	3450	5374	4682
290147	7713	4123	5801	4273
277034	8223	3912	6444	4207
272974	7780	5162	6605	4815
273890	7933	3865	6187	4670
280373	8033	4309	6712	4601
266809	9262	4417	6244	4852

Amygdala RIGHT	Accumbens RIGHT	Cereb.Cortex LEFT	Thalamus LEFT	Caudate LEFT
1616	670	257398	7426	3850
1771	747	268491	7037	3521
1753	730	285573	7195	4178
1715	730	258074	7197	3180
1862	543	280577	9294	3877
1439	528	243335	6993	3325
1790	814	269974	7745	3444
1901	557	258938	7481	3588
1743	760	298728	7339	4531
1408	677	259052	7658	3750
1588	569	236037	6825	3297
1623	708	280532	8786	4565
1577	680	239629	7083	3492
1518	746	866374	6440	3215
1754	847	280800	7120	3647
1408	555	251730	6889	3846
1448	586	244468	7534	3856
1809	771	296623	7225	3029
1591	606	242359	7529	3380
1852	704	266700	7682	3888
1781	668	274881	8458	4464
1718	505	219171	7015	3239
2092	618	289069	7058	3825
1771	698	254314	6911	3923
1624	667	251425	8122	3832
1821	683	251854	7126	3545
1356	593	205155	7416	3220
1260	657	229918	6238	3568
1411	717	261621	7166	3538
1810	796	253319	7194	4639
1861	619	250966	7100	2887
1843	637	264360	7448	4021
1824	697	301418	8406	5271
1768	527	248467	7629	3895
1795	965	291851	7378	4007
1576	566	269092	7208	3725
1873	663	297973	8451	4083
1836	905	275105	7991	3715
1738	646	259494	8525	3883
1691	760	285600	7786	3662
1730	842	276895	8066	4006
1715	958	280403	7624	5488
1806	780	279796	7278	3673
1751	754	273639	7872	4198
1786	752	265440	9044	4307

Putamen LEFT	Hippocampus LEFT	Amygdala LEFT	Accumbens LEFT	WMHI
6012	4101	1533	444	1298
5895	4725	1733	563	1097
5992	4498	1792	656	1254
5644	4016	1899	498	726
7075	5078	1874	812	999
6209	3705	1448	515	1014
5742	4431	1671	661	2201
5801	4696	1852	620	1406
6891	4926	1834	778	1603
6846	4298	1665	521	2485
6232	3904	1631	453	958
6140	4263	1579	602	1122
5441	3531	1488	642	1216
5000	4387	1501	474	1478
5891	4670	1724	618	1247
5685	4442	1727	596	769
6720	4233	1532	541	1665
6647	4468	1867	777	1694
6451	4845	1755	451	1292
6481	5163	2060	662	3158
6257	4036	1755	610	617
5282	4039	1632	440	155
5693	4062	2056	393	686
6142	4115	1626	555	1576
5533	4218	1659	563	1056
6426	4632	1748	568	1386
5539	3921	1323	430	889
5241	4089	1388	482	723
6130	4198	1642	554	1529
6193	4150	1813	631	1995
6049	4144	1515	630	2243
6474	4357	1731	612	1384
6773	4651	2013	629	844
5879	4572	1822	513	1530
6946	4485	1700	928	1252
6329	3916	1469	467	2189
5961	5148	1773	620	2365
6974	4769	1746	731	1704
6029	4976	1878	559	2009
6021	4575	1343	560	3615
6500	3946	1645	599	1328
7319	4698	1904	843	620
6894	4736	1755	638	844
6650	4739	1856	602	2030
5973	4886	1867	645	1297

CC_Posterior	CC_MidPosterior	CC_Central	CC_MidAnterior	CC_Anterior	CC_Whole
775	397	411	386	837	2806
805	441	388	390	918	2942
994	568	455	432	856	3305
938	467	690	562	664	3321
1119	499	502	574	1177	3871
694	382	481	390	781	2728
1037	367	477	529	1097	3507
792	433	434	417	865	2941
1172	587	551	519	1072	3901
877	525	439	522	874	3237
880	533	657	540	1014	3624
1137	593	581	744	1013	4068
1265	590	559	701	988	4103
887	419	640	712	784	3442
818	431	443	446	664	2802
813	444	481	499	838	3075
657	391	412	409	829	2698
1024	556	577	532	1046	3735
1256	536	476	467	964	3699
734	465	489	479	917	3084
747	271	407	493	962	2880
934	487	688	641	812	3562
1124	640	558	530	955	3807
855	396	381	422	707	2761
988	508	495	600	931	3522
891	559	442	416	762	3070
767	458	606	569	801	3201
947	461	426	502	732	3068
825	475	478	457		2235
999	458	522	587	1028	3594
978	487	475	517	974	3431
936	378	393	367	937	3010
1094	627	679	691	1122	4213
898	402	388	453	980	3121
1033	517	470	467	908	3395
925	472	436	470	1033	3336
1180	462	404	398	936	3380
1007	412	533	535	761	3248
1063	587	558	553	934	3695
893	506	616		1166	3181
913	443	395	452	932	3135
851	505	502	484	899	3241
748	403	563	473	650	2837
947	448	440	509	840	3184
938	579		551	985	3053

	Gray Matter SNPs						
Name	rs6265	s10780961	rs1822420	rs4304401	rs980455	rs230530	rs1609798
M87109984	AA	AB	BB	AA	AB	AB	BB
M87113317	AB	AB	BB	AB	AA	AB	BB
M87115517	AA	AB	BB	AB	AB	AB	AB
M87118004	AB	AB	BB	AB	AA	AB	BB
M87120980	BB	BB	AB	AA	BB	AA	AB
M87123990	AB	AA	BB	AA	AB	AB	BB
M87129006	BB	BB	BB	AA	AA	AB	BB
M87131456	BB	BB	BB	AB	BB	AA	AA
M87136065	BB	AB	AB	AA	AB	AB	AB
M87137660	BB	BB	BB	AA	AA	AB	AB
M87144978	AB	BB	AB	AA	AB	AA	AB
M87144991	BB	AB	BB	AB	BB	AA	AA
M87146401	BB	AB	AB	AA	AA	AB	BB
M87146463	AB	BB	BB	AB	AB	AB	AB
M87147975	BB	AA	BB	AA	BB	AA	AA
M87169984	AB	AB	BB	AA	AB	AB	AB
M87177119	BB	BB	AB	AA	AA	AB	BB
M87178340	BB	AA	BB	NC	BB	AB	AB
M87180407	BB	AB	BB	AA	AB	AB	BB
M87180947	AA	AB	BB	AA	AA	BB	BB
M87181072	BB	AB	BB	AA	AA	BB	BB
M87182419	AB	AB	BB	AA	AB	AB	AB
M87182832	BB	BB	BB	AB	BB	AA	AA
M87185249	BB	AA	BB	AA	AA	AB	BB
M87189298	BB	AB	BB	AB	BB	AA	AA
M87196594	BB	AB	BB	AA	AB	AA	AB
M87109470	BB	AB	BB	AB	AB	AB	AB
M87112783	BB	AB	AB	AA	AA	BB	BB
M87114670	BB	BB	BB	AB	AB	AA	AB
M87117785	BB	AB	BB	AB	BB	AA	BB
M87118605	AB	AA	BB	AA	AB	AB	AB
M87119370	AB	AA	BB	AA	AB	AB	BB
M87120670	AB	AB	AB	AA	AB	AB	BB
M87122697	BB	AB	BB	AA	BB	AA	AA
M87148033	BB	BB	BB	AA	AB	AA	BB
M87148957	BB	BB	BB	AB	AA	AB	BB
M87151676	BB	AB	BB	AB	AA	BB	BB
M87157736	BB	AA	BB	AA	AA	BB	BB
M87165919	BB	BB	BB	AB	AB	AB	BB
M87173074	BB	AB	AB	AA	AB	AB	BB
M87188301	BB	AA	BB	AA	AB	AB	AB
M87189597	BB	AB	AB	AA	AB	AB	AB
M87195743	BB	AB	BB	AA	AB	AA	AB
M87150951	BB	AA	BB	AA	AB	AB	AB
M87198790	BB	BB	AB	AB	AB	AB	AB
Chr	11	9	9	9	4	4	4
AA Freq	0.066667	0.2	0	0.659091	0.288889	0.288889	0.133333
AB Freq	0.222222	0.511111	0.222222	0.340909	0.511111	0.6	0.4
BB Freq	0.711111	0.288889	0.777778	0	0.2	0.111111	0.466667
Minor Freq	0.177778	0.455556	0.111111	0.170455	0.455556	0.411111	0.333333

APPENDIX IV: RAW WHITE MATTER DATA

Sample ID	Study	adscon	adsobs	adsper	adsphy	adstot	ADS
M87109984	fMRI	3	0	1	3	7	0
M87113317	07-226-362	5	1	1	0	6	0
M87115517	fMRI	1	0	1	1	3	0
M87118004	fMRI	3	1	1	2	6	0
M87120980	fMRI	5	1	1	1	7	0
M87123990	07226-397	5	0	0	0	5	0
M87129006	fMRI	5	0	0	2	7	0
M87131456	fMRI	3	0	1	3	7	0
M87137660	fMRI	1	1	4	1	6	0
M87146463	07226-441	3	0	0	2	5	0
M87169984	fMRI	5	0	0	2	7	0
M87177119	07226-407	3	0	1	0	4	0
M87178340	07226-395	1	0	0	1	2	0
M87180407	07-226-354	3	0	1	1	5	0
M87180947	fMRI	3	0	1	1	5	0
M87181072	fMRI	3	0	0	0	3	0
M87182419	07226-413	1	1	1	1	3	0
M87182832	fMRI	6	0	1	0	7	0
M87185249	fMRI	4	1	0	0	4	0
M87189298	fMRI	1	0	1	0	2	0
M87196594	fMRI	3	0	0	0	3	0
M87109470	Tx	16	3	8	4	28	1
M87112783	07226-384	8	1	2	5	15	1
M87114670	fMRI	9	0	2	4	15	1
M87117785	07226-432	10	1	1	4	15	1
M87120670	07226-433	8	0	6	5	19	1
M87122697	Tx	11	2	5	1	17	1
M87148033	Tx	9	0	1	5	15	1
M87148957	Tx	11	0	2	4	17	1
M87151676	fMRI	11	2	5	4	20	1
M87165919	07-228-199	12	3	1	6	19	1
M87188301	fMRI	11	1	2	3	16	1
M87189597	fMRI	11	0	1	3	15	1
M87195743	fMRI	11	0	2	3	16	1
M87150951	fMRI	10	1	3	3	16	1
M87198790	fMRI	10	0	3	2	15	1

adsgroup	maxdrinks	ethnic	gender	cigs	bditot	BDI
	14	latino	male	0	1.5	0
	13	white	male	0	3	0
0	6	mixed	female	0	0	0
	30	mixed	male	0	12	2
	15	white	male	12	5	2
0	15	Latino	male	3	7	2
	12	latino	female	0	0	0
	18	Native	male	1	0	0
	16	Asian	male	0	19	1
	10	white	female	0	1.5	0
	21	mixed	male	0	2.5	0
0	17	white	male	0	9	2
0	15	white	male	0	1	0
0	15	white	male	2.5	0	0
0	10	white	male	0	0	0
0	12	white	male	0	1.5	0
0	8	white	female	1	14	1
	20	mixed	male	0	6.5	2
0	10	white	male	0	0	0
0	6	latino	female	0	2.5	0
0	5	white	female	0	0	0
1	20	white	female	40	28.5	1
	10	Latino	female	0	8.5	2
	12	latino	male	0	10.5	2
	12	white	male	2	6.5	2
1	12	white	male	0	12	2
1	12	latino	male	0	4	2
	10	mixed	male	0	24	1
1	7	mixed	male	2	10.5	2
1	26	mixed	male	0	13.5	2
1	26	white	Male	3	6.5	2
	34	mixed	male	2	18	1
	15	latino	male	0	6	2
	12	white	male	0	22.5	1
	12	white	male	4	7.5	2
	15	mixed	male	0	4	2

bdigroup	age	bmi
	21	26.5
	27	26.63
0	22	22.92
	28	26.39
	22	20.22
	23	28.06
0	21	25.68
0	28	71.91
	24	26.57
	22	24.33
	21	20.45
	23	27.13
0	25	26.57
0	28	25.84
0	26	25.77
	21	21.18
	24	19.77
	22	25.64
0	23	25.8
	27	21.08
0	23	19.74
1	30	22
	27	21.79
	21	26.63
	24	21.97
	29	22.89
	28	21.3
1	28	31.9
	25	27.4
	21	25.37
	28	26.6
	25	36.87
	28	25.09
1	22	23.5
	30	22.47
	22	22.6

Cingulum Bundle (hippocampal part) RIGHT						
VOL	FA	MD	L1 / Axial D	L2	L3	Radial D
560	0.4164	0.00098	0.00146	0.00082	0.00066	0.00074
1112	0.39933	0.00081	0.00119	0.00069	0.00054	0.00062
704	0.363951	0.00088	0.00125	0.00078	0.00061	0.0007
1296	0.3683	0.00083	0.00117	0.00075	0.00056	0.00066
2512	0.41914	0.00082	0.00123	0.0007	0.00052	0.00061
856	0.38152	0.00085	0.00122	0.00079	0.00056	0.00067
2008	0.38228	0.00094	0.00136	0.00084	0.00063	0.00073
672	0.38862	0.00089	0.00127	0.00081	0.00058	0.00069
888	0.41976	0.00089	0.00131	0.00076	0.00058	0.00067
1392	0.40741	0.00085	0.00125	0.00077	0.00054	0.00065
296	0.31915	0.00101	0.00137	0.00092	0.00074	0.00083
600	0.37765	0.00083	0.00119	0.00075	0.00055	0.00065
1216	0.40757	0.00082	0.00121	0.00073	0.00053	0.00063
480	0.45912	0.00076	0.00117	0.00064	0.00046	0.00055
264	0.38885	0.00096	0.00139	0.00084	0.00066	0.00075
2008	0.371975	0.00093	0.00132	0.00084	0.00064	0.00074
272	0.42914	0.00083	0.00124	0.0007	0.00054	0.00062
936	0.34463	0.00087	0.00121	0.0008	0.00061	0.00071
304	0.3922	0.00097	0.00142	0.0008	0.0007	0.00075
1360	0.340584	0.00102	0.00142	0.00092	0.00072	0.00082
1704	0.37832	0.00087	0.00125	0.00078	0.00059	0.00068
1128	0.38554	0.00102	0.00146	0.00088	0.0007	0.00079
1488	0.41081	0.00083	0.00123	0.00071	0.00054	0.00063
416	0.398637	0.00084	0.00124	0.00071	0.00057	0.00064
1048	0.44654	0.00081	0.00123	0.00073	0.00048	0.0006
1888	0.43471	0.00082	0.00123	0.00072	0.0005	0.00061
2056	0.47036	0.00081	0.00128	0.00067	0.00049	0.00058
1200	0.37926	0.00083	0.0012	0.00078	0.00054	0.00065
616	0.37273	0.00083	0.00118	0.00071	0.00058	0.00065
1936	0.400181	0.00081	0.00119	0.00073	0.00052	0.00062
1080	0.44886	0.00081	0.00124	0.00071	0.00049	0.0006
1400	0.40272	0.00085	0.00124	0.00076	0.00054	0.00065
1088	0.353868	0.00084	0.00118	0.00074	0.00059	0.00067
792	0.408643	0.00083	0.00124	0.00072	0.00055	0.00063
432	0.36002	0.00088	0.00124	0.00076	0.00063	0.0007
768	0.390789	0.00088	0.00128	0.00078	0.0006	0.00069

Cingulum Bundle (hippocampal part) LEFT						
VOL	FA	MD	L1 / Axial D	L2	L3	Radial D
864	0.3778	0.00088	0.00126	0.00078	0.0006	0.00069
1024	0.45771	0.00076	0.00118	0.00063	0.00047	0.00055
632	0.420578	0.00087	0.0013	0.00073	0.00057	0.00065
544	0.36902	0.00071	0.00102	0.00064	0.00049	0.00056
1048	0.39485	0.00079	0.00115	0.00073	0.00051	0.00062
920	0.4091	0.00076	0.00112	0.00066	0.00049	0.00057
1600	0.41054	0.00082	0.0012	0.00075	0.00051	0.00063
680	0.45603	0.00069	0.00104	0.00061	0.00043	0.00052
520	0.41263	0.00074	0.0011	0.00064	0.00049	0.00056
1440	0.46124	0.00076	0.00116	0.00066	0.00044	0.00055
1872	0.41024	0.0008	0.00119	0.00071	0.00051	0.00061
1472	0.41184	0.00076	0.00112	0.00067	0.00048	0.00057
2296	0.46296	0.00076	0.00119	0.00065	0.00045	0.00055
680	0.45083	0.00074	0.00113	0.00065	0.00044	0.00055
1496	0.44416	0.0008	0.00122	0.00071	0.00048	0.00059
1040	0.357011	0.00079	0.00111	0.00071	0.00056	0.00063
872	0.45481	0.00095	0.00145	0.00081	0.0006	0.0007
976	0.38995	0.00073	0.00104	0.00068	0.00047	0.00057
1776	0.37893	0.00078	0.00114	0.00069	0.00053	0.00061
1344	0.32111	0.00077	0.00104	0.00073	0.00055	0.00064
872	0.41847	0.00081	0.00122	0.0007	0.00051	0.00061
1616	0.3997	0.00082	0.00119	0.00073	0.00052	0.00063
2136	0.45647	0.00079	0.00124	0.00067	0.00048	0.00057
544	0.409376	0.00073	0.00109	0.00061	0.00048	0.00055
448	0.44715	0.00069	0.00105	0.00061	0.00042	0.00051
1096	0.42883	0.0007	0.00105	0.00062	0.00043	0.00053
816	0.3867	0.00078	0.00112	0.00069	0.00052	0.00061
1896	0.40455	0.00078	0.00114	0.00071	0.00051	0.00061
1240	0.43756	0.00069	0.00103	0.00059	0.00043	0.00051
1784	0.397275	0.0008	0.00117	0.0007	0.00052	0.00061
480	0.40123	0.00072	0.00106	0.00064	0.00047	0.00056
1064	0.37808	0.00082	0.00118	0.00072	0.00057	0.00065
920	0.421229	0.00082	0.0012	0.00071	0.00055	0.00063
1272	0.354391	0.00078	0.00109	0.00071	0.00054	0.00063
960	0.38379	0.00079	0.00115	0.0007	0.00053	0.00062
520	0.346083	0.00079	0.0011	0.0007	0.00057	0.00064

Cingulum Bundle (gyrus) RIGHT						
VOL	FA	MD	L1 / Axial D	L2	L3	Radial D
1872	0.45191	0.00076	0.00117	0.00066	0.00045	0.00055
1344	0.42927	0.00087	0.00131	0.00076	0.00053	0.00065
560	0.472534	0.00078	0.00124	0.00064	0.00047	0.00055
1984	0.44452	0.0008	0.00123	0.00071	0.00048	0.00059
3392	0.44246	0.00079	0.00121	0.00068	0.00048	0.00058
1792	0.44279	0.00078	0.00118	0.00069	0.00046	0.00058
1640	0.41244	0.00079	0.00117	0.00071	0.00049	0.0006
712	0.46678	0.00083	0.00129	0.00074	0.00046	0.0006
1568	0.44007	0.00081	0.00121	0.00075	0.00047	0.00061
1984	0.46548	0.0008	0.00126	0.00069	0.00047	0.00058
2224	0.43892	0.00085	0.00127	0.00077	0.0005	0.00063
560	0.49398	0.00084	0.00135	0.00069	0.00048	0.00058
1040	0.5473	0.00076	0.00129	0.00062	0.00037	0.0005
1968	0.46278	0.00082	0.00126	0.00073	0.00046	0.0006
1368	0.4412	0.00083	0.00126	0.00075	0.00049	0.00062
3456	0.446557	0.00079	0.00122	0.00068	0.00048	0.00058
1016	0.44063	0.00088	0.00134	0.00078	0.00052	0.00065
2600	0.48421	0.00078	0.00125	0.00065	0.00045	0.00055
1904	0.46252	0.00078	0.00122	0.00069	0.00045	0.00057
1608	0.440046	0.00081	0.00124	0.0007	0.00049	0.0006
2432	0.43078	0.0008	0.00121	0.00071	0.00049	0.0006
3248	0.40245	0.00082	0.0012	0.00074	0.00051	0.00063
808	0.43678	0.00082	0.00122	0.00079	0.00046	0.00062
488	0.531765	0.00074	0.00123	0.00062	0.00039	0.0005
2424	0.49088	0.00076	0.00121	0.00065	0.00041	0.00053
1976	0.53207	0.00078	0.00131	0.00063	0.00041	0.00052
4744	0.4641	0.00077	0.0012	0.00067	0.00044	0.00055
1568	0.47765	0.00078	0.00123	0.00069	0.00043	0.00058
632	0.47479	0.00085	0.00132	0.00078	0.00046	0.00062
656	0.458171	0.00079	0.00121	0.0007	0.00045	0.00057
7848	0.45908	0.00075	0.00116	0.00066	0.00043	0.00054
464	0.46115	0.00078	0.0012	0.00072	0.00043	0.00058
1368	0.45371	0.00082	0.00126	0.00075	0.00046	0.00061
848	0.460768	0.00083	0.00128	0.00072	0.00048	0.0006
2472	0.4216	0.00077	0.00114	0.00069	0.00047	0.00058
2232	0.462198	0.00088	0.00136	0.00077	0.00051	0.00064

Cingulum Bundle (gyrus) LEFT						
VOL	FA	MD	L1 / Axial D	L2	L3	Radial D
4128	0.44787	0.0008	0.00122	0.00069	0.00048	0.00058
2264	0.51635	0.00076	0.00125	0.00063	0.0004	0.00052
1568	0.509081	0.00076	0.00126	0.00062	0.00041	0.00052
1768	0.48632	0.00079	0.00126	0.00069	0.00043	0.00056
3024	0.04845	0.00078	0.00125	0.00065	0.00045	0.00055
2200	0.45183	0.00079	0.00121	0.00069	0.00047	0.00058
2848	0.45839	0.0082	0.00127	0.0007	0.00048	0.00059
3464	0.47894	0.00083	0.00129	0.00073	0.00046	0.00059
2368	0.48707	0.00078	0.00123	0.00067	0.00043	0.00055
2776	0.51412	0.00078	0.00129	0.00064	0.00041	0.00053
6288	0.4558	0.00082	0.00126	0.00074	0.00047	0.0006
2864	0.50618	0.00074	0.0012	0.00062	0.00039	0.00051
1256	0.57502	0.00073	0.00127	0.00058	0.00033	0.00046
1424	0.52366	0.00078	0.00128	0.00068	0.00038	0.00053
2384	0.46315	0.00085	0.00132	0.00076	0.00048	0.00062
4144	0.490502	0.00075	0.00121	0.00062	0.00042	0.00052
1552	0.47184	0.00083	0.0013	0.00073	0.00046	0.0006
3776	0.49139	0.00078	0.00125	0.00066	0.00043	0.00055
2744	0.48236	0.00082	0.0013	0.00068	0.00046	0.00057
2312	0.434563	0.00082	0.00124	0.00073	0.0005	0.00061
2072	0.48268	0.0008	0.00127	0.00067	0.00046	0.00056
2064	0.45341	0.00084	0.00129	0.00073	0.00049	0.00061
776	0.45244	0.0008	0.00123	0.00073	0.00046	0.00059
656	0.519238	0.0007	0.00115	0.00066	0.00037	0.00047
4184	0.4997	0.00073	0.00118	0.0006	0.0004	0.0005
6736	0.51238	0.00078	0.00127	0.00066	0.00041	0.00053
3304	0.50998	0.00073	0.0012	0.00061	0.00039	0.0005
2984	0.48978	0.00081	0.00129	0.00068	0.00045	0.00057
2080	0.45461	0.00082	0.00126	0.00073	0.00047	0.0006
1696	0.490954	0.00079	0.00126	0.00067	0.00043	0.00055
6296	0.49594	0.00078	0.00126	0.00065	0.00043	0.00054
2912	0.49307	0.00078	0.00125	0.00066	0.00043	0.00054
5680	0.476207	0.00082	0.00129	0.00071	0.00045	0.00058
968	0.510274	0.0008	0.00131	0.00067	0.00042	0.00054
6472	0.44442	0.00081	0.00124	0.00069	0.00049	0.00059
3064	0.493966	0.0008	0.00129	0.00068	0.00044	0.00056

Inferior-frontal occipital fasciculus RIGHT						
VOL	FA	MD	L1 / Axial D	L2	L3	Radial D
5512	0.46815	0.00083	0.0013	0.00072	0.00049	0.0006
13816	0.43595	0.00085	0.00128	0.00075	0.00052	0.00063
7664	0.44349	0.00084	0.00128	0.00073	0.00051	0.00062
9064	0.451	0.00082	0.00126	0.00071	0.00049	0.0006
11200	0.46546	0.00081	0.00127	0.00069	0.00047	0.00058
9240	0.48057	0.0008	0.00126	0.0007	0.00044	0.00057
5944	0.46086	0.00089	0.00139	0.00076	0.00053	0.00065
1296	0.44901	0.009	0.00137	0.00079	0.00053	0.00066
11272	0.47057	0.00083	0.00129	0.00071	0.00048	0.00059
7288	0.47725	0.00081	0.00129	0.00069	0.00047	0.00058
8656	0.44711	0.00086	0.00132	0.00077	0.0005	0.00064
6880	0.49043	0.00079	0.00126	0.00067	0.00043	0.00055
13256	0.46987	0.00078	0.00122	0.00068	0.00045	0.00056
10328	0.45882	0.00082	0.00125	0.00072	0.00047	0.0006
4024	0.46834	0.00082	0.00128	0.00074	0.00046	0.0006
13496	0.45888	0.00083	0.00129	0.0007	0.0005	0.0006
3880	0.47693	0.00084	0.00131	0.00073	0.00047	0.0006
11792	0.48134	0.00082	0.00129	0.0007	0.00046	0.00058
10424	0.46268	0.00081	0.00125	0.00071	0.00046	0.00058
7456	0.48149	0.00082	0.0013	0.00069	0.00046	0.00058
9904	0.45019	0.00084	0.00129	0.00072	0.0005	0.00061
7992	0.461	0.00087	0.00135	0.00076	0.00051	0.00063
2856	0.43166	0.00091	0.00135	0.00081	0.00056	0.00069
1496	0.5202	0.00082	0.00136	0.00069	0.00042	0.00056
11312	0.49842	0.00078	0.00125	0.00066	0.00043	0.00054
7904	0.52636	0.00082	0.00134	0.00067	0.00044	0.00056
10056	0.46658	0.00081	0.00126	0.00069	0.00048	0.00058
8864	0.46556	0.00083	0.0013	0.00071	0.00049	0.0006
9592	0.49564	0.00078	0.00125	0.00068	0.00042	0.00055
12232	0.4549	0.00079	0.00122	0.00068	0.00047	0.0006716
8064	0.48588	0.00086	0.00135	0.00073	0.00049	0.00061
4744	0.46724	0.00087	0.00134	0.00075	0.0005	0.00063
13664	0.45923	0.00082	0.00127	0.0007	0.00048	0.00059
7144	0.45478	0.00085	0.00131	0.00074	0.0005	0.00062
4104	0.44597	0.00086	0.0013	0.00074	0.00053	0.00063
10312	0.47496	0.00083	0.00131	0.0007	0.00048	0.00059

Inferior-frontal occipital fasciculus LEFT						
VOL	FA	MD	L1 / Axial D	L2	L3	Radial D
11864	0.47921	0.00082	0.00129	0.0007	0.00047	0.00059
15408	0.45418	0.00084	0.0013	0.00073	0.00051	0.00062
11656	0.4539	0.0008	0.00123	0.00071	0.00046	0.00059
15312	0.4584	0.0008	0.00124	0.00069	0.00048	0.00058
15192	0.47764	0.00078	0.00123	0.00066	0.00044	0.00055
7424	0.50145	0.00084	0.00134	0.00072	0.00046	0.00059
10632	0.46902	0.00085	0.00134	0.00073	0.00049	0.00061
6192	0.46153	0.00084	0.00129	0.00076	0.00049	0.00062
14600	0.4576	0.00081	0.00125	0.00071	0.00048	0.0006
9024	0.49455	0.0008	0.00128	0.00068	0.00044	0.00056
4672	0.50337	0.00081	0.00131	0.00069	0.00044	0.00057
5128	0.49494	0.00078	0.00125	0.00066	0.00043	0.00055
12520	0.48389	0.00079	0.00125	0.00067	0.00044	0.00056
9840	0.46696	0.00081	0.00126	0.00071	0.00046	0.00059
9760	0.46043	0.00083	0.00129	0.00073	0.00048	0.00061
4992	0.51653	0.00084	0.00138	0.00067	0.00047	0.00057
6672	0.4789	0.00079	0.00124	0.0007	0.00044	0.00057
12584	0.4881	0.00081	0.00128	0.00069	0.00044	0.00057
4880	0.49496	0.00082	0.00131	0.00068	0.00047	0.00058
3168	0.51845	0.00079	0.00129	0.00068	0.00041	0.00055
14696	0.45828	0.00081	0.00126	0.0007	0.00047	0.00059
5808	0.46264	0.00082	0.00127	0.00071	0.00048	0.00059
5936	0.46248	0.00083	0.00129	0.00072	0.00049	0.0006
6176	0.51192	0.00079	0.00129	0.00067	0.00043	0.00055
8480	0.51978	0.00078	0.00128	0.00065	0.00042	0.00053
15384	0.50607	0.00077	0.00124	0.00066	0.00041	0.00054
11496	0.47816	0.00078	0.00122	0.00066	0.00045	0.00055
9960	0.47848	0.00083	0.00131	0.00072	0.00047	0.00059
11592	0.51424	0.00076	0.00123	0.00066	0.00039	0.00053
15976	0.43523	0.00081	0.00123	0.0007	0.00049	0.0006
9152	0.5015	0.00079	0.00127	0.00067	0.00043	0.00055
8864	0.46673	0.00086	0.00134	0.00074	0.00051	0.00062
8848	0.48016	0.00084	0.00132	0.00071	0.00049	0.0006
8248	0.49148	0.0008	0.00128	0.00069	0.00044	0.00057
8952	0.45484	0.00083	0.00128	0.00071	0.0005	0.0006
11160	0.48881	0.00083	0.00131	0.0007	0.00046	0.00058

Inferior longitudinal fasciculus RIGHT						
VOL	FA	MD	L1 / Axial D	L2	L3	Radial D
10320	0.49087	0.00081	0.00129	0.00068	0.00046	0.00057
5832	0.43334	0.00089	0.00135	0.00076	0.00056	0.00066
10768	0.72328	0.00087	0.00129	0.00077	0.00054	0.00065
4488	0.42686	0.00084	0.00126	0.00074	0.00051	0.00063
2552	0.48959	0.00087	0.00139	0.00072	0.0005	0.00061
4920	0.47156	0.00085	0.00132	0.00075	0.00048	0.00061
2640	0.46987	0.00095	0.00148	0.00081	0.00055	0.00068
4672	0.44152	0.00088	0.00134	0.00078	0.00052	0.00065
5232	0.45813	0.0008	0.00125	0.00069	0.00047	0.00058
4536	0.465	0.00082	0.00127	0.00071	0.00047	0.00059
7848	0.43658	0.00087	0.00133	0.00078	0.00052	0.00065
1912	0.4799	0.00084	0.00133	0.00073	0.00047	0.0006
2104	0.46491	0.00081	0.00126	0.00069	0.00049	0.00059
3336	0.43275	0.00092	0.00137	0.00083	0.00057	0.0007
7144	0.4339	0.00084	0.00126	0.00075	0.0005	0.00062
7976	0.45201	0.00093	0.00143	0.00079	0.00058	0.00068
6832	0.44958	0.00081	0.00124	0.00073	0.00047	0.0006
5344	0.47355	0.0008	0.00126	0.00069	0.00045	0.00057
2088	0.42932	0.00084	0.00126	0.00076	0.00051	0.00064
10560	0.46643	0.00082	0.00128	0.0007	0.00047	0.00059
7952	0.44729	0.00083	0.00128	0.00074	0.00049	0.00061
7680	0.43488	0.00089	0.00134	0.00078	0.00054	0.00066
5680	0.42476	0.00084	0.00125	0.00076	0.00051	0.00063
2504	0.49027	0.00082	0.00131	0.00071	0.00045	0.00058
10192	0.46676	0.00084	0.0013	0.00073	0.00049	0.00061
7224	0.50848	0.00078	0.00126	0.00067	0.00041	0.00054
4048	0.47977	0.00086	0.00134	0.00074	0.00049	0.00062
6016	0.43433	0.00083	0.00127	0.00073	0.00051	0.00062
3160	0.48652	0.00081	0.00128	0.00072	0.00044	0.00058
7776	0.43049	0.0008	0.00121	0.00071	0.00049	0.0006
4976	0.49465	0.00082	0.00131	0.00068	0.00045	0.00057
5232	0.44979	0.00082	0.00126	0.00073	0.00048	0.0006
7328	0.44751	0.00083	0.00127	0.00072	0.0005	0.00061
7576	0.4421	0.00084	0.00128	0.00073	0.0005	0.00061
8872	0.42233	0.00084	0.00126	0.00076	0.00052	0.00064
6304	0.45398	0.00084	0.00129	0.00073	0.0005	0.00061

Inferior longitudinal fasciculus LEFT						
VOL	FA	MD	L1 / Axial D	L2	L3	Radial D
7968	0.47679	0.0008	0.00126	0.00068	0.00046	0.00057
6144	0.46433	0.00085	0.00133	0.00072	0.00051	0.00062
6616	0.46633	0.00078	0.00121	0.00069	0.00044	0.00056
6840	0.46111	0.00077	0.00119	0.00067	0.00044	0.00056
1712	0.47716	0.00077	0.00123	0.00069	0.00044	0.00054
6216	0.49414	0.00077	0.00125	0.00065	0.00043	0.00054
6184	0.45561	0.00086	0.00132	0.00076	0.00051	0.00063
8168	0.45673	0.00083	0.00128	0.00074	0.00047	0.00061
7064	0.47807	0.00078	0.00124	0.00067	0.00045	0.00056
5088	0.50633	0.00077	0.00125	0.00064	0.00041	0.00053
6176	0.47811	0.0008	0.00126	0.00068	0.00044	0.00056
4512	0.49802	0.00075	0.00122	0.00064	0.00041	0.00052
11032	0.48185	0.00076	0.00121	0.00064	0.00043	0.00054
5056	0.46014	0.00075	0.00117	0.00066	0.00043	0.00055
5576	0.46742	0.00083	0.0013	0.00071	0.00048	0.00059
4864	0.47427	0.00082	0.00129	0.00069	0.00047	0.00058
6808	0.47062	0.00076	0.00118	0.00067	0.00042	0.00054
7448	0.4778	0.00077	0.00121	0.00067	0.00042	0.00055
3624	0.51056	0.00081	0.00131	0.00069	0.00044	0.00057
10152	0.05001	0.00079	0.00127	0.00068	0.00042	0.00055
10992	0.4474	0.00082	0.00126	0.0007	0.00049	0.00059
6224	0.46379	0.00082	0.00129	0.00071	0.00048	0.00059
5680	0.42476	0.00084	0.00125	0.00076	0.00051	0.00063
3968	0.52595	0.00078	0.0013	0.00064	0.00041	0.00053
7768	0.4929	0.00075	0.00121	0.00063	0.00041	0.00052
6752	0.49757	0.00075	0.00121	0.00065	0.0004	0.00052
5144	0.49314	0.00076	0.00121	0.00064	0.00042	0.00053
11952	0.45658	0.00082	0.00126	0.00071	0.00047	0.00059
2576	0.54224	0.00072	0.00122	0.00059	0.00036	0.00048
8360	0.44268	0.00083	0.00128	0.00071	0.00051	0.00061
9096	0.49619	0.00076	0.00122	0.00065	0.00042	0.00053
5088	0.47517	0.00082	0.0013	0.0007	0.00047	0.00058
6432	0.48031	0.0008	0.00127	0.00067	0.00046	0.00057
9024	0.47314	0.00078	0.00123	0.00068	0.00044	0.00056
7960	0.44958	0.00084	0.00128	0.00073	0.0005	0.00061
4584	0.49486	0.00079	0.00125	0.00067	0.00044	0.00056

Superior longgitudinal fasciculus RIGHT						
VOL	FA	MD	L1 / Axial D	L2	L3	Radial D
11776	0.43136	0.00076	0.00114	0.00069	0.00045	0.00057
9192	0.39534	0.00083	0.00121	0.00076	0.00053	0.00064
6808	0.41962	0.00078	0.00116	0.0007	0.00048	0.00059
9312	0.41576	0.00079	0.00117	0.00072	0.00048	0.0006
880	0.44054	0.00077	0.00118	0.00068	0.00047	0.00056
11936	0.43542	0.00075	0.00113	0.00067	0.00044	0.00056
10752	0.41416	0.00082	0.00121	0.00074	0.00051	0.00062
6760	0.41012	0.00083	0.00122	0.00076	0.00051	0.00064
8192	0.43329	0.00079	0.00119	0.00071	0.00047	0.00059
7256	0.45438	0.00077	0.00119	0.00068	0.00045	0.00056
2912	0.44397	0.00082	0.00123	0.00079	0.00045	0.00062
8512	0.45618	0.00073	0.00113	0.00065	0.00042	0.00053
15680	0.44684	0.00073	0.00112	0.00066	0.00042	0.00054
7608	0.43386	0.00078	0.00117	0.0007	0.00046	0.00058
7664	0.39459	0.00084	0.00122	0.00079	0.00052	0.00066
10224	0.43083	0.00076	0.00114	0.00069	0.00045	0.00057
6256	0.44817	0.00078	0.00119	0.00071	0.00044	0.00058
9944	0.44138	0.00076	0.00116	0.00069	0.00044	0.00057
9688	0.41503	0.00076	0.00112	0.00069	0.00046	0.00058
9304	0.41408	0.00078	0.00114	0.00072	0.00047	0.00059
9624	0.39475	0.00084	0.00121	0.00077	0.00053	0.00065
3528	0.43077	0.00074	0.00112	0.00066	0.00045	0.00055
1392	0.44126	0.00071	0.00107	0.00066	0.00041	0.00053
13704	0.45348	0.00073	0.00111	0.00065	0.00042	0.00053
9760	0.47102	0.00073	0.00113	0.00065	0.0004	0.00053
15608	0.43722	0.00074	0.00112	0.00066	0.00044	0.00055
12936	0.39214	0.00082	0.00119	0.00075	0.00052	0.00063
4760	0.42398	0.00086	0.00127	0.00081	0.00051	0.00066
15800	0.43848	0.00074	0.00111	0.00067	0.00043	0.00055
17584	0.42241	0.00074	0.0011	0.00067	0.00045	0.00056
7128	0.4066	0.0008	0.00116	0.00076	0.00048	0.00062
13296	0.42561	0.00079	0.00118	0.00071	0.00047	0.00059
8128	0.41295	0.00081	0.00119	0.00075	0.00049	0.00062
12968	0.41517	0.00077	0.00114	0.0007	0.00047	0.00058
9376	0.42133	0.00081	0.00121	0.00074	0.00049	0.00062

Superior longitudinal fasciculus LEFT						
VOL	FA	MD	L1 / Axial D	L2	L3	Radial D
9872	0.45047	0.00072	0.00111	0.00065	0.00042	0.00053
7712	0.44851	0.00077	0.00117	0.0007	0.00044	0.00057
6184	0.42979	0.00072	0.00107	0.00066	0.00042	0.00054
5120	0.43992	0.00075	0.00112	0.00069	0.00043	0.00056
10792	0.43519	0.00073	0.0011	0.00068	0.00042	0.00055
10032	0.46518	0.00071	0.00103	0.00064	0.00039	0.00052
8264	0.45253	0.00077	0.00117	0.00069	0.00044	0.00057
10696	0.44232	0.00075	0.00113	0.00069	0.00044	0.00056
4752	0.44061	0.00076	0.00114	0.0007	0.00044	0.00057
13040	0.44782	0.00074	0.00112	0.00067	0.00042	0.00055
2912	0.44397	0.00082	0.00123	0.00079	0.00045	0.00062
8216	0.46931	0.00068	0.00108	0.00061	0.00036	0.00048
8256	0.49945	0.00069	0.0011	0.0006	0.00036	0.00048
2824	0.48267	0.00074	0.00116	0.00066	0.00039	0.00053
8360	0.44045	0.00078	0.00117	0.00073	0.00044	0.00058
14064	0.44447	0.00071	0.00107	0.00064	0.00041	0.00052
6448	0.43256	0.00075	0.00113	0.00069	0.00044	0.00057
7544	0.46942	0.00071	0.00111	0.00065	0.00038	0.00052
7984	0.45592	0.00072	0.00111	0.00066	0.0004	0.00053
11648	0.42909	0.00076	0.00114	0.0007	0.00045	0.00057
10240	0.41796	0.00076	0.00111	0.00071	0.00045	0.00058
2960	0.41561	0.00072	0.00104	0.00069	0.00042	0.00056
6088	0.49344	0.00067	0.00106	0.00062	0.00034	0.00048
10856	0.49421	0.00069	0.00109	0.00062	0.00035	0.00049
11360	0.46886	0.0007	0.00109	0.00064	0.00036	0.0005
13080	0.46027	0.00069	0.00106	0.00062	0.00038	0.0005
6184	0.44755	0.00073	0.0011	0.00068	0.00042	0.00054
2256	0.49238	0.00078	0.00119	0.00076	0.00038	0.00057
9800	0.43963	0.00073	0.00111	0.00067	0.00042	0.00055
12112	0.47684	0.00069	0.00109	0.00062	0.00038	0.0005
10272	0.44109	0.00073	0.00111	0.00066	0.00043	0.00054
70008	0.47077	0.00072	0.00112	0.00064	0.0004	0.00052
8968	0.45526	0.00074	0.00114	0.00067	0.00042	0.00055
11064	0.43557	0.00074	0.00111	0.00067	0.00043	0.00056
8808	0.4493	0.00076	0.00115	0.0007	0.00043	0.00056

Uncinate fasciculus RIGHT						
VOL	FA	MD	L1 / Axial D	L2	L3	Radial D
1032	0.39778	0.00085	0.00125	0.00077	0.00055	0.00066
5320	0.396428	0.00086	0.00125	0.00077	0.00056	0.00067
5328	0.38007	0.00086	0.00123	0.00076	0.00057	0.00067
6048	0.39254	0.00085	0.00123	0.00076	0.00055	0.00066
2432	0.41353	0.00086	0.00127	0.00078	0.00054	0.00066
3936	0.37295	0.00089	0.00128	0.0008	0.00061	0.0007
5992	0.3728	0.00085	0.00121	0.00077	0.00057	0.00067
3168	0.39313	0.00084	0.00123	0.00075	0.00056	0.00065
816	0.44842	0.00082	0.00127	0.00069	0.00051	0.0006
3448	0.38281	0.00088	0.00125	0.00081	0.00057	0.00069
1736	0.43261	0.00081	0.00123	0.00069	0.00051	0.0006
2496	0.42322	0.00079	0.00118	0.0007	0.00049	0.00059
2992	0.39108	0.00081	0.00118	0.00073	0.00053	0.00063
4064	0.38632	0.00091	0.00131	0.00081	0.0006	0.00071
4448	0.385596	0.00077	0.00112	0.0007	0.00051	0.0006
4456	0.38542	0.00084	0.00121	0.00077	0.00054	0.00066
4376	0.40717	0.00081	0.0012	0.00071	0.00052	0.00061
3336	0.40199	0.0008	0.00117	0.00073	0.00051	0.00062
6152	0.409442	0.00081	0.0012	0.00071	0.00052	0.00061
2936	0.39012	0.00084	0.00122	0.00075	0.00055	0.00065
3296	0.35518	0.0009	0.00126	0.00082	0.00062	0.00072
2000	0.34396	0.00083	0.00115	0.00076	0.00057	0.00066
4464	0.39519	0.00078	0.00114	0.00069	0.00051	0.0006
2960	0.44215	0.00077	0.00117	0.00067	0.00046	0.00057
9592	0.43931	0.00075	0.00113	0.00067	0.00045	0.00056
5200	0.3962	0.0008	0.00116	0.00073	0.00051	0.00062
4832	0.40571	0.0008	0.00118	0.00071	0.00052	0.00061
2152	0.40601	0.0008	0.00118	0.00071	0.00051	0.00061
2288	0.37838	0.0008	0.00116	0.00071	0.00054	0.00063
2880	0.39436	0.00079	0.00116	0.0007	0.00052	0.00061
752	0.44292	0.00086	0.00131	0.00072	0.00054	0.00063
5184	0.394065	0.00083	0.00121	0.00075	0.00054	0.00065
4808	0.378329	0.00084	0.0012	0.00077	0.00055	0.00066
4704	0.36482	0.00082	0.00117	0.00073	0.00057	0.00066
7200	0.39912	0.00081	0.00118	0.00073	0.00052	0.00062

Uncinate fasciculus LEFT						
VOL	FA	MD	L1 / Axial D	L2	L3	Radial D
4760	0.38389	0.00083	0.00119	0.00074	0.00054	0.00064
2912	0.40638	0.00083	0.00123	0.00074	0.00054	0.00064
7552	0.392028	0.00082	0.00119	0.00074	0.00054	0.00064
6280	0.38667	0.00083	0.0012	0.00073	0.00055	0.00064
1736	0.4276	0.00078	0.00118	0.00069	0.00048	0.00059
3328	0.39708	0.00084	0.00123	0.00076	0.00055	0.00065
2584	0.40428	0.00083	0.00122	0.00073	0.00053	0.00063
3880	0.38738	0.00077	0.00111	0.00069	0.0005	0.0006
4752	0.39739	0.00081	0.00118	0.00073	0.00052	0.00062
864	0.47919	0.00078	0.00124	0.00066	0.00045	0.00055
2456	0.39969	0.00083	0.00122	0.00073	0.00054	0.00063
976	0.41728	0.00079	0.00118	0.00071	0.0005	0.0006
3656	0.42032	0.00077	0.00115	0.00067	0.00048	0.00058
5096	0.41036	0.00078	0.00114	0.0007	0.00049	0.00059
4928	0.39613	0.00082	0.0012	0.00074	0.00053	0.00064
3688	0.388267	0.00076	0.0011	0.00068	0.0005	0.00059
6000	0.40775	0.00077	0.00114	0.0007	0.00048	0.00059
6432	0.39313	0.0008	0.00117	0.0007	0.00052	0.00061
4864	0.40196	0.0008	0.00117	0.00072	0.00051	0.00062
5072	0.386497	0.00082	0.00119	0.00074	0.00053	0.00064
4008	0.38994	0.00083	0.00118	0.00075	0.00054	0.00065
3984	0.38519	0.0008	0.00116	0.00072	0.00053	0.00063
2384	0.38682	0.00078	0.00113	0.0007	0.00051	0.00061
3368	0.407211	0.00076	0.00111	0.00068	0.00048	0.00058
5160	0.42256	0.00075	0.00112	0.00067	0.00046	0.00057
5632	0.46329	0.00074	0.00114	0.00064	0.00043	0.00053
3840	0.41212	0.00075	0.00112	0.00066	0.00048	0.00057
3248	0.41651	0.00083	0.00123	0.00073	0.00053	0.00063
4744	0.42497	0.00078	0.00117	0.00069	0.00049	0.00059
3256	0.388449	0.00081	0.00117	0.00072	0.00053	0.00063
4480	0.41561	0.00075	0.00111	0.00066	0.00047	0.00056
5248	0.41345	0.00084	0.00125	0.00074	0.00054	0.00064
6384	0.4037	0.00084	0.00122	0.00076	0.00053	0.00064
3768	0.403115	0.00082	0.00119	0.00074	0.00052	0.00063
4608	0.38751	0.00081	0.00118	0.00072	0.00055	0.00063
7040	0.419318	0.0008	0.00118	0.0007	0.0005	0.0006

Forceps Minor						
VOL	FA	MD	L1 / Axial D	L2	L3	Radial D
4336	0.48249	0.00081	0.00129	0.00068	0.00046	0.00057
8368	0.50226	0.00079	0.00128	0.00067	0.00044	0.00055
21528	0.48133	0.00083	0.00132	0.00071	0.00047	0.00059
9176	0.50426	0.0008	0.0013	0.00067	0.00043	0.00055
3880	0.52252	0.00079	0.00132	0.00065	0.00041	0.00053
3800	0.53412	0.00085	0.00141	0.00071	0.00043	0.00057
2744	0.49075	0.00085	0.00136	0.00072	0.00047	0.0006
8248	0.49911	0.00085	0.00137	0.00071	0.00047	0.00059
11504	0.51546	0.00078	0.00128	0.00065	0.00041	0.00053
9216	0.50362	0.00081	0.00133	0.00067	0.00044	0.00056
712	0.50375	0.00076	0.00126	0.00062	0.00042	0.00052
6456	0.51123	0.00074	0.00121	0.00064	0.00038	0.00051
4120	0.56256	0.00077	0.00134	0.00062	0.00037	0.00049
4880	0.53431	0.0008	0.00132	0.00065	0.00041	0.00053
2568	0.47607	0.0009	0.00142	0.00076	0.00051	0.00063
10912	0.47085	0.0008	0.00127	0.00069	0.00046	0.00057
5040	0.49535	0.00077	0.00123	0.00066	0.0004	0.00053
6720	0.50878	0.00079	0.0013	0.00066	0.00042	0.00054
15088	0.49354	0.00079	0.00126	0.00067	0.00043	0.00055
5608	0.50833	0.00076	0.00124	0.00064	0.0004	0.00052
10904	0.47593	0.0008	0.00127	0.00067	0.00046	0.00057
952	0.47267	0.0008	0.00126	0.00066	0.00047	0.00057
2928	0.44626	0.00091	0.00139	0.0008	0.00054	0.00067
6688	0.50388	0.00076	0.00124	0.00062	0.00042	0.00052
3088	0.53749	0.00076	0.00129	0.0006	0.0004	0.0005
8264	0.55882	0.00076	0.00131	0.00061	0.00038	0.00049
7760	0.54407	0.00078	0.00134	0.00063	0.00039	0.00051
3248	0.41651	0.00083	0.00123	0.00073	0.00053	0.00063
4872	0.54237	0.00075	0.00127	0.00061	0.00038	0.0005
10976	0.49801	0.00083	0.00134	0.00069	0.00046	0.00058
2432	0.53351	0.00077	0.00129	0.00063	0.00041	0.00052
2208	0.53209	0.00081	0.00136	0.00065	0.00043	0.00054
5688	0.4873	0.0008	0.00128	0.00066	0.00044	0.00055
3072	0.48978	0.00083	0.00133	0.00071	0.00045	0.00058
3224	0.49779	0.00081	0.00132	0.00066	0.00045	0.00056
6368	0.51058	0.0008	0.0013	0.00069	0.00041	0.00055

Forceps Major						
VOL	FA	MD	L1 / Axial D	L2	L3	Radial D
12592	0.51671	0.00086	0.00142	0.00067	0.00048	0.00057
6776	0.51892	0.00088	0.00146	0.0007	0.00049	0.00059
6776	0.55246	0.00083	0.00164	0.00064	0.00043	0.00053
5688	0.56405	0.00082	0.00144	0.00061	0.00042	0.00051
13520	0.51658	0.00083	0.0014	0.00064	0.00047	0.00055
9904	0.5311	0.00082	0.00141	0.00063	0.00044	0.00053
11184	0.47417	0.00091	0.00144	0.00074	0.00054	0.00064
11088	0.50805	0.00091	0.00151	0.00072	0.00051	0.00061
10192	0.50242	0.00086	0.00141	0.00068	0.00048	0.00058
12224	0.5493	0.00082	0.00143	0.00062	0.00043	0.00052
8344	0.54955	0.00089	0.00154	0.00067	0.00048	0.00057
4896	0.6095	0.00086	0.00158	0.00058	0.00041	0.0005
9192	0.57197	0.00085	0.00148	0.00065	0.00044	0.00054
6208	0.55517	0.00084	0.00146	0.00065	0.00042	0.00053
5392	0.5634	0.00086	0.00151	0.00063	0.00043	0.00053
6744	0.49204	0.00095	0.00154	0.00075	0.00057	0.00066
6560	0.58551	0.00087	0.00156	0.00062	0.00043	0.00053
12672	0.53605	0.00083	0.00142	0.00064	0.00044	0.00054
7152	0.56625	0.00084	0.00148	0.00061	0.00042	0.00052
10808	0.50924	0.00087	0.00144	0.00068	0.00049	0.00059
13048	0.49721	0.00086	0.0014	0.00068	0.00049	0.00059
10536	0.52743	0.00086	0.00146	0.00065	0.00047	0.00056
3248	0.52493	0.00084	0.00141	0.00067	0.00045	0.00056
4224	0.617	0.00085	0.00157	0.00068	0.0004	0.00049
12632	0.54373	0.00083	0.00141	0.00065	0.00043	0.00054
10304	0.57592	0.00081	0.00142	0.00062	0.00038	0.0005
5904	0.59946	0.00082	0.00149	0.00057	0.00039	0.00048
10432	0.51626	0.00089	0.00147	0.00069	0.0005	0.00059
5936	0.57649	0.00084	0.00149	0.00063	0.00042	0.00052
12432	0.051748	0.00083	0.00138	0.00066	0.00046	0.00056
6984	0.58211	0.00086	0.00154	0.00061	0.00044	0.00053
3008	0.5521	0.00089	0.00154	0.00066	0.00047	0.00057
3672	0.55061	0.00093	0.0016	0.00069	0.00051	0.0006
5592	0.54264	0.00094	0.00159	0.0007	0.00052	0.00061
11640	0.51362	0.0009	0.00149	0.00071	0.00051	0.00061
3352	0.59369	0.0009	0.00162	0.00063	0.00046	0.00054

Antertio Thalamic Radiation RIGHT						
VOL	FA	MD	L1 / Axial D	L2	L3	Radial D
6216	0.43189	0.00079	0.0012	0.00069	0.00049	0.00059
11952	0.45144	0.00076	0.00116	0.00067	0.00044	0.00056
14008	0.043406	0.00079	0.0012	0.00069	0.00048	0.00059
8768	0.45864	0.00076	0.00118	0.00068	0.00044	0.00056
8808	0.44389	0.00075	0.00114	0.00068	0.00043	0.00056
7000	0.46369	0.00076	0.00117	0.00067	0.00043	0.00055
11464	0.43751	0.0008	0.00121	0.00071	0.00048	0.0006
10208	0.45368	0.00079	0.0012	0.00069	0.00046	0.00058
7232	0.47521	0.00077	0.00121	0.00066	0.00044	0.00055
10640	0.45706	0.00078	0.0012	0.00068	0.00045	0.00057
6448	0.47587	0.00074	0.00116	0.00065	0.00041	0.00053
8408	0.49879	0.00074	0.00119	0.00063	0.0004	0.00051
4136	0.4732	0.00077	0.0012	0.00067	0.00044	0.00056
9416	0.43411	0.00081	0.00121	0.00073	0.00048	0.0006
9120	0.46421	0.00075	0.00117	0.00065	0.00043	0.00054
6824	0.43398	0.00079	0.00117	0.00072	0.00046	0.00059
8824	0.44822	0.00077	0.00118	0.00068	0.00045	0.00057
4024	0.44522	0.00075	0.00113	0.00067	0.00044	0.00055
9536	0.44057	0.00077	0.00116	0.0007	0.00045	0.00057
4048	0.44406	0.00076	0.00116	0.00068	0.00045	0.00057
5304	0.43573	0.00081	0.00122	0.00071	0.00049	0.0006
8648	0.46068	0.0008	0.00123	0.00069	0.00047	0.00058
7880	0.46588	0.00078	0.0012	0.00067	0.00045	0.00056
6584	0.47064	0.00073	0.00113	0.00064	0.00041	0.00052
9424	0.45491	0.00072	0.0011	0.00065	0.00041	0.00053
12120	0.45684	0.00078	0.0012	0.00068	0.00046	0.00057
4784	0.44894	0.00077	0.00118	0.00068	0.00045	0.00056
12144	0.47497	0.00076	0.0012	0.00067	0.00043	0.00055
12320	0.43327	0.00079	0.00119	0.00069	0.00049	0.00059
8584	0.433	0.00074	0.0011	0.00068	0.00043	0.00055
7960	0.4678	0.0008	0.00125	0.00069	0.00046	0.00058
4704	0.46753	0.00078	0.00122	0.00068	0.00045	0.00056
8184	0.4544	0.00081	0.00124	0.00071	0.00047	0.00059
10768	0.42681	0.00078	0.00118	0.0007	0.00048	0.00059
5584	0.48165	0.00083	0.0013	0.00072	0.00046	0.00059

Anterior Thalamic Radiation LEFT						
VOL	FA	MD	L1 / Axial D	L2	L3	Radial D
6640	0.46116	0.00081	0.00125	0.0007	0.00048	0.00059
8936	0.45897	0.00078	0.00119	0.0007	0.00045	0.00057
9360	0.43729	0.00078	0.00117	0.00068	0.00047	0.00058
5416	0.41466	0.00077	0.00114	0.00069	0.00048	0.00059
8976	0.46521	0.00077	0.00119	0.00067	0.00045	0.00056
7360	0.47397	0.00076	0.00118	0.00068	0.00043	0.00055
7784	0.44232	0.00082	0.00124	0.00073	0.00049	0.00061
3640	0.5051	0.00074	0.00119	0.00064	0.0004	0.00052
6296	0.48879	0.00077	0.00122	0.00066	0.00042	0.00054
11296	0.45148	0.00079	0.00121	0.00069	0.00047	0.00058
5048	0.40855	0.00081	0.00118	0.00075	0.0005	0.00062
10944	0.47005	0.00075	0.00117	0.00066	0.00043	0.00054
6528	0.52354	0.00073	0.00121	0.00061	0.00038	0.0005
7760	0.44864	0.00079	0.0012	0.0007	0.00047	0.00058
9224	0.45883	0.0008	0.00123	0.00071	0.00046	0.00059
14400	0.45626	0.00075	0.00116	0.00065	0.00044	0.00055
8520	0.44294	0.00079	0.00119	0.00071	0.00046	0.00058
9000	0.47673	0.00075	0.00117	0.00065	0.00042	0.00053
9128	0.49997	0.00077	0.00124	0.00065	0.00043	0.00054
4912	0.43717	0.00083	0.00126	0.00075	0.0005	0.00062
6288	0.42872	0.00078	0.00117	0.00071	0.00047	0.00059
4768	0.42758	0.0008	0.00119	0.00072	0.00048	0.0006
1816	0.46798	0.00077	0.00119	0.00068	0.00044	0.00056
5968	0.45786	0.00077	0.00118	0.00067	0.00045	0.00056
6632	0.52245	0.00073	0.00119	0.00061	0.00038	0.00049
10584	0.51039	0.00073	0.00118	0.00063	0.00038	0.0005
9864	0.44857	0.00077	0.00118	0.00068	0.00046	0.00057
7760	0.4695	0.00075	0.00117	0.00068	0.00042	0.00054
14680	0.47307	0.00077	0.00119	0.00068	0.00043	0.00055
17360	0.43977	0.00079	0.00121	0.0007	0.00048	0.00059
4808	0.44169	0.00076	0.00114	0.00069	0.00045	0.00057
8944	0.44345	0.00081	0.00122	0.00072	0.00048	0.0006
4920	0.47238	0.00076	0.00117	0.00067	0.00042	0.00055
4704	0.46145	0.00076	0.00119	0.00067	0.00042	0.00054
1512	0.44496	0.00076	0.00116	0.00068	0.00044	0.00056
8176	0.4639	0.0008	0.00123	0.00071	0.00045	0.00058

Corticospinal tract RIGHT						
VOL	FA	MD	L1 / Axial D	L2	L3	Radial D
3376	0.536	0.00076	0.00128	0.00061	0.00039	0.0005
3760	0.5099	0.00077	0.00125	0.00065	0.00041	0.00053
4936	0.52095	0.00077	0.00128	0.00061	0.00041	0.00051
4080	0.52463	0.00076	0.00125	0.00063	0.00039	0.00051
1208	0.55838	0.00076	0.00132	0.00061	0.00036	0.00048
5248	0.53918	0.00076	0.00127	0.00062	0.00038	0.0005
1096	0.53732	0.00078	0.00131	0.00063	0.0004	0.00051
3496	0.52524	0.0008	0.00132	0.00068	0.00041	0.00054
1816	0.53235	0.00079	0.00132	0.00066	0.0004	0.00053
1808	0.57017	0.00079	0.00137	0.00063	0.00038	0.0005
2888	0.55054	0.00078	0.00131	0.00064	0.00038	0.00051
1616	0.56224	0.00072	0.00126	0.00057	0.00034	0.00046
2168	0.55537	0.00078	0.00133	0.00062	0.00038	0.0005
1696	0.49706	0.00083	0.00135	0.00068	0.00046	0.00057
8264	0.51599	0.00074	0.00121	0.00063	0.00038	0.0005
1520	0.53669	0.00079	0.00132	0.00065	0.00039	0.00052
1992	0.57192	0.00075	0.00132	0.00058	0.00036	0.00047
3912	0.53364	0.00076	0.00127	0.00062	0.00039	0.0005
3048	0.52845	0.00078	0.00013	0.00063	0.0004	0.00052
1360	0.51584	0.00079	0.00131	0.00063	0.00042	0.00052
2192	0.50233	0.0008	0.0013	0.00068	0.00043	0.00056
400	0.48535	0.00077	0.0012	0.00067	0.00042	0.00055
3440	0.53325	0.00076	0.00127	0.00062	0.00038	0.0005
1536	0.58096	0.00076	0.00134	0.00059	0.00036	0.00048
1088	0.58301	0.00073	0.00127	0.00058	0.00033	0.00045
1624	0.57807	0.00077	0.00136	0.00058	0.00037	0.00047
1368	0.53311	0.00078	0.00131	0.00063	0.00041	0.00052
2088	0.55853	0.00077	0.00131	0.00062	0.00037	0.00049
1472	0.49685	0.00079	0.00128	0.00064	0.00044	0.00054
1344	0.54282	0.00078	0.00132	0.00063	0.00039	0.00051
864	0.53256	0.00079	0.00132	0.00064	0.0004	0.00052
3344	0.50523	0.0008	0.00128	0.00069	0.00042	0.00056
3416	0.51476	0.00078	0.00128	0.00064	0.0004	0.00052
896	0.54979	0.00075	0.00128	0.00062	0.00036	0.00049
4024	0.52986	0.00077	0.00128	0.00063	0.00039	0.00051

Corticospinal Tract LEFT						
VOL	FA	MD	L1 / Axial D	L2	L3	Radial D
2784	0.55074	0.00074	0.00125	0.0006	0.00036	0.00048
6864	0.54739	0.00072	0.00123	0.00059	0.00036	0.00047
5104	0.53154	0.00075	0.00125	0.00061	0.00039	0.0005
1976	0.56871	0.00074	0.00129	0.00058	0.00036	0.00047
4320	0.56303	0.00073	0.00126	0.00058	0.00035	0.00047
3232	0.58143	0.00074	0.00129	0.00058	0.00034	0.00046
3048	0.55826	0.00077	0.00131	0.00064	0.00037	0.0005
3472	0.5424	0.00073	0.00123	0.0006	0.00036	0.00048
4112	0.55447	0.00075	0.00127	0.00062	0.00037	0.00049
1480	0.56697	0.00076	0.00132	0.00061	0.00037	0.00049
3584	0.55487	0.00072	0.00122	0.0006	0.00033	0.00047
3816	0.59295	0.00069	0.00123	0.00054	0.0003	0.00042
7760	0.44864	0.00079	0.0012	0.0007	0.00047	0.00058
3672	0.62854	0.00077	0.00129	0.00064	0.0004	0.00052
7200	0.52689	0.00074	0.00123	0.00061	0.00039	0.0005
2760	0.5201	0.00083	0.00137	0.00068	0.00045	0.00057
4920	0.55362	0.00074	0.00125	0.00061	0.00036	0.00048
6136	0.5699	0.00075	0.0013	0.0006	0.00036	0.00048
3984	0.5389	0.00075	0.000124	0.00062	0.00037	0.0005
5328	0.53904	0.00076	0.00129	0.00061	0.00039	0.0005
2472	0.5278	0.00075	0.00123	0.00064	0.00038	0.00051
688	0.59481	0.0008	0.00143	0.00059	0.00039	0.00049
1816	0.57093	0.00071	0.00124	0.00057	0.00033	0.00045
3736	0.59954	0.00074	0.00132	0.00056	0.00033	0.00044
1472	0.5762	0.00074	0.00127	0.00061	0.00036	0.00048
2032	0.56742	0.00071	0.00125	0.00056	0.00034	0.00045
1672	0.56986	0.00069	0.0012	0.00055	0.00032	0.00044
576	0.54963	0.00074	0.00125	0.00061	0.00037	0.00049
2960	0.533	0.00075	0.00125	0.0006	0.00039	0.00049
1544	0.58769	0.00071	0.00126	0.00056	0.00032	0.00044
2216	0.55408	0.00075	0.00128	0.0006	0.00038	0.00049
1984	0.53302	0.00073	0.00122	0.00061	0.00037	0.00049
2616	0.54402	0.00074	0.00125	0.0006	0.00037	0.00048
920	0.58645	0.00071	0.00126	0.00056	0.00032	0.00044
3592	0.54083	0.00075	0.00125	0.00062	0.00037	0.0005

	White Matter SNPs			
Name	rs720308	rs2301600	rs3746248	rs762178
M87109984	AA	BB	AB	AA
M87113317	AB	AB	AB	AB
M87115517	AA	BB	AB	AB
M87118004	AA	BB	BB	BB
M87120980	AA	AB	BB	AB
M87123990	AB	AB	AB	AB
M87129006	AB	AA	BB	AA
M87131456	BB	AA	BB	AB
M87137660	AB	AB	AB	AB
M87146463	AA	BB	AA	AB
M87169984	AA	BB	BB	AB
M87177119	AA	AB	BB	AA
M87178340	AB	AB	BB	BB
M87180407	AA	BB	AB	AB
M87180947	AA	BB	BB	BB
M87181072	AB	AB	BB	AA
M87182419	AA	BB	BB	AB
M87182832	AA	AA	BB	AB
M87185249	AA	BB	BB	BB
M87189298	AA	AB	AB	AB
M87196594	AA	AB	BB	AB
M87109470	AA	BB	AA	BB
M87112783	AA	AB	BB	AB
M87114670	AA	BB	BB	AA
M87117785	AA	BB	BB	AA
M87120670	AA	BB	AB	AB
M87122697	AB	AB	BB	AA
M87148033	AB	AB	BB	BB
M87148957	AA	AB	BB	BB
M87151676	AA	BB	BB	AB
M87165919	AA	BB	BB	AB
M87188301	AB	AB	BB	AA
M87189597	BB	AA	BB	AB
M87195743	AA	AB	AB	BB
M87150951	AA	BB	AB	AB
M87198790	AB	AB	BB	AB
Chr	19	19	19	21
AA Freq	0.6888889	0.1111111	0.06666667	0.2
AB Freq	0.2444444	0.4222222	0.3111111	0.5777778
BB Freq	0.06666667	0.4666667	0.6222222	0.2222222
Minor Freq	0.1888889	0.3222222	0.2222222	0.4888889

REFERENCES

Agartz I, Momenan R, Rawlings RR, Kerich MJ, Hommer DW (Hippocampal volume in patients with alcohol dependence. Arch Gen Psychiatry 56:356-363.1999).

Aggleton JP, Vann SD, Oswald CJ, Good M (Identifying cortical inputs to the rat hippocampus that subserve allocentric spatial processes: a simple problem with a complex answer. Hippocampus 10:466-474.2000).

Alvarez Retuerto AI, Cantor RM, Gleeson JG, Ustaszewska A, Schackwitz WS, Pennacchio LA, Geschwind DH (Association of common variants in the Joubert syndrome gene (AHI1) with autism. Hum Mol Genet 17:3887-3896.2008).

Anokhin AP, Heath AC, Myers E (Genetic and environmental influences on frontal EEG asymmetry: a twin study. Biol Psychol 71:289-295.2006).

Anokhin AP, Muller V, Lindenberger U, Heath AC, Myers E (Genetic influences on dynamic complexity of brain oscillations. Neurosci Lett 397:93-98.2006).

Arfanakis K, Haughton VM, Carew JD, Rogers BP, Dempsey RJ, Meyerand ME (Diffusion tensor MR imaging in diffuse axonal injury. AJNR Am J Neuroradiol 23:794-802.2002).

Bakalkin G, Yakovleva T, Terenius L (NF-kappa B-like factors in the murine brain. Developmentally-regulated and tissue-specific expression. Brain Res Mol Brain Res 20:137-146.1993).

Basser PJ, Jones DK (Diffusion-tensor MRI: theory, experimental design and data analysis - a technical review. NMR Biomed 15:456-467.2002).

Beck AT, Beamesderfer A (Assessment of depression: the depression inventory. Mod Probl Pharmacopsychiatry 7:151-169.1974).

Benters R, Niemeyer CM, Wohrle D (Dendrimer-activated solid supports for nucleic acid and protein microarrays. Chembiochem 2:686-694.2001).

Beohar N, Kawamoto S (Transcriptional regulation of the human nonmuscle myosin II heavy chain-A gene. Identification of three clustered cis-elements in intron-1 which modulate transcription in a cell type- and differentiation state-dependent manner. J Biol Chem 273:9168-9178.1998).

Bernstein HG, Stanarius A, Baumann B, Henning H, Krell D, Danos P, Falkai P, Bogerts B (Nitric oxide synthase-containing neurons in the human hypothalamus: reduced number of immunoreactive cells in the paraventricular nucleus of depressive patients and schizophrenics. Neuroscience 83:867-875.1998).

Bhave SV, Ghoda L, Hoffman PL (Brain-derived neurotrophic factor mediates the anti-apoptotic effect of NMDA in cerebellar granule neurons: signal transduction cascades and site of ethanol action. J Neurosci 19:3277-3286.1999).

Bonsch D, Lenz B, Kornhuber J, Bleich S (DNA hypermethylation of the alpha synuclein promoter in patients with alcoholism. Neuroreport 16:167-170.2005).

Bowirrat A, Oscar-Berman M (Relationship between dopaminergic neurotransmission, alcoholism, and Reward Deficiency syndrome. Am J Med Genet B Neuropsychiatr Genet 132B:29-37.2005).

Bramham CR, Messaoudi E (BDNF function in adult synaptic plasticity: the synaptic consolidation hypothesis. Prog Neurobiol 76:99-125.2005).

Brewer C, Perrett L (Brain damage due to alcohol consumption: an air-encephalographic, psychometric and electroencephalographic study. Br J Addict Alcohol Other Drugs 66:170-182.1971).

Buck KJ, Metten P, Belknap JK, Crabbe JC (Quantitative trait loci involved in genetic predisposition to acute alcohol withdrawal in mice. J Neurosci 17:3946-3955.1997).

Cargill M, Altshuler D, Ireland J, Sklar P, Ardlie K, Patil N, Shaw N, Lane CR, Lim EP, Kalyanaraman N, Nemesh J, Ziaugra L, Friedland L, Rolfe A, Warrington J, Lipshutz R, Daley GQ, Lander ES (Characterization of single-nucleotide polymorphisms in coding regions of human genes. Nat Genet 22:231-238.1999).

Chenevert TL, Brunberg JA, Pipe JG (Anisotropic diffusion in human white matter: demonstration with MR techniques in vivo. Radiology 177:401-405.1990).

Clerget-Darpoux F, Goldin LR, Gershon ES (Clinical methods in psychiatric genetics. III. Environmental stratification may simulate a genetic effect in adoption studies. Acta Psychiatr Scand 74:305-311.1986).

Compton MT, Whicker NE, Hochman KM (Alcohol and cannabis use in Urban, African American, first-episode schizophrenia-spectrum patients: associations with positive and negative symptoms. J Clin Psychiatry 68:1939-1945.2007).

Conturo TE, Lori NF, Cull TS, Akbudak E, Snyder AZ, Shimony JS, McKinstry RC, Burton H, Raichle ME (Tracking neuronal fiber pathways in the living human brain. Proc Natl Acad Sci U S A 96:10422-10427.1999).

Covault J, Gelernter J, Hesselbrock V, Nellissery M, Kranzler HR (Allelic and haplotypic association of GABRA2 with alcohol dependence. Am J Med Genet B Neuropsychiatr Genet 129B:104-109.2004).

Crabb DW (Biological markers for increased risk of alcoholism and for quantitation of alcohol consumption. J Clin Invest 85:311-315.1990).

Crow TJ (Temporal lobe asymmetries as the key to the etiology of schizophrenia. Schizophr Bull 16:433-443.1990).

Dale AM, Fischl B, Sereno MI (Cortical surface-based analysis. I. Segmentation and surface reconstruction. Neuroimage 9:179-194.1999).

Davis KL, Haroutunian V (Global expression-profiling studies and oligodendrocyte dysfunction in schizophrenia and bipolar disorder. Lancet 362:758.2003).

Davis KL, Stewart DG, Friedman JI, Buchsbaum M, Harvey PD, Hof PR, Buxbaum J, Haroutunian V (White matter changes in schizophrenia: evidence for myelin-related dysfunction. Arch Gen Psychiatry 60:443-456.2003).

de la Monte SM (Disproportionate atrophy of cerebral white matter in chronic alcoholics. Arch Neurol 45:990-992.1988).

Desai NS, Rutherford LC, Turrigiano GG (BDNF regulates the intrinsic excitability of cortical neurons. Learn Mem 6:284-291.1999).

Dick DM, Aliev F, Wang JC, Saccone S, Hinrichs A, Bertelsen S, Budde J, Saccone N, Foroud T, Nurnberger J, Jr., Xuei X, Conneally PM, Schuckit M, Almasy L, Crowe R, Kuperman S, Kramer J, Tischfield JA, Hesselbrock V, Edenberg HJ, Porjesz B, Rice JP, Bierut L, Goate A (A Systematic single nucleotide polymorphism screen to fine-map alcohol dependence genes on chromosome 7 identifies association with a novel susceptibility gene ACN9. Biol Psychiatry 63:1047-1053.2008).

Dick DM, Foroud T (Genetic strategies to detect genes involved in alcoholism and alcohol-related traits. Alcohol Res Health 26:172-180.2002).

Dick DM, Jones K, Saccone N, Hinrichs A, Wang JC, Goate A, Bierut L, Almasy L, Schuckit M, Hesselbrock V, Tischfield J, Foroud T, Edenberg H, Porjesz B, Begleiter H (Endophenotypes successfully lead to gene identification: results from the collaborative study on the genetics of alcoholism. Behav Genet 36:112-126.2006).

Dick DM, Jones K, Saccone N, Hinrichs A, Wang JC, Goate A, Bierut L, Almasy L, Schuckit M, Hesselbrock V, Tischfield J, Foroud T, Edenberg H, Porjesz B, Begleiter H (Endophenotypes successfully lead to gene identification: results from the collaborative study on the genetics of alcoholism. Behav Genet 36:112-126.2006).

Dorsey SG, Bambrick LL, Balice-Gordon RJ, Krueger BK (Failure of brain-derived neurotrophic factor-dependent neuron survival in mouse trisomy 16. J Neurosci 22:2571-2578.2002).

Ducci F, Goldman D (Genetic approaches to addiction: genes and alcohol. Addiction 103:1414-1428.2008).

Duman RS, Heninger GR, Nestler EJ (A molecular and cellular theory of depression. Arch Gen Psychiatry 54:597-606.1997).

Duong TQ, Ackerman JJ, Ying HS, Neil JJ (Evaluation of extra- and intracellular apparent diffusion in normal and globally ischemic rat brain via 19F NMR. Magn Reson Med 40:1-13.1998).

Edenberg HJ, Bierut LJ, Boyce P, Cao M, Cawley S, Chiles R, Doheny KF, Hansen M, Hinrichs T, Jones K, Kelleher M, Kennedy GC, Liu G, Marcus G, McBride C, Murray SS, Oliphant A, Pettengill J, Porjesz B, Pugh EW, Rice JP, Rubano T,

Shannon S, Steeke R, Tischfield JA, Tsai YY, Zhang C, Begleiter H (Description of the data from the Collaborative Study on the Genetics of Alcoholism (COGA) and single-nucleotide polymorphism genotyping for Genetic Analysis Workshop 14. BMC Genet 6 Suppl 1:S2.2005).

Edenberg HJ, Foroud T (The genetics of alcoholism: identifying specific genes through family studies. Addict Biol 11:386-396.2006).

Edenberg HJ, Kranzler HR (The contribution of genetics to addiction therapy approaches. Pharmacol Ther 108:86-93.2005).

Edenberg HJ, Xuei X, Chen HJ, Tian H, Wetherill LF, Dick DM, Almasy L, Bierut L, Bucholz KK, Goate A, Hesselbrock V, Kuperman S, Nurnberger J, Porjesz B, Rice J, Schuckit M, Tischfield J, Begleiter H, Foroud T (Association of alcohol dehydrogenase genes with alcohol dependence: a comprehensive analysis. Hum Mol Genet 15:1539-1549.2006).

Edwards G, Gross MM (Alcohol dependence: provisional description of a clinical syndrome. Br Med J 1:1058-1061.1976).

Egan MF, Kojima M, Callicott JH, Goldberg TE, Kolachana BS, Bertolino A, Zaitsev E, Gold B, Goldman D, Dean M, Lu B, Weinberger DR (The BDNF val66met polymorphism affects activity-dependent secretion of BDNF and human memory and hippocampal function. Cell 112:257-269.2003).

Egan MF, Weinberger DR, Lu B (Schizophrenia, III: brain-derived neurotropic factor and genetic risk. Am J Psychiatry 160:1242.2003).

Ehlers CL, Wall TL, Betancourt M, Gilder DA (The clinical course of alcoholism in 243 Mission Indians. Am J Psychiatry 161:1204-1210.2004).

Eide FF, Vining ER, Eide BL, Zang K, Wang XY, Reichardt LF (Naturally occurring truncated trkB receptors have dominant inhibitory effects on brain-derived neurotrophic factor signaling. J Neurosci 16:3123-3129.1996).

Estruch R, Nicolas JM, Salamero M, Aragon C, Sacanella E, Fernandez-Sola J, Urbano-Marquez A (Atrophy of the corpus callosum in chronic alcoholism. J Neurol Sci 146:145-151.1997).

Evans DM, Cardon LR (A comparison of linkage disequilibrium patterns and estimated population recombination rates across multiple populations. Am J Hum Genet 76:681-687.2005).

Fein G, Di Sclafani V, Cardenas VA, Goldmann H, Tolou-Shams M, Meyerhoff DJ (Cortical gray matter loss in treatment-naive alcohol dependent individuals. Alcohol Clin Exp Res 26:558-564.2002).

Fein G, Di Sclafani V, Meyerhoff DJ (Prefrontal cortical volume reduction associated with frontal cortex function deficit in 6-week abstinent crack-cocaine dependent men. Drug Alcohol Depend 68:87-93.2002).

Filipek PA (Neurobiologic correlates of developmental dyslexia: how do dyslexics' brains differ from those of normal readers? J Child Neurol 10 Suppl 1:S62-69.1995).

Filipek PA (Quantitative magnetic resonance imaging in autism: the cerebellar vermis. Curr Opin Neurol 8:134-138.1995).

Fischl B, Salat DH, Busa E, Albert M, Dieterich M, Haselgrove C, van der Kouwe A, Killiany R, Kennedy D, Klaveness S, Montillo A, Makris N, Rosen B, Dale AM

(Whole brain segmentation: automated labeling of neuroanatomical structures in the human brain. Neuron 33:341-355.2002).

Fischl B, Salat DH, van der Kouwe AJ, Makris N, Segonne F, Quinn BT, Dale AM (Sequence-independent segmentation of magnetic resonance images. Neuroimage 23 Suppl 1:S69-84.2004).

Fischl B, Sereno MI, Dale AM (Cortical surface-based analysis. II: Inflation, flattening, and a surface-based coordinate system. Neuroimage 9:195-207.1999).

Fischl B, van der Kouwe A, Destrieux C, Halgren E, Segonne F, Salat DH, Busa E, Seidman LJ, Goldstein J, Kennedy D, Caviness V, Makris N, Rosen B, Dale AM (Automatically parcellating the human cerebral cortex. Cereb Cortex 14:11-22.2004).

Fleisher A, Grundman M, Jack CR, Jr., Petersen RC, Taylor C, Kim HT, Schiller DH, Bagwell V, Sencakova D, Weiner MF, DeCarli C, DeKosky ST, van Dyck CH, Thal LJ (Sex, apolipoprotein E epsilon 4 status, and hippocampal volume in mild cognitive impairment. Arch Neurol 62:953-957.2005).

Fuster JM (Jackson and the frontal executive hierarchy. Int J Psychophysiol 64:106-107.2007).

Gabriel SB, Schaffner SF, Nguyen H, Moore JM, Roy J, Blumenstiel B, Higgins J, DeFelice M, Lochner A, Faggart M, Liu-Cordero SN, Rotimi C, Adeyemo A, Cooper R, Ward R, Lander ES, Daly MJ, Altshuler D (The structure of haplotype blocks in the human genome. Science 296:2225-2229.2002).

Gazdzinski S, Durazzo TC, Studholme C, Song E, Banys P, Meyerhoff DJ (Quantitative brain MRI in alcohol dependence: preliminary evidence for effects of concurrent

chronic cigarette smoking on regional brain volumes. Alcohol Clin Exp Res 29:1484-1495.2005).

Ge Y, Grossman RI, Babb JS, Rabin ML, Mannon LJ, Kolson DL (Age-related total gray matter and white matter changes in normal adult brain. Part I: volumetric MR imaging analysis. AJNR Am J Neuroradiol 23:1327-1333.2002).

Ge Y, Grossman RI, Babb JS, Rabin ML, Mannon LJ, Kolson DL (Age-related total gray matter and white matter changes in normal adult brain. Part II: quantitative magnetization transfer ratio histogram analysis. AJNR Am J Neuroradiol 23:1334-1341.2002).

Geller B, Badner JA, Tillman R, Christian SL, Bolhofner K, Cook EH, Jr. (Linkage disequilibrium of the brain-derived neurotrophic factor Val66Met polymorphism in children with a prepubertal and early adolescent bipolar disorder phenotype. Am J Psychiatry 161:1698-1700.2004).

Gershon ES, Goldin LR (Clinical methods in psychiatric genetics. I. Robustness of genetic marker investigative strategies. Acta Psychiatr Scand 74:113-118.1986).

Giedd JN, Blumenthal J, Jeffries NO, Rajapakse JC, Vaituzis AC, Liu H, Berry YC, Tobin M, Nelson J, Castellanos FX (Development of the human corpus callosum during childhood and adolescence: a longitudinal MRI study. Prog Neuropsychopharmacol Biol Psychiatry 23:571-588.1999).

Glabus MF, Blackwood DH, Ebmeier KP, Souza V, Walker MT, Sharp CW, Dunan JT, Muir W (Methodological considerations in measurement of the P300 component of the auditory oddball ERP in schizophrenia. Electroencephalogr Clin Neurophysiol 90:123-134.1994).

Glahn DC, Bearden CE, Niendam TA, Escamilla MA (The feasibility of neuropsychological endophenotypes in the search for genes associated with bipolar affective disorder. Bipolar Disord 6:171-182.2004).

Glahn DC, Paus T, Thompson PM (Imaging genomics: mapping the influence of genetics on brain structure and function. Hum Brain Mapp 28:461-463.2007).

Glahn DC, Thompson PM, Blangero J (Neuroimaging endophenotypes: strategies for finding genes influencing brain structure and function. Hum Brain Mapp 28:488-501.2007).

Glatt CE, Freimer NB (Association analysis of candidate genes for neuropsychiatric disease: the perpetual campaign. Trends Genet 18:307-312.2002).

Gokhan S, Marin-Husstege M, Yung SY, Fontanez D, Casaccia-Bonnefil P, Mehler MF (Combinatorial profiles of oligodendrocyte-selective classes of transcriptional regulators differentially modulate myelin basic protein gene expression. J Neurosci 25:8311-8321.2005).

Goldin LR, Nurnberger JI, Jr., Gershon ES (Clinical methods in psychiatric genetics. II. The high risk approach. Acta Psychiatr Scand 74:119-128.1986).

Goldman-Rakic PS (Circuitry of the frontal association cortex and its relevance to dementia. Arch Gerontol Geriatr 6:299-309.1987).

Goldstein BI, Diamantouros A, Schaffer A, Naranjo CA (Pharmacotherapy of alcoholism in patients with co-morbid psychiatric disorders. Drugs 66:1229-1237.2006).

Gong G, Jiang T, Zhu C, Zang Y, He Y, Xie S, Xiao J (Side and handedness effects on the cingulum from diffusion tensor imaging. Neuroreport 16:1701-1705.2005).

Good CD, Johnsrude IS, Ashburner J, Henson RN, Friston KJ, Frackowiak RS (A voxel-based morphometric study of ageing in 465 normal adult human brains. Neuroimage 14:21-36.2001).

Goodwin DW (Genetic determinants of alcohol addiction. Adv Exp Med Biol 56:339-355.1975).

Gothelf D, Furfaro JA, Penniman LC, Glover GH, Reiss AL (The contribution of novel brain imaging techniques to understanding the neurobiology of mental retardation and developmental disabilities. Ment Retard Dev Disabil Res Rev 11:331-339.2005).

Gottesman, II, Gould TD (The endophenotype concept in psychiatry: etymology and strategic intentions. Am J Psychiatry 160:636-645.2003).

Gratacos M, Gonzalez JR, Mercader JM, de Cid R, Urretavizcaya M, Estivill X (Brain-derived neurotrophic factor Val66Met and psychiatric disorders: meta-analysis of case-control studies confirm association to substance-related disorders, eating disorders, and schizophrenia. Biol Psychiatry 61:911-922.2007).

Gratacos M, Soria V, Urretavizcaya M, Gonzalez JR, Crespo JM, Bayes M, de Cid R, Menchon JM, Vallejo J, Estivill X (A brain-derived neurotrophic factor (BDNF) haplotype is associated with antidepressant treatment outcome in mood disorders. Pharmacogenomics J 8:101-112.2008).

Green AE, Munafo MR, Deyoung CG, Fossella JA, Fan J, Gray JR (Using genetic data in cognitive neuroscience: from growing pains to genuine insights. Nat Rev Neurosci.2008).

Greene LA, Kaplan DR (Early events in neurotrophin signalling via Trk and p75 receptors. Curr Opin Neurobiol 5:579-587.1995).

Grobin AC, Matthews DB, Devaud LL, Morrow AL (The role of GABA(A) receptors in the acute and chronic effects of ethanol. Psychopharmacology (Berl) 139:2-19.1998).

Haapasalo A, Koponen E, Hoppe E, Wong G, Castren E (Truncated trkB.T1 is dominant negative inhibitor of trkB.TK+-mediated cell survival. Biochem Biophys Res Commun 280:1352-1358.2001).

Halushka MK, Mathews DJ, Bailey JA, Chakravarti A (GIST: A web tool for collecting gene information. Physiol Genomics 1:75-81.1999).

Harding AJ, Wong A, Svoboda M, Kril JJ, Halliday GM (Chronic alcohol consumption does not cause hippocampal neuron loss in humans. Hippocampus 7:78-87.1997).

Hariri AR, Drabant EM, Weinberger DR (Imaging genetics: perspectives from studies of genetically driven variation in serotonin function and corticolimbic affective processing. Biol Psychiatry 59:888-897.2006).

Hariri AR, Goldberg TE, Mattay VS, Kolachana BS, Callicott JH, Egan MF, Weinberger DR (Brain-derived neurotrophic factor val66met polymorphism affects human memory-related hippocampal activity and predicts memory performance. J Neurosci 23:6690-6694.2003).

Hariri AR, Goldberg TE, Mattay VS, Kolachana BS, Callicott JH, Egan MF, Weinberger DR (Brain-derived neurotrophic factor val66met polymorphism affects human memory-related hippocampal activity and predicts memory performance. J Neurosci 23:6690-6694.2003).

Harper C, Kril J (Brain atrophy in chronic alcoholic patients: a quantitative pathological study. J Neurol Neurosurg Psychiatry 48:211-217.1985).

Harper C, Kril J (Pathological changes in alcoholic brain shrinkage. Med J Aust 144:3-4.1986).

Harper C, Kril J (Patterns of neuronal loss in the cerebral cortex in chronic alcoholic patients. J Neurol Sci 92:81-89.1989).

Harper C, Kril J (If you drink your brain will shrink. Neuropathological considerations. Alcohol Alcohol Suppl 1:375-380.1991).

Harper C, Kril J (An introduction to alcohol-induced brain damage and its causes. Alcohol Alcohol Suppl 2:237-243.1994).

Harper C, Kril J, Daly J (Are we drinking our neurones away? Br Med J (Clin Res Ed) 294:534-536.1987).

Harper CG, Kril JJ (Neuropathology of alcoholism. Alcohol Alcohol 25:207-216.1990).

Harper CG, Kril JJ, Holloway RL (Brain shrinkage in chronic alcoholics: a pathological study. Br Med J (Clin Res Ed) 290:501-504.1985).

Harris GJ, Jaffin SK, Hodge SM, Kennedy D, Caviness VS, Marinkovic K, Papadimitriou GM, Makris N, Oscar-Berman M (Frontal white matter and cingulum diffusion tensor imaging deficits in alcoholism. Alcohol Clin Exp Res 32:1001-1013.2008).

Hartmann M, Brigadski T, Erdmann KS, Holtmann B, Sendtner M, Narz F, Lessmann V (Truncated TrkB receptor-induced outgrowth of dendritic filopodia involves the p75 neurotrophin receptor. J Cell Sci 117:5803-5814.2004).

Hasan KM, Ewing-Cobbs L, Kramer LA, Fletcher JM, Narayana PA (Diffusion tensor quantification of the macrostructure and microstructure of human midsagittal corpus callosum across the lifespan. NMR Biomed 21:1094-1101.2008).

Hasan KM, Halphen C, Boska MD, Narayana PA (Diffusion tensor metrics, T2 relaxation, and volumetry of the naturally aging human caudate nuclei in healthy young and middle-aged adults: possible implications for the neurobiology of human brain aging and disease. Magn Reson Med 59:7-13.2008).

Hasan KM, Kamali A, Kramer LA, Papnicolaou AC, Fletcher JM, Ewing-Cobbs L (Diffusion tensor quantification of the human midsagittal corpus callosum subdivisions across the lifespan. Brain Res 1227:52-67.2008).

Hasin DS, Keyes KM, Hatzenbuehler ML, Aharonovich EA, Alderson D (Alcohol consumption and posttraumatic stress after exposure to terrorism: effects of proximity, loss, and psychiatric history. Am J Public Health 97:2268-2275.2007).

Hermoye L, Saint-Martin C, Cosnard G, Lee SK, Kim J, Nassogne MC, Menten R, Clapuyt P, Donohue PK, Hua K, Wakana S, Jiang H, van Zijl PC, Mori S (Pediatric diffusion tensor imaging: normal database and observation of the white matter maturation in early childhood. Neuroimage 29:493-504.2006).

Hill SY, Shen S, Zezza N, Hoffman EK, Perlin M, Allan W (A genome wide search for alcoholism susceptibility genes. Am J Med Genet B Neuropsychiatr Genet 128B:102-113.2004).

Hodgkinson CA, Yuan Q, Xu K, Shen PH, Heinz E, Lobos EA, Binder EB, Cubells J, Ehlers CL, Gelernter J, Mann J, Riley B, Roy A, Tabakoff B, Todd RD, Zhou Z,

Goldman D (Addictions biology: haplotype-based analysis for 130 candidate genes on a single array. Alcohol Alcohol 43:505-515.2008).

Hommer D, Momenan R, Rawlings R, Ragan P, Williams W, Rio D, Eckardt M (Decreased corpus callosum size among alcoholic women. Arch Neurol 53:359-363.1996).

Jernigan TL, Butters N, DiTraglia G, Schafer K, Smith T, Irwin M, Grant I, Schuckit M, Cermak LS (Reduced cerebral grey matter observed in alcoholics using magnetic resonance imaging. Alcohol Clin Exp Res 15:418-427.1991).

Jiang H, van Zijl PC, Kim J, Pearlson GD, Mori S (DtiStudio: resource program for diffusion tensor computation and fiber bundle tracking. Comput Methods Programs Biomed 81:106-116.2006).

Kaltschmidt C, Kaltschmidt B, Neumann H, Wekerle H, Baeuerle PA (Constitutive NF-kappa B activity in neurons. Mol Cell Biol 14:3981-3992.1994).

Kang H, Schuman EM (Long-lasting neurotrophin-induced enhancement of synaptic transmission in the adult hippocampus. Science 267:1658-1662.1995).

Kang HJ, Schuman EM (Neurotrophin-induced modulation of synaptic transmission in the adult hippocampus. J Physiol Paris 89:11-22.1995).

Katoh-Semba R, Takeuchi IK, Semba R, Kato K (Distribution of brain-derived neurotrophic factor in rats and its changes with development in the brain. J Neurochem 69:34-42.1997).

Katz LC, Shatz CJ (Synaptic activity and the construction of cortical circuits. Science 274:1133-1138.1996).

Kessler DA (Alcohol marketing and youth: the challenge for public health. J Public Health Policy 26:292-295.2005).

Klein R, Conway D, Parada LF, Barbacid M (The trkB tyrosine protein kinase gene codes for a second neurogenic receptor that lacks the catalytic kinase domain. Cell 61:647-656.1990).

Klein R, Martin-Zanca D, Barbacid M, Parada LF (Expression of the tyrosine kinase receptor gene trkB is confined to the murine embryonic and adult nervous system. Development 109:845-850.1990).

Koob GF (Alcoholism: allostasis and beyond. Alcohol Clin Exp Res 27:232-243.2003).

Kubicki M, Westin CF, Maier SE, Mamata H, Frumin M, Ersner-Hershfield H, Kikinis R, Jolesz FA, McCarley R, Shenton ME (Diffusion tensor imaging and its application to neuropsychiatric disorders. Harv Rev Psychiatry 10:324-336.2002).

Lander ES, Linton LM, Birren B, Nusbaum C, Zody MC, Baldwin J, Devon K, Dewar K, Doyle M, FitzHugh W, Funke R, Gage D, Harris K, Heaford A, Howland J, Kann L, Lehoczky J, LeVine R, McEwan P, McKernan K, Meldrim J, Mesirov JP, Miranda C, Morris W, Naylor J, Raymond C, Rosetti M, Santos R, Sheridan A, Sougnez C, Stange-Thomann N, Stojanovic N, Subramanian A, Wyman D, Rogers J, Sulston J, Ainscough R, Beck S, Bentley D, Burton J, Clee C, Carter N, Coulson A, Deadman R, Deloukas P, Dunham A, Dunham I, Durbin R, French L, Grafham D, Gregory S, Hubbard T, Humphray S, Hunt A, Jones M, Lloyd C, McMurray A, Matthews L, Mercer S, Milne S, Mullikin JC, Mungall A, Plumb R, Ross M, Shownkeen R, Sims S, Waterston RH, Wilson RK, Hillier LW, McPherson JD, Marra MA, Mardis ER, Fulton LA, Chinwalla AT, Pepin KH,

Gish WR, Chissoe SL, Wendl MC, Delehaunty KD, Miner TL, Delehaunty A, Kramer JB, Cook LL, Fulton RS, Johnson DL, Minx PJ, Clifton SW, Hawkins T, Branscomb E, Predki P, Richardson P, Wenning S, Slezak T, Doggett N, Cheng JF, Olsen A, Lucas S, Elkin C, Uberbacher E, Frazier M, Gibbs RA, Muzny DM, Scherer SE, Bouck JB, Sodergren EJ, Worley KC, Rives CM, Gorrell JH, Metzker ML, Naylor SL, Kucherlapati RS, Nelson DL, Weinstock GM, Sakaki Y, Fujiyama A, Hattori M, Yada T, Toyoda A, Itoh T, Kawagoe C, Watanabe H, Totoki Y, Taylor T, Weissenbach J, Heilig R, Saurin W, Artiguenave F, Brottier P, Bruls T, Pelletier E, Robert C, Wincker P, Smith DR, Doucette-Stamm L, Rubenfield M, Weinstock K, Lee HM, Dubois J, Rosenthal A, Platzer M, Nyakatura G, Taudien S, Rump A, Yang H, Yu J, Wang J, Huang G, Gu J, Hood L, Rowen L, Madan A, Qin S, Davis RW, Federspiel NA, Abola AP, Proctor MJ, Myers RM, Schmutz J, Dickson M, Grimwood J, Cox DR, Olson MV, Kaul R, Shimizu N, Kawasaki K, Minoshima S, Evans GA, Athanasiou M, Schultz R, Roe BA, Chen F, Pan H, Ramser J, Lehrach H, Reinhardt R, McCombie WR, de la Bastide M, Dedhia N, Blocker H, Hornischer K, Nordsiek G, Agarwala R, Aravind L, Bailey JA, Bateman A, Batzoglou S, Birney E, Bork P, Brown DG, Burge CB, Cerutti L, Chen HC, Church D, Clamp M, Copley RR, Doerks T, Eddy SR, Eichler EE, Furey TS, Galagan J, Gilbert JG, Harmon C, Hayashizaki Y, Haussler D, Hermjakob H, Hokamp K, Jang W, Johnson LS, Jones TA, Kasif S, Kaspryzk A, Kennedy S, Kent WJ, Kitts P, Koonin EV, Korf I, Kulp D, Lancet D, Lowe TM, McLysaght A, Mikkelsen T, Moran JV, Mulder N, Pollara VJ, Ponting CP, Schuler G, Schultz J, Slater G, Smit AF, Stupka E, Szustakowski J, Thierry-

Mieg D, Thierry-Mieg J, Wagner L, Wallis J, Wheeler R, Williams A, Wolf YI, Wolfe KH, Yang SP, Yeh RF, Collins F, Guyer MS, Peterson J, Felsenfeld A, Wetterstrand KA, Patrinos A, Morgan MJ, de Jong P, Catanese JJ, Osoegawa K, Shizuya H, Choi S, Chen YJ (Initial sequencing and analysis of the human genome. Nature 409:860-921.2001).

Lauterbur PC (Image formation by induced local interactions. Examples employing nuclear magnetic resonance. 1973. Clin Orthop Relat Res 3-6.1989).

Levine ES, Dreyfus CF, Black IB, Plummer MR (Brain-derived neurotrophic factor rapidly enhances synaptic transmission in hippocampal neurons via postsynaptic tyrosine kinase receptors. Proc Natl Acad Sci U S A 92:8074-8077.1995).

Lewohl JM, Wang L, Miles MF, Zhang L, Dodd PR, Harris RA (Gene expression in human alcoholism: microarray analysis of frontal cortex. Alcohol Clin Exp Res 24:1873-1882.2000).

Liang T, Spence J, Liu L, Strother WN, Chang HW, Ellison JA, Lumeng L, Li TK, Foroud T, Carr LG (alpha-Synuclein maps to a quantitative trait locus for alcohol preference and is differentially expressed in alcohol-preferring and -nonpreferring rats. Proc Natl Acad Sci U S A 100:4690-4695.2003).

Lipsky RH, Xu K, Zhu D, Kelly C, Terhakopian A, Novelli A, Marini AM (Nuclear factor kappaB is a critical determinant in N-methyl-D-aspartate receptor-mediated neuroprotection. J Neurochem 78:254-264.2001).

Lohof AM, Ip NY, Poo MM (Potentiation of developing neuromuscular synapses by the neurotrophins NT-3 and BDNF. Nature 363:350-353.1993).

Long JC, Knowler WC, Hanson RL, Robin RW, Urbanek M, Moore E, Bennett PH, Goldman D (Evidence for genetic linkage to alcohol dependence on chromosomes 4 and 11 from an autosome-wide scan in an American Indian population. Am J Med Genet 81:216-221.1998).

Lu QR, Yuk D, Alberta JA, Zhu Z, Pawlitzky I, Chan J, McMahon AP, Stiles CD, Rowitch DH (Sonic hedgehog--regulated oligodendrocyte lineage genes encoding bHLH proteins in the mammalian central nervous system. Neuron 25:317-329.2000).

MacQueen GM, Yucel K, Taylor VH, Macdonald K, Joffe R (Posterior hippocampal volumes are associated with remission rates in patients with major depressive disorder. Biol Psychiatry 64:880-883.2008).

Mahadev K, Vemuri MC (Effect of ethanol on chromatin and nonhistone nuclear proteins in rat brain. Neurochem Res 23:1179-1184.1998).

Mahadev K, Vemuri MC (Ethanol-induced changes in hepatic chromatin and nonhistone nuclear protein composition in the rat. Alcohol 15:207-211.1998).

Makris N, Oscar-Berman M, Jaffin SK, Hodge SM, Kennedy DN, Caviness VS, Marinkovic K, Breiter HC, Gasic GP, Harris GJ (Decreased volume of the brain reward system in alcoholism. Biol Psychiatry 64:192-202.2008).

Malhotra AK, Goldman D (Benefits and pitfalls encountered in psychiatric genetic association studies. Biol Psychiatry 45:544-550.1999).

Manji H (Depression, III: treatments. Am J Psychiatry 160:24.2003).

Marini AM, Jiang X, Wu X, Tian F, Zhu D, Okagaki P, Lipsky RH (Role of brain-derived neurotrophic factor and NF-kappaB in neuronal plasticity and survival: From genes to phenotype. Restor Neurol Neurosci 22:121-130.2004).

Marinkovic K, Halgren E, Klopp J, Maltzman I (Alcohol effects on movement-related potentials: a measure of impulsivity? J Stud Alcohol 61:24-31.2000).

Marinkovic K, Oscar-Berman M, Urban T, O'Reilly CE, Howard JA, Sawyer K, Harris GJ (Alcoholism and dampened temporal limbic activation to emotional faces. Alcohol Clin Exp Res 33:1880-1892.2009).

Marshall CA, Novitch BG, Goldman JE (Olig2 directs astrocyte and oligodendrocyte formation in postnatal subventricular zone cells. J Neurosci 25:7289-7298.2005).

McAllister AK, Lo DC, Katz LC (Neurotrophins regulate dendritic growth in developing visual cortex. Neuron 15:791-803.1995).

McDonald C, Bullmore ET, Sham PC, Chitnis X, Wickham H, Bramon E, Murray RM (Association of genetic risks for schizophrenia and bipolar disorder with specific and generic brain structural endophenotypes. Arch Gen Psychiatry 61:974-984.2004).

McGough NN, He DY, Logrip ML, Jeanblanc J, Phamluong K, Luong K, Kharazia V, Janak PH, Ron D (RACK1 and brain-derived neurotrophic factor: a homeostatic pathway that regulates alcohol addiction. J Neurosci 24:10542-10552.2004).

Meberg PJ, Kinney WR, Valcourt EG, Routtenberg A (Gene expression of the transcription factor NF-kappa B in hippocampus: regulation by synaptic activity. Brain Res Mol Brain Res 38:179-190.1996).

Meffert MK, Baltimore D (Physiological functions for brain NF-kappaB. Trends Neurosci 28:37-43.2005).

Meffert MK, Chang JM, Wiltgen BJ, Fanselow MS, Baltimore D (NF-kappa B functions in synaptic signaling and behavior. Nat Neurosci 6:1072-1078.2003).

Merikangas KR, Gelernter CS (Comorbidity for alcoholism and depression. Psychiatr Clin North Am 13:613-632.1990).

Merikangas KR, Risch NJ, Weissman MM (Comorbidity and co-transmission of alcoholism, anxiety and depression. Psychol Med 24:69-80.1994).

Moldin SO (Detection and replication of linkage to a complex human disease. Genet Epidemiol 14:1023-1028.1997).

Moseley I (Neuroimaging. Curr Opin Neurol Neurosurg 3:863.1990).

Mukherjee P, Berman JI, Chung SW, Hess CP, Henry RG (Diffusion tensor MR imaging and fiber tractography: theoretic underpinnings. AJNR Am J Neuroradiol 29:632-641.2008).

Mukherjee P, Chung SW, Berman JI, Hess CP, Henry RG (Diffusion tensor MR imaging and fiber tractography: technical considerations. AJNR Am J Neuroradiol 29:843-852.2008).

Mukherjee P, Miller JH, Shimony JS, Conturo TE, Lee BC, Almli CR, McKinstry RC (Normal brain maturation during childhood: developmental trends characterized with diffusion-tensor MR imaging. Radiology 221:349-358.2001).

Nauta WJ (The problem of the frontal lobe: a reinterpretation. J Psychiatr Res 8:167-187.1971).

Nauta WJ (Neural associations of the frontal cortex. Acta Neurobiol Exp (Wars) 32:125-140.1972).

Nelson E, Rice J, Rochberg N, Endicott J, Coryell W, Akiskal HS (Affective illness in family members and matched controls. Acta Psychiatr Scand 91:146-151.1995).

Nestler EJ (Is there a common molecular pathway for addiction? Nat Neurosci 8:1445-1449.2005).

Nestler EJ, Guitart X, Ortiz J, Trevisan L (Second messenger and protein phosphorylation mechanisms underlying possible genetic vulnerability to alcoholism. Ann N Y Acad Sci 708:108-118.1994).

Neves-Pereira M, Mundo E, Muglia P, King N, Macciardi F, Kennedy JL (The brain-derived neurotrophic factor gene confers susceptibility to bipolar disorder: evidence from a family-based association study. Am J Hum Genet 71:651-655.2002).

Nurnberger JI, Jr., Foroud T, Flury L, Meyer ET, Wiegand R (Is there a genetic relationship between alcoholism and depression? Alcohol Res Health 26:233-240.2002).

Oishi M, Mochizuki Y (Frontal lobe atrophy and central motor conduction time in chronic alcoholics. Clin Electroencephalogr 30:76-78.1999).

Oishi M, Mochizuki Y, Shikata E (Corpus callosum atrophy and cerebral blood flow in chronic alcoholics. J Neurol Sci 162:51-55.1999).

Oscar-Berman M, Bowirrat A (Genetic influences in emotional dysfunction and alcoholism-related brain damage. Neuropsychiatr Dis Treat 1:211-229.2005).

Oscar-Berman M, Marinkovic K (Alcoholism and the brain: an overview. Alcohol Res Health 27:125-133.2003).

Oscar-Berman M, Marinkovic K (Alcohol: effects on neurobehavioral functions and the brain. Neuropsychol Rev 17:239-257.2007).

Patterson SL, Abel T, Deuel TA, Martin KC, Rose JC, Kandel ER (Recombinant BDNF rescues deficits in basal synaptic transmission and hippocampal LTP in BDNF knockout mice. Neuron 16:1137-1145.1996).

Paula-Barbosa MM, Tavares MA (Long term alcohol consumption induces microtubular changes in the adult rat cerebellar cortex. Brain Res 339:195-199.1985).

Pezawas L, Verchinski BA, Mattay VS, Callicott JH, Kolachana BS, Straub RE, Egan MF, Meyer-Lindenberg A, Weinberger DR (The brain-derived neurotrophic factor val66met polymorphism and variation in human cortical morphology. J Neurosci 24:10099-10102.2004).

Pfefferbaum A (Alcoholism damages the brain, but does moderate alcohol use? Lancet Neurol 3:143-144.2004).

Pfefferbaum A, Adalsteinsson E, Sullivan EV (Supratentorial profile of white matter microstructural integrity in recovering alcoholic men and women. Biol Psychiatry 59:364-372.2006).

Pfefferbaum A, Lim KO, Desmond JE, Sullivan EV (Thinning of the corpus callosum in older alcoholic men: a magnetic resonance imaging study. Alcohol Clin Exp Res 20:752-757.1996).

Pfefferbaum A, Lim KO, Zipursky RB, Mathalon DH, Rosenbloom MJ, Lane B, Ha CN, Sullivan EV (Brain gray and white matter volume loss accelerates with aging in

chronic alcoholics: a quantitative MRI study. Alcohol Clin Exp Res 16:1078-1089.1992).

Pfefferbaum A, Sullivan EV (Disruption of brain white matter microstructure by excessive intracellular and extracellular fluid in alcoholism: evidence from diffusion tensor imaging. Neuropsychopharmacology 30:423-432.2005).

Pfefferbaum A, Sullivan EV, Adalsteinsson E, Garrick T, Harper C (Postmortem MR imaging of formalin-fixed human brain. Neuroimage 21:1585-1595.2004).

Pierpaoli C, Basser PJ (Toward a quantitative assessment of diffusion anisotropy. Magn Reson Med 36:893-906.1996).

Pishkin V, Lovallo WR, Bourne LE, Jr. (Chronic alcoholism in males: cognitive deficit as a function of age of onset, age, and duration. Alcohol Clin Exp Res 9:400-406.1985).

Porjesz B, Rangaswamy M, Kamarajan C, Jones KA, Padmanabhapillai A, Begleiter H (The utility of neurophysiological markers in the study of alcoholism. Clin Neurophysiol 116:993-1018.2005).

Poupon C, Clark CA, Frouin V, Regis J, Bloch I, Le Bihan D, Mangin J (Regularization of diffusion-based direction maps for the tracking of brain white matter fascicles. Neuroimage 12:184-195.2000).

Pritchard JK, Rosenberg NA (Use of unlinked genetic markers to detect population stratification in association studies. Am J Hum Genet 65:220-228.1999).

Pruessner JC, Li LM, Serles W, Pruessner M, Collins DL, Kabani N, Lupien S, Evans AC (Volumetry of hippocampus and amygdala with high-resolution MRI and

three-dimensional analysis software: minimizing the discrepancies between laboratories. Cereb Cortex 10:433-442.2000).

Radel M, Vallejo RL, Iwata N, Aragon R, Long JC, Virkkunen M, Goldman D (Haplotype-based localization of an alcohol dependence gene to the 5q34 {gamma}-aminobutyric acid type A gene cluster. Arch Gen Psychiatry 62:47-55.2005).

Rahman SZ, Singhal KC (Postal stamps on drug and alcohol abuse. Indian J Physiol Pharmacol 43:147-150.1999).

Ramsey SE, Brown RA, Stuart GL, Burgess ES, Miller IW (Cognitive variables in alcohol dependent patients with elevated depressive symptoms: changes and predictive utility as a function of treatment modality. Subst Abus 23:171-182.2002).

Reich T, Edenberg HJ, Goate A, Williams JT, Rice JP, Van Eerdewegh P, Foroud T, Hesselbrock V, Schuckit MA, Bucholz K, Porjesz B, Li TK, Conneally PM, Nurnberger JI, Jr., Tischfield JA, Crowe RR, Cloninger CR, Wu W, Shears S, Carr K, Crose C, Willig C, Begleiter H (Genome-wide search for genes affecting the risk for alcohol dependence. Am J Med Genet 81:207-215.1998).

Ribases M, Gratacos M, Badia A, Jimenez L, Solano R, Vallejo J, Fernandez-Aranda F, Estivill X (Contribution of NTRK2 to the genetic susceptibility to anorexia nervosa, harm avoidance and minimum body mass index. Mol Psychiatry 10:851-860.2005).

Roberto M, Nelson TE, Ur CL, Gruol DL (Long-term potentiation in the rat hippocampus is reversibly depressed by chronic intermittent ethanol exposure. J Neurophysiol 87:2385-2397.2002).

Rodd ZA, Bertsch BA, Strother WN, Le-Niculescu H, Balaraman Y, Hayden E, Jerome RE, Lumeng L, Nurnberger JI, Jr., Edenberg HJ, McBride WJ, Niculescu AB (Candidate genes, pathways and mechanisms for alcoholism: an expanded convergent functional genomics approach. Pharmacogenomics J 7:222-256.2007).

Rosenbloom M, Sullivan EV, Pfefferbaum A (Using magnetic resonance imaging and diffusion tensor imaging to assess brain damage in alcoholics. Alcohol Res Health 27:146-152.2003).

Rowitch DH, Lu QR, Kessaris N, Richardson WD (An 'oligarchy' rules neural development. Trends Neurosci 25:417-422.2002).

Saarelainen T, Vaittinen S, Castren E (trkB-receptor activation contributes to the kainate-induced increase in BDNF mRNA synthesis. Cell Mol Neurobiol 21:429-435.2001).

Saiki RK, Gelfand DH, Stoffel S, Scharf SJ, Higuchi R, Horn GT, Mullis KB, Erlich HA (Primer-directed enzymatic amplification of DNA with a thermostable DNA polymerase. Science 239:487-491.1988).

Salgado-Pineda P, Delaveau P, Blin O, Nieoullon A (Dopaminergic contribution to the regulation of emotional perception. Clin Neuropharmacol 28:228-237.2005).

Schachner M, Bartsch U (Multiple functions of the myelin-associated glycoprotein MAG (siglec-4a) in formation and maintenance of myelin. Glia 29:154-165.2000).

Schmahmann JD, Caplan D (Cognition, emotion and the cerebellum. Brain 129:290-292.2006).

Sebat J (Major changes in our DNA lead to major changes in our thinking. Nat Genet 39:S3-5.2007).

Sen S, Nesse RM, Stoltenberg SF, Li S, Gleiberman L, Chakravarti A, Weder AB, Burmeister M (A BDNF coding variant is associated with the NEO personality inventory domain neuroticism, a risk factor for depression. Neuropsychopharmacology 28:397-401.2003).

Shear PK, Sullivan EV, Lane B, Pfefferbaum A (Mammillary body and cerebellar shrinkage in chronic alcoholics with and without amnesia. Alcohol Clin Exp Res 20:1489-1495.1996).

Shen J, Chan KW, Chen BT, Philippe J, Sehba F, Duttaroy A, Carroll J, Yoburn BC (The effect of in vivo ethanol consumption on cyclic AMP and delta-opioid receptors in mouse striatum. Brain Res 770:65-71.1997).

Sher KJ, Grekin ER, Williams NA (The development of alcohol use disorders. Annu Rev Clin Psychol 1:493-523.2005).

Shimizu E, Hashimoto K, Iyo M (Ethnic difference of the BDNF 196G/A (val66met) polymorphism frequencies: the possibility to explain ethnic mental traits. Am J Med Genet B Neuropsychiatr Genet 126B:122-123.2004).

Shimizu E, Hashimoto K, Iyo M ([Major depressive disorders and BDNF (brain-derived neurotrophic factor)]. Nihon Shinkei Seishin Yakurigaku Zasshi 24:147-150.2004).

Skinner HA, Allen BA (Alcohol dependence syndrome: measurement and validation. J Abnorm Psychol 91:199-209.1982).

Sklar P, Gabriel SB, McInnis MG, Bennett P, Lim YM, Tsan G, Schaffner S, Kirov G, Jones I, Owen M, Craddock N, DePaulo JR, Lander ES (Family-based association study of 76 candidate genes in bipolar disorder: BDNF is a potential risk locus. Brain-derived neutrophic factor. Mol Psychiatry 7:579-593.2002).

Smith SM, Johansen-Berg H, Jenkinson M, Rueckert D, Nichols TE, Miller KL, Robson MD, Jones DK, Klein JC, Bartsch AJ, Behrens TE (Acquisition and voxelwise analysis of multi-subject diffusion data with tract-based spatial statistics. Nat Protoc 2:499-503.2007).

Sobell LC, Maisto SA, Sobell MB, Cooper AM (Reliability of alcohol abusers' self-reports of drinking behavior. Behav Res Ther 17:157-160.1979).

Sobell LC, VanderSpek R, Saltman P (Utility of portable breath alcohol testers for drunken driving offenders. J Stud Alcohol 41:930-934.1980).

Sowell ER, Thompson PM, Holmes CJ, Batth R, Jernigan TL, Toga AW (Localizing age-related changes in brain structure between childhood and adolescence using statistical parametric mapping. Neuroimage 9:587-597.1999).

Specht K, Willmes K, Shah NJ, Jancke L (Assessment of reliability in functional imaging studies. J Magn Reson Imaging 17:463-471.2003).

Stoilov P, Castren E, Stamm S (Analysis of the human TrkB gene genomic organization reveals novel TrkB isoforms, unusual gene length, and splicing mechanism. Biochem Biophys Res Commun 290:1054-1065.2002).

Sullivan EV, Pfefferbaum A (Neurocircuitry in alcoholism: a substrate of disruption and repair. Psychopharmacology (Berl) 180:583-594.2005).

Sullivan EV, Sable HJ, Strother WN, Friedman DP, Davenport A, Tillman-Smith H, Kraft RA, Wyatt C, Szeliga KT, Buchheimer NC, Daunais JB, Adalsteinsson E, Pfefferbaum A, Grant KA (Neuroimaging of rodent and primate models of alcoholism: initial reports from the integrative neuroscience initiative on alcoholism. Alcohol Clin Exp Res 29:287-294.2005).

Sun T, Walsh CA (Molecular approaches to brain asymmetry and handedness. Nat Rev Neurosci 7:655-662.2006).

Sunyaev S, Hanke J, Brett D, Aydin A, Zastrow I, Lathe W, Bork P, Reich J (Individual variation in protein-coding sequences of human genome. Adv Protein Chem 54:409-437.2000).

Sunyaev SR, Lathe WC, 3rd, Ramensky VE, Bork P (SNP frequencies in human genes an excess of rare alleles and differing modes of selection. Trends Genet 16:335-337.2000).

Szeszko PR, Lipsky R, Mentschel C, Robinson D, Gunduz-Bruce H, Sevy S, Ashtari M, Napolitano B, Bilder RM, Kane JM, Goldman D, Malhotra AK (Brain-derived neurotrophic factor val66met polymorphism and volume of the hippocampal formation. Mol Psychiatry 10:631-636.2005).

Tapia-Arancibia L, Rage F, Givalois L, Dingeon P, Arancibia S, Beauge F (Effects of alcohol on brain-derived neurotrophic factor mRNA expression in discrete regions of the rat hippocampus and hypothalamus. J Neurosci Res 63:200-208.2001).

Thoenen H (Neurotrophins and neuronal plasticity. Science 270:593-598.1995).

Tsankova N, Renthal W, Kumar A, Nestler EJ (Epigenetic regulation in psychiatric disorders. Nat Rev Neurosci 8:355-367.2007).

Uhl GR, Liu QR, Walther D, Hess J, Naiman D (Polysubstance abuse-vulnerability genes: genome scans for association, using 1,004 subjects and 1,494 single-nucleotide polymorphisms. Am J Hum Genet 69:1290-1300.2001).

Varnas K, Lawyer G, Jonsson EG, Kulle B, Nesvag R, Hall H, Terenius L, Agartz I (Brain-derived neurotrophic factor polymorphisms and frontal cortex morphology in schizophrenia. Psychiatr Genet 18:177-183.2008).

Venter JC, Adams MD, Myers EW, Li PW, Mural RJ, Sutton GG, Smith HO, Yandell M, Evans CA, Holt RA, Gocayne JD, Amanatides P, Ballew RM, Huson DH, Wortman JR, Zhang Q, Kodira CD, Zheng XH, Chen L, Skupski M, Subramanian G, Thomas PD, Zhang J, Gabor Miklos GL, Nelson C, Broder S, Clark AG, Nadeau J, McKusick VA, Zinder N, Levine AJ, Roberts RJ, Simon M, Slayman C, Hunkapiller M, Bolanos R, Delcher A, Dew I, Fasulo D, Flanigan M, Florea L, Halpern A, Hannenhalli S, Kravitz S, Levy S, Mobarry C, Reinert K, Remington K, Abu-Threideh J, Beasley E, Biddick K, Bonazzi V, Brandon R, Cargill M, Chandramouliswaran I, Charlab R, Chaturvedi K, Deng Z, Di Francesco V, Dunn P, Eilbeck K, Evangelista C, Gabrielian AE, Gan W, Ge W, Gong F, Gu Z, Guan P, Heiman TJ, Higgins ME, Ji RR, Ke Z, Ketchum KA, Lai Z, Lei Y, Li Z, Li J, Liang Y, Lin X, Lu F, Merkulov GV, Milshina N, Moore HM, Naik AK, Narayan VA, Neelam B, Nusskern D, Rusch DB, Salzberg S, Shao W, Shue B, Sun J, Wang Z, Wang A, Wang X, Wang J, Wei M, Wides R, Xiao C, Yan C, Yao A,

Ye J, Zhan M, Zhang W, Zhang H, Zhao Q, Zheng L, Zhong F, Zhong W, Zhu S, Zhao S, Gilbert D, Baumhueter S, Spier G, Carter C, Cravchik A, Woodage T, Ali F, An H, Awe A, Baldwin D, Baden H, Barnstead M, Barrow I, Beeson K, Busam D, Carver A, Center A, Cheng ML, Curry L, Danaher S, Davenport L, Desilets R, Dietz S, Dodson K, Doup L, Ferriera S, Garg N, Gluecksmann A, Hart B, Haynes J, Haynes C, Heiner C, Hladun S, Hostin D, Houck J, Howland T, Ibegwam C, Johnson J, Kalush F, Kline L, Koduru S, Love A, Mann F, May D, McCawley S, McIntosh T, McMullen I, Moy M, Moy L, Murphy B, Nelson K, Pfannkoch C, Pratts E, Puri V, Qureshi H, Reardon M, Rodriguez R, Rogers YH, Romblad D, Ruhfel B, Scott R, Sitter C, Smallwood M, Stewart E, Strong R, Suh E, Thomas R, Tint NN, Tse S, Vech C, Wang G, Wetter J, Williams S, Williams M, Windsor S, Winn-Deen E, Wolfe K, Zaveri J, Zaveri K, Abril JF, Guigo R, Campbell MJ, Sjolander KV, Karlak B, Kejariwal A, Mi H, Lazareva B, Hatton T, Narechania A, Diemer K, Muruganujan A, Guo N, Sato S, Bafna V, Istrail S, Lippert R, Schwartz R, Walenz B, Yooseph S, Allen D, Basu A, Baxendale J, Blick L, Caminha M, Carnes-Stine J, Caulk P, Chiang YH, Coyne M, Dahlke C, Mays A, Dombroski M, Donnelly M, Ely D, Esparham S, Fosler C, Gire H, Glanowski S, Glasser K, Glodek A, Gorokhov M, Graham K, Gropman B, Harris M, Heil J, Henderson S, Hoover J, Jennings D, Jordan C, Jordan J, Kasha J, Kagan L, Kraft C, Levitsky A, Lewis M, Liu X, Lopez J, Ma D, Majoros W, McDaniel J, Murphy S, Newman M, Nguyen T, Nguyen N, Nodell M, Pan S, Peck J, Peterson M, Rowe W, Sanders R, Scott J, Simpson M, Smith T, Sprague A, Stockwell T,

Turner R, Venter E, Wang M, Wen M, Wu D, Wu M, Xia A, Zandieh A, Zhu X (The sequence of the human genome. Science 291:1304-1351.2001).

Verdejo-Garcia A, Bechara A, Recknor EC, Perez-Garcia M (Executive dysfunction in substance dependent individuals during drug use and abstinence: an examination of the behavioral, cognitive and emotional correlates of addiction. J Int Neuropsychol Soc 12:405-415.2006).

Verdejo-Garcia A, Vilar-Lopez R, Perez-Garcia M, Podell K, Goldberg E (Altered adaptive but not veridical decision-making in substance dependent individuals. J Int Neuropsychol Soc 12:90-99.2006).

Viding E, Williamson DE, Hariri AR (Developmental imaging genetics: challenges and promises for translational research. Dev Psychopathol 18:877-892.2006).

Wagner T, Krampe H, Stawicki S, Reinhold J, Jahn H, Mahlke K, Barth U, Sieg S, Maul O, Galwas C, Aust C, Kroner-Herwig B, Brunner E, Poser W, Henn F, Ruther E, Ehrenreich H (Substantial decrease of psychiatric comorbidity in chronic alcoholics upon integrated outpatient treatment - results of a prospective study. J Psychiatr Res 38:619-635.2004).

Wakana S, Caprihan A, Panzenboeck MM, Fallon JH, Perry M, Gollub RL, Hua K, Zhang J, Jiang H, Dubey P, Blitz A, van Zijl P, Mori S (Reproducibility of quantitative tractography methods applied to cerebral white matter. Neuroimage 36:630-644.2007).

Wang J, El-Guebaly N (Sociodemographic factors associated with comorbid major depressive episodes and alcohol dependence in the general population. Can J Psychiatry 49:37-44.2004).

Watkins KE, Paus T, Lerch JP, Zijdenbos A, Collins DL, Neelin P, Taylor J, Worsley KJ, Evans AC (Structural asymmetries in the human brain: a voxel-based statistical analysis of 142 MRI scans. Cereb Cortex 11:868-877.2001).

Webster MJ, Weickert CS, Herman MM, Kleinman JE (BDNF mRNA expression during postnatal development, maturation and aging of the human prefrontal cortex. Brain Res Dev Brain Res 139:139-150.2002).

Williams JT, Blangero J (Asymptotic power of likelihood-ratio tests for detecting quantitative trait loci using the COGA data. Genet Epidemiol 17 Suppl 1:S397-402.1999).

Wong DF, Maini A, Rousset OG, Brasic JR (Positron emission tomography--a tool for identifying the effects of alcohol dependence on the brain. Alcohol Res Health 27:161-173.2003).

Xu K, Anderson TR, Neyer KM, Lamparella N, Jenkins G, Zhou Z, Yuan Q, Virkkunen M, Lipsky RH (Nucleotide sequence variation within the human tyrosine kinase B neurotrophin receptor gene: association with antisocial alcohol dependence. Pharmacogenomics J 7:368-379.2007).

Xue R, van Zijl PC, Crain BJ, Solaiyappan M, Mori S (In vivo three-dimensional reconstruction of rat brain axonal projections by diffusion tensor imaging. Magn Reson Med 42:1123-1127.1999).

Yeh PH, Simpson K, Durazzo TC, Gazdzinski S, Meyerhoff DJ (Tract-Based Spatial Statistics (TBSS) of diffusion tensor imaging data in alcohol dependence: abnormalities of the motivational neurocircuitry. Psychiatry Res 173:22-30.2009).

Zoeller RT, Butnariu OV, Fletcher DL, Riley EP (Limited postnatal ethanol exposure permanently alters the expression of mRNAS encoding myelin basic protein and myelin-associated glycoprotein in cerebellum. Alcohol Clin Exp Res 18:909-916.1994).

Zou J, Crews F (CREB and NF-kappaB transcription factors regulate sensitivity to excitotoxic and oxidative stress induced neuronal cell death. Cell Mol Neurobiol 26:385-405.2006).